

THESIS

2

2000

MICHIGAN STATE UNIVERSITY LIBRARIES



3 1293 02079 9395

This is to certify that the

dissertation entitled

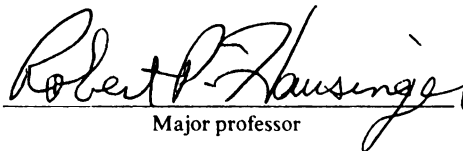
Characterization and Function of
2,4-Dichlorophenoxyacetic Acid/ alpha-Keto-
glutarate Dioxygenase and Related Enzymes

presented by

Deborah Ann Hogan

has been accepted towards fulfillment
of the requirements for

Ph.D. degree in Microbiology


Major professor

Date 12/13/99

LIBRARY
Michigan State
University

CHARACTERIZATION AND FUNCTION OF 2,4-DICHLORO-
PHENOXYACETIC ACID/ α -KETOGLUTARATE-DEPENDENT DIOXYGENASE
AND RELATED ENZYMES

By

Deborah Ann Hogan

A DISSERTATION

Submitted to
Michigan State University
in partial fulfillment of the requirements
for the degree of

DOCTOR OF PHILOSOPHY

Department of Microbiology

1999

ABSTRACT

CHARACTERIZATION AND FUNCTION OF 2,4-DICHLORO-PHENOXYACETIC ACID/ α -KETOGLUTARATE-DEPENDENT DIOXYGENASE AND RELATED ENZYMES

By

Deborah Ann Hogan

The rapid degradation of the herbicide 2,4-dichlorophenoxyacetic acid (2,4-D) in soils is mediated by bacteria containing the enzyme 2,4-D/ α -ketoglutarate (α -KG) dioxygenase, or TfdA. TfdA is among the more than forty Fe(II)-dependent enzymes that comprise the α -KG-dependent dioxygenase superfamily. Most of these enzymes couple the oxidative decarboxylation of α -KG to diverse oxidations including hydroxylations, cyclizations, desaturations, and ring expansion reactions. A small group of related enzymes within the superfamily have been characterized through various biochemical, spectroscopic and structural studies, but none of these sequences exhibit any overall identity to TfdA or its relatives.

To better understand the mechanism of TfdA, site-directed mutagenesis experiments were performed to identify the ligands to the Fe(II) metallocenter as well as other residues that may be critical for activity. Nine histidines and one aspartate were individually substituted with alanines, and the effects of the mutations were assessed by kinetic and spectroscopic analyses. Electron paramagnetic resonance (EPR) and electron spin-echo envelope modulation (ESEEM) spectroscopies were used to determine that alteration of His 113 and Asp 115 caused dramatic changes to the metal binding site of TfdA. A second histidine ligand was tentatively identified as His 262. Two residues, His

213 and His 216, were implicated in catalysis and the former may play a role in substrate binding.

In addition to serving as a model enzyme for mechanistic studies of α -KG-dependent dioxygenases, TfdA performs a novel reaction in the degradation of aromatic compounds. A search for other enzymes with TfdA-like activity found a hypothetical protein, encoded by YLL057c, in *Saccharomyces cerevisiae* with 27% identity to TfdA. All of the residues involved in TfdA metallocenter formation are conserved in this sequence. To determine if this protein catalyzed a reaction similar to that of TfdA, YLL057c was cloned and found to encode a sulfonate/ α -KG dioxygenase with activity towards a number of different sulfonates including isethionate and taurocholate, a conjugated bile salt. Studies with a *S. cerevisiae* strain which lacked this gene indicated that sulfonate/ α -KG dioxygenase is involved in utilization of sulfonates as alternative sources of sulfur.

The presence of α -KG-dependent dioxygenases with activities similar to TfdA was also assessed in a collection of diverse soil bacteria. Thirty seven percent of the seventy-seven isolates tested appeared to contain a *tfdA*-like element as determined by a PCR-based method. Results from three different assays suggested that none of the isolates could degrade 2,4-D. The high identity between *tfdA*-like genes from distantly related bacteria suggests that extensive horizontal transfer was responsible for its distribution. Although the function of *tfdA*-like elements in these bacterial isolates is not known, the widespread presence of this gene implies its importance in the environment. It is proposed that these genes are involved in the degradation of the aromatic compounds prevalent in soils such as those released from lignin degradation.

To my family for their love and support

ACKNOWLEDGMENTS

My appreciation and thanks first go to my advisor, Bob Hausinger. His tireless enthusiasm for being a both scientist and a mentor creates a wonderful environment for a graduate student. I particularly value his dedication, directness, friendship and sense of humor and I look forward to being his colleague. I would also like to thank my guidance committee members, John Breznak, Pat Oriel, Cindy Nakatsu, and C. A. Reddy, for their support. Each committee member had a unique influence on my graduate education. I owe special thanks Cindy Nakatsu for sharing her expertise in molecular biology and her interest in my project. I would also like to acknowledge the invaluable experience I gained during my eight-month internship at Parke-Davis with Ruth VanBogelen, who is a true bacterial physiologist and a great role model.

The supportive environment in the Hausinger Lab has been valuable to me. I would particularly like to thank Gerry Colpas and Matt Ryle for their willingness to be my spectroscopy gurus. I am very appreciative of the help given to me by Julie Dunning-Hotopp, Linda Michel, and Ruth Saari. I can't express enough gratitude to Tommy Auchtung, who made major contributions to the yeast dioxygenase project, while curating the lab aquarium and playing the Beatles. In addition, I would like to thank past and present lab members (Tim Brayman, Aileen Soriano, Mary Beth Moncrief, Padmakumar Raghavakaimal, Ruth Schaller and Vladimir Romanov) for their advice and conversation.

Thanks to all of the members of my class who have been great friends ever since our first post-exam celebration at the Peanut Barrel as students in Biochemistry 801.

Among the friends I have made here, I owe particular thanks to Mary Ellen Davey, Dan Buckley, Joe Graber, Mark Johnson, Brad Stevenson, and Joel Klappenbach. I would also like to mention my family and friends from home whose support from afar was essential.

I would like to thank the ROME Lab and John McCracken for use of space and equipment. I have enjoyed support from the College of Natural Science, the Biotechnology Training Program, and the Center for Microbial Ecology for which I am grateful. Finally, I would like to express my gratitude to the departmental staff and faculty whose assistance was important and appreciated.

TABLE OF CONTENTS

List of Tables	x
List of Figures	xi
List of Schemes	xiii
List of Equations	xiv
Key to Abbreviations	xv
 CHAPTER 1 INTRODUCTION	 1
Sequence analysis of α -KG-dependent dioxygenases	3
IPNS-like α -KG-dependent dioxygenases (Group I)	5
Enzymes with similarity to TfdA (Group II)	7
Group III α -KG-dependent dioxygenases	10
Summary of α -KG-dependent dioxygenase sequence analyses	11
Biochemical and biophysical characterization of α -KG-dependent dioxygenases	12
Biochemistry of TfdA and related enzymes	12
Biochemical studies of other α -KG-dependent dioxygenases	16
Site-directed mutagenesis and chemical modification studies of α -KG-dependent dioxygenases	19
Spectroscopic experiments for metallocenter characterization of α -KG-dependent dioxygenases	21
Crystal structures of IPNS and DAOCS	23
Mechanism of α -KG-dependent dioxygenases	25
Degradation of 2,4-D and Ecology of TfdA	27
Overview of thesis	33
Literature cited	35
 CHAPTER 2 CHARACTERIZATION OF THE ACTIVE SITE OF 2,4- DICHLOROPHENOXYACETIC ACID/ α -KETOGLUTARATE DIOXYGENASE ..	 48
Introduction	49
Experimental Procedures	51
Recombinant Plasmids	51
Protein Purification	53
Analysis of Kinetic Parameters	54
Native Protein Analysis by Gel Filtration	55
Spectroscopic Analysis	55
Results	56
Production of the mutant TfdAs	56
Kinetic analyses of altered TfdAs	57
Evaluation of the Structural Consequences of the Mutations	58
EPR Spectroscopic Characterization of Variants with Altered Metal Sites	59

ESEEM Spectroscopic Characterization of Variants with Altered Metal Sites.....	65
Discussion.....	74
Literature Cited.....	81
CHAPTER 3 CLONING AND CHARACTERIZATION OF A SULFONATE/ α -	
KETOGLUTARATE DIOXYGENASE FROM <i>Saccharomyces cerevisiae</i>	85
Introduction	86
Materials and Methods	87
Cloning and expression of YLL057c.	87
Production and purification of YLL057c gene product.	88
Characterization of MBP-dioxygenase fusion protein.	89
Studies with the YLL057c deletion mutant.....	89
Results and Discussion	90
Additional properties of <i>S. cerevisiae</i> sulfonate dioxygenase.....	95
Phenotype of <i>S. cerevisiae</i> YLL057c deletion mutant.....	95
Role of sulfonate/ α -KG dioxygenase in <i>S. cerevisiae</i>	97
Literature cited.....	98
CHAPTER 4 DISTRIBUTION OF <i>tfdA</i> IN THE ENVIRONMENT	100
Introduction	101
Materials and Methods	102
Bacterial strains	102
16S rDNA partial sequence analyses	103
PCR Amplification of the <i>tfdA</i> gene.....	103
Dot Blot of PCR products	104
Analysis of 2,4-D degradation and TfdA activity	105
Incorporation of radiolabel from ^{14}C -2,4-D	105
Results	106
Composition of the LTER collection	106
Identification of <i>tfdA</i> in LTER collection	107
2,4-D degradation by LTER isolates.....	110
Experiments to determine if the <i>tfdA</i> -like gene encodes a functional TfdA	110
Discussion.....	113
Acknowledgements.	116
Literature cited.....	117
CHAPTER 5 CONCLUSIONS AND FUTURE RESEARCH	121
Understanding the mechanism of α -KG-dependent dioxygenases.....	122
Biological significance and potential applications of α -KG-dependent	
dioxygenases	129
Role of TfdA in the environment	131
Literature cited	137

APPENDIX A AMINO ACID SEQUENCE ALIGNMENTS.....	142
Literature cited.....	151
APPENDIX B STEREOSPECIFIC DEGRADATION OF THE PHENOXY- PROPIONATE HERBICIDE MECPROP.....	152

LIST OF TABLES

Table 1. Characterized enzymes in the α -KG-dependent dioxygenase superfamily.....	4
Table 2. Conserved amino acids among subgroups within the α -KG-dependent dioxygenase superfamily.....	6
Table 3. Amino acid sequence comparisons between α -KG-dependent dioxygenases.....	8
Table 4. Sequences of mutagenic primers used to create altered <i>tfdA</i> genes	52
Table 5. Summary of the kinetic parameters for active TfdA variants.....	58
Table 6. Summary of the EPR spectral parameters for Cu(II)-substituted TfdA variants.....	63
Table 7. Sulfonate specificity and kinetic parameters for sulfonate/ α -KG dioxygenase.	93
Table 8. Distribution of isolates with <i>tfdA</i> among the different phylogenetic groups within the LTER collection.	112

LIST OF FIGURES

Figure 1. Substrates of Group II enzymes.	14
Figure 2. Oxyferryl mechanistic model for α -KG-dependent dioxygenases.....	26
Figure 3. Pathway for the degradation of 2,4-D by <i>Ralstonia eutropha</i> JMP134(pJP4)..	28
Figure 4. Restriction maps of the plasmids used in construction of <i>tfdA</i> mutants.....	52
Figure 5. X-band CW-EPR spectra of Cu(II)-substituted TfdA variants.	60
Figure 6. 3-Pulse ESEEM spectra of Cu-substituted wild-type TfdA with 2-histidine simulation data.	67
Figure 7. 3-Pulse ESEEM time-domain spectra of TfdA variants.....	69
Figure 8. Spectral simulation of ESEEM data for D115A-Cu-TfdA.....	70
Figure 9. Spectral simulation of ESEEM data for MBP-H167A-Cu-TfdA.....	71
Figure 10. 3-pulse ESEEM of D115A TfdA (4.2K).....	73
Figure 11. Model for the active site of TfdA.	79
Figure 12. Structures of substrates for <i>S. cerevisiae</i> sulfonate/ α -KG dioxygenase.....	91
Figure 13. Substrate concentration dependence of sulfonate/ α -KG dioxygenase activity.....	94
Figure 14. Role of YLL057c in the utilization of different sulfur sources.	96
Figure 15. 16S rDNA phylogeny of the LTER isolates.....	108
Figure 16. Hybridization of amplified products from LTER isolates to a digoxigenin- labeled fragment internal to the <i>tfdA</i> gene.	111
Figure 17. Comparison of the proposed reaction mechanisms for an α -KG-dependent hydroxylase and IPNS.....	125
Figure 18. Substrates of TfdA.....	132
Figure 19. Structures of the major intermonomeric linkages in lignin.	132

LIST OF FIGURES (CON'T)

Figure 20. Open reading frames adjacent to a putative α -KG-dependent dioxygenase in <i>Bordetella pertussis</i> . Genbank accession numbers are shown in parentheses.	134
Figure 21. Scheme for lignin degradation in <i>S. paucimobilis</i>	135
Figure 22. Alignment of Group II α -KG-dependent dioxygenases.....	143
Figure 23. Alignment of Group III α -KG-dependent dioxygenases	147
Figure 24. Alignment of complete and partial TfdA sequences	149

LIST OF SCHEMES

Scheme 1. Reaction catalyzed by TfdA.....	2
Scheme 2. Reactions catalyzed by IPNS, DAOCS and clavamate synthase.....	18
Scheme 3. Reaction mechanism of <i>S. cerevisiae</i> sulfonate/ α -KG dioxygenase.....	91

LIST OF EQUATIONS

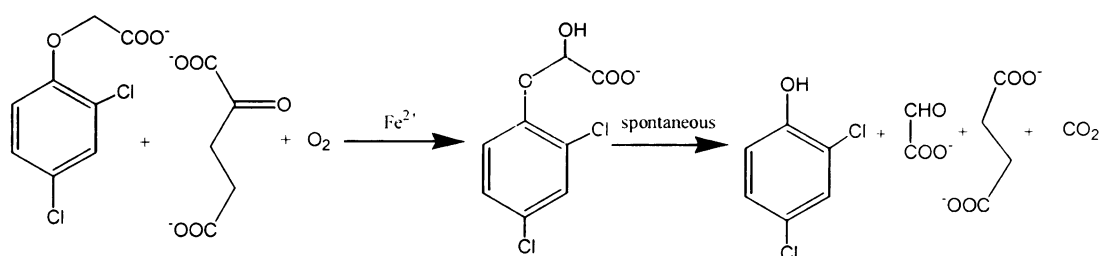
Equation 1 Equation for substrate inhibition	92
--	----

KEY TO ABBREVIATIONS

2,4-D	2,4-dichlorophenoxyacetic acid
3-CBA	3-chlorobenzoate
4-AAP	4-aminoantipyrene
4-HPPD	4-hydroxyphenylpyruvate dioxygenase
α -KG	α -ketoglutarate
ACC	aminocyclopropane carboxylate
ACV	L- α -amino- δ -adipoyl-L-cysteinyl-D-valine
DAOCS	deacetoxycephalosporin synthase
EDTA	ethylenediaminetetraacetic acid
EPR	electron paramagnetic resonance
ESEEM	electron spin-echo envelope modulation
GST	glutathione S-transferase
IPNS	isopenicillin <i>N</i> synthase
LTER	long-term ecological research
MBP	maltose binding protein
TfdA	2,4-D/ α -KG dioxygenase

CHAPTER 1
INTRODUCTION

2,4-Dichlorophenoxyacetic acid (2,4-D)/ α -ketoglutarate (α -KG) dioxygenase (TfdA) encodes the first enzyme in a well-characterized degradative pathway for the herbicide 2,4-D by bacteria (35). TfdA is a non-heme Fe(II)-dependent enzyme that couples the oxidative cleavage of α -KG, yielding CO₂ and succinate, to the decomposition of 2,4-D to form 2,4-dichlorophenol and glyoxalate (26) (Scheme 1). Based on its requirement for Fe(II) and its use of α -KG as a cosubstrate, TfdA is included in the α -KG-dependent-dioxygenase superfamily (90).



Scheme 1. Reaction catalyzed by TfdA.

In this introduction, I first compare the amino acid sequences of members of the α -KG-dependent dioxygenase superfamily to indicate relationships and differences between these enzymes. Next, I summarize previous research on TfdA and other biochemically characterized α -KG-dependent dioxygenases. Finally, I review studies on the occurrence of the *tfdA* gene, which encodes TfdA, in various 2,4-D degrading soil bacterial isolates and communities. The introductory chapter will conclude with an overview of the research presented in this dissertation.

α -KG-dependent dioxygenases are common in plants, animals, and the majority of aerobic microorganisms. Furthermore, data from recent genome sequence projects

suggest their presence in nematodes and insects (γ -butyrobetaine hydroxylase in *Caenorhabditis elegans*, Genbank # Z66523 and *Drosophila melanogaster*, Genbank # AL109630, respectively). Since 1967, when prolyl hydroxylase was characterized as the first α -KG-dependent dioxygenase (45), this class of enzymes has come to include more than forty members (Table 1). The reactions catalyzed by these enzymes range from steps in the synthesis of hormones (36, 91), antibiotics (58), collagen (54), and compatible solutes (30, 44) to the decomposition of pyrimidines (111, 115), amino acids (21) and other small molecules (21, 27, 40). In light of the diversity of substrates for α -KG dependent dioxygenases and the different types of oxidative reactions they catalyze, it is not surprising that their sequences exhibit little overall similarity.

Amino acid sequence analysis of α -KG-dependent dioxygenases

Although there is no overall sequence identity uniting all enzymes in the α -KG-dependent dioxygenase superfamily, comparison of their primary structures finds subgroups of related proteins. More than twenty distinct enzymes with significant levels of sequence identity to isopenicillin-*N*-synthase (IPNS) (Table 1) have been described (8, 58). The IPNS-like enzymes (Group I) include the majority of characterized α -KG-dependent dioxygenases. A second cluster of enzymes related by sequence (Group II) is comprised of TfdA, four previously characterized α -KG-dependent dioxygenases, and four putative enzymes yet to be studied. The Group II enzymes do not exhibit significant

Table 1. Characterized enzymes in the α -KG-dependent dioxygenase superfamily.

Enzyme	Source for purified enzyme	References
Group I IPNS-like enzymes		
Isopenicillin <i>N</i> synthase (IPNS) ^a	Fungi, Bacteria	(93)
Deacetoxycephalosporin C synthetase (DAOCS)	Fungi, Bacteria	(56)
Deacetylcephalosporin C synthase	Fungi, Bacteria	(102)
Aminocyclopropane carboxylate (ACC) oxidase ^a	Plant	(135)
Ethylene-forming enzyme	Bacteria	(83)
Deacetoxyvindoline 4-hydroxylase	Plant	(14)
Hyocyanine-6S-hydroxylase	Plant	(69)
Flavone synthase I	Plant	(9)
Flavanol synthase	Plant	(43)
Flavanone 3-hydroxylase	Plant	(10)
Leucoanthocyanidin hydroxylase	Plant	(99)
Gibberellin-2 β -hydroxylase	Plant	(37) for review
Gibberellin 3 β -hydroxylase	Plant	"
Gibberellin-7-oxidase	Plant	"
Gibberellin 13-oxidase	Plant	"
Gibberellin-20-oxidase	Plant	"
Procollagen Prolyl-4-Hydroxylase	Mammal, Bird, Virus	(54) for review, (23)
Procollagen Aspartyl Hydroxylase	Mammal	(55, 129)
Procollagen Lysyl Hydroxylase	Mammal	(74, 81, 89, 125)
Group II TfdA-like enzymes		
TfdA	Bacteria	(27)
Taurine/ α -KG dioxygenase (TauD)	Bacteria	(21)
Sulfonate/ α -KG dioxygenase	Fungi	(40)
Clavamate synthase (CS)	Bacteria	(11)
γ -Butyrobetaine hydroxylase	Bacteria, Mammal	(30, 62)
Group III		
Proline-4-Hydroxylase	Bacteria	(106)
Phytanoyl-CoA Hydroxylase	Mammal	(46)
Miscellaneous		
Thymine hydroxylase ^b	Fungi	(115)
Pyrimidine-deoxynucleoside-1-dioxygenase ^b	Fungi	(111)
Trimethyl-lysine dioxygenase ^b	Mammal	(44)
Proline 3-hydroxylase ^c	Bacteria	(77)

^a Enzyme does not use α -KG as a cosubstrate

^b No sequence is available for this enzyme

^c Enzyme does not have any sequence identity to other characterized enzymes



similarity to IPNS and other Group I enzymes. Group III contains four enzymes that, despite their very disparate substrates, have obvious sequence relatedness. Future studies on the structure and activity of enzymes in this class may uncover a relationship between Group III and either of the other two groups of α -KG-dependent dioxygenases; at present, however, sequence comparisons predict that they form a distinct cluster. Table 2 summarizes the elements common to the enzymes in each group. Finally, a fourth group contains α -KG-dependent dioxygenases that either exhibit no sequence similarity to enzymes in the other three classes or their amino acid sequence is not yet published.

IPNS-like α -KG-dependent dioxygenases (Group I)

IPNS is an Fe(II)-dependent enzyme that converts L- α -amino- δ -adipoyl-L-cysteiny-D-valine (ACV) to isopenicillin *N* (Scheme 2) with chemistry that is similar to the mechanism of α -KG-dependent dioxygenases (although α -KG is not used as a co-substrate). IPNS has between 25 and 35% amino acid identity to over twenty enzymes involved in antibiotic synthesis (58) and the formation of plant hormones (91). For comparison, sequences for the same enzyme from different plant genera have, on average, more than 60% amino acid identity. Alignment of Group I sequences indicates that a His-X-Asp-X₅₅-His motif is found in all of these enzymes (8) (Table 2 A). Crystal structures of IPNS (94) and the related enzyme deacetoxycephalosporin C synthase (DAOCS) (122) supported biophysical studies that predicted these residues to be ligands to the iron metallocenter. These same structures, combined with further sequence comparisons (58, 63), reveal a conserved Arg-X-Ser arrangement involved in α -KG binding in Group I enzymes.

A. Group I

	H D	X	H R/K S
IPNS	DHLDVSMITV	47	HRV KFINAERLS
DAOCS	PHYDLSMVTI	52	HHVAAPRRDQIAGSSRTS
FL3H	RHTDPGTILL	50	HQA VVNGESSRLS
VanB	AHTDFDCLTL	65	HRV . KNPADHEYQGARYS
P4H	PHFDFAKDE	63	HAA CPVLVGKQVVS
LysH	PHHDASTFTI	44	HEG LPTTKGTRYIAVS

B. Group II

	H D	X	DN H	X	R
TfdA	WHSDSSFQ	147	WNVGDLVMWDNRCVLH	10	R
TauD	WHTDVTFI	153	WQPNDAIWDNRVTQH	10	R
YSD	WHTDVVSF	147	WEPHSVVIWDNRVRQH	11	R
AtsK	WHTDVTFV	134	WEAGDVAIWDNRATQH	10	R
PvcB	LHWGMYL	147	WRSDDLVIADNLTLLH	10	R
CarC	FHADGGLL	148	WEDGDLIMDNRRVIH	11	R
SyrI	YHNESSHL	192	WRKGDVVMLDNMLAAH	8	R
γ -BBH	LHTDLPTR	139	LEAGQLWCDFNRRVLH	11	R
CS	FHTEMAYH	123	LEPGDLLIVDNFRTH	11	K X R

C. Group III

	H D	X	PG H	X	H N R
Pro4H	WHQDYIF	34	VPGETH	65	HGSGTNMSPHPR
HtxA	WHQDWAF	30	LPGETH	52	HGSGPNHSTIRR
PPHYH	LHQDLHY	31	LPGETH	51	HGSGQNKTQGFR
MmcH	LHADQTF	33	VPGETH	36	HQTGANTTDRPR

Table 2. Conserved amino acids among subgroups within the α -KG-dependent dioxygenase superfamily.

Amino acids in common among the IPNS-like α -KG-dependent dioxygenases (A), the TfdA-like enzymes (B) and the proline 4-hydroxylase group (C) in the α -KG-dependent dioxygenase superfamily are shown. The numbers in columns labeled “X” represent the number of amino acids intervening between the conserved regions. The unique identifiers for the protein sequences in Group I are IPNS, isopenicillin N synthase (IPNS_STRJU); DAOCS, Deacetoxycephalosporin synthase (pir2:A39204); FL3H, Flavanone 3-hydroxylase (SW:FL3H_HORVU); VanB, vanillate biosynthesis enzyme B (AF009673); P4H, human prolyl 4-hydroxylase (P13674); LysH, human lysyl hydroxylase (Q02809). The sequences in Group II are TfdA, 2,4-D/ α -KG dioxygenase (M16730); TauD, taurine/ α -KG dioxygenase (P37610); YSD, *S. cerevisiae* sulfonate/ α -KG dioxygenase (Q12358); AtsK, putative α -KG dioxygenase from sulfate-ester transport gene cluster (AF126201) PvcB, pyoverdine biosynthesis enzyme (AF002222); CarC, carbapenem biosynthesis enzyme C (AAD38231); SyrI, syringomycin biosynthesis enzyme I (AAB63253); γ -BBH, γ -butyrobetaine hydroxylase (P80193); CS, clavaminic synthase (A44241). Group III sequences are Pro4H, proline 4-hydroxylase (D78338); HtxA, putative hypophosphite/ α -KG dioxygenase (AF023463); PPHYH, Phytanoyl-CoA hydroxylase (NP_006205); MmcH, mitomycin C biosynthesis protein (AF127374).

Several enzymes involved in the hydroxylation of peptidyl amino acids are grouped together by activity and placed into Group I based on the presence of the above motif. Although these key active site residues are maintained in prolyl-4-hydroxylase (15, 23), lysyl hydroxylase (74, 81, 125), and aspartyl hydroxylase (47), their sequences lack detectable levels of similarity to other Group I enzymes. The importance of the amino acids in the above motif for activity has been confirmed by mutagenesis studies (described below). 4-Hydroxyphenylpyruvate dioxygenase (4-HPPD) is an Fe(II)-dependent enzyme that catalyzes ring hydroxylation concomitant with decarboxylation of the α -keto acid side chain. Mechanistic similarities in addition to seeming conservation of the above motif prompted inclusion of 4-HPPD with Group I enzymes of α -KG dependent dioxygenase superfamily. Upon introduction of less related 4-HPPD sequences into alignments, the H-X-D motif was no longer absolutely conserved, casting doubt on the relationship of this enzyme to the α -KG-dependent dioxygenases. A recently released crystal structure of 4-HPPD indicates a protein fold more similar to that of extradiol (ring-cleaving) dioxygenases than IPNS and DAOCS.

Enzymes with similarity to TfdA (Group II)

As recently as 1995, no enzymes with significant sequence similarity to TfdA were known. Over the past five years, however, multiple TfdA homologs have been identified due to the dramatic increase in genome sequence data and the development of more powerful sequence analysis tools, such as BLASTP (1) and Position-Specific Iterative (PSI)-BLAST (2). Now, it is apparent that TfdA is related to four characterized

	γ -BBH CE	γ -BBH	PvcB	CS2	CS1	YSD	SyrB1	AtsK	CarC	TauD	TfdA
γ -BBH CE	-	31/383	23/180	22/159	21/159	22/171	25/147	13/243	16/222	15/236	16/159
γ -BBH		-	21/206	22/280	25/179	14/167	15/266	14/265	17/258	20/160	15/221
PvcB			-	24/87	14/177	17/252	19/323	20/269	17/251	22/177	27/176
CS2				-	81/320	14/180	28/66	15/318	18/268	25/54	14/189
CS1					-	14/182	28/66	16/231	20/184	25/54	15/179
YSD						-	18/300	28/295	18/171	31/291	28/262
SyrB1							-	22/324	14/318	17/288	17/286
AtsK								-		38/279	29/270
CarC									-	15/298	28/156
TauD										-	29/285
TfdA											-

Table 3. Amino acid sequence comparisons between α -KG-dependent dioxygenases.

Both percent identity (first number) and the length of sequence over which the sequence this level of identity was found (second number) are presented. Sequence comparisons were performed by either BLASTP analysis or PSI-BLAST analysis. The algorithm for creating an optimal alignment is the same in each technique. The percent identities and length of homologous regions change slightly depending on which enzyme is used as the query sequence. The sequences used above are γ -BBH, γ -butyrobetaine hydroxylase from *Pseudomonas* sp. (P80193); γ -BBH CE, γ -butyrobetaine hydroxylase from *Caenorhabditis elegans* (Z66523); PvcB, pyoverdine biosynthesis enzyme (AF002222); CS2, clavamate synthase 2 (L06214); CS1, clavamate synthase (A44241); YSD, *S. cerevisiae* sulfonate/ α -KG dioxygenase (Q12358); Syr1, syringomycin biosynthesis enzyme I (AAB63253); AtsK, putative α -KG dioxygenase

α -KG-dependent dioxygenases and to sequences of several putative α -KG-dependent dioxygenases. Amino acid sequence identities from pairwise comparisons range from fifteen to forty percent (Table 3).

TfdA is most closely related to taurine/ α -KG dioxygenase (TauD) (21), *Saccharomyces cerevisiae* sulfonate/ α -KG dioxygenase (YSD) (40) and three putative α -KG-dependent dioxygenases: PvcB, involved in synthesis of the siderophore pyoverdine (109), CarC, which is necessary for formation of the β -lactamase inhibitor carbapenem (72), and AtsK, a putative dioxygenase in a sulfate-ester degradation gene cluster in *Pseudomonas putida* (127). Although they have not been biochemically characterized, the roles of PvcB, CarC and AtsK were identified through various transposon mutagenesis studies. The relationships between these six sequences are detected by a standard BLASTP analysis. More sensitive analyses with PSI-BLAST find relationships between TfdA and more distantly related α -KG-dependent dioxygenases. PSI-BLAST detects lower levels of relatedness by creating a position-specific matrix of conserved amino acids to rescore and realign sequences that receive low BLAST scores. As this process is repeated, unrelated sequences with chance high scores are downgraded as the matrix of positionally-conserved amino acids improves. By these methods, relationships between TfdA and two other well-characterized α -KG-dependent dioxygenases, γ -butyrobetaine hydroxylase and clavamate synthase (Table 3), become evident. In addition, the sequence of a third enzyme, SyrB, which is required for synthesis of syringomycin, also aligns with the TfdA-like sequences. Of the twenty nine sequences identified as relatives of TfdA after six iterations of PSI-BLAST, all were either

previously characterized α -KG dependent dioxygenases or hypothetical proteins with the characteristic conserved amino acids described below.

Comparison of all nine Group II α -KG-dependent dioxygenase sequences finds several strictly conserved residues (Table 2B, Appendix A). As in the Group I enzymes, an H-X-D-like motif is present in all sequences, although in both clavamate synthase and SyrB, the aspartate is replaced by a chemically-equivalent glutamate residue. A stretch of amino acids near the C-terminus with high levels of similarity across these sequences, contains the only other invariant histidine, suggesting that this residue may be analogous to the third metal ligand in the Group I motif described above. Conserved asparagine and arginine residues near this histidine are also apparent and the latter may play a role similar to the α -KG-binding arginine in IPNS and DAOCS.

Group III α -KG-dependent dioxygenases

A third group within the α -KG-dependent dioxygenase superfamily contains two characterized enzymes, proline 4-hydroxylase (73) and phytanoyl-CoA hydroxylase (46), and two putative α -KG-dioxygenases, hypophosphite oxidase (HtxA) (73) and MmcH which is involved in mitomycin C biosynthesis (67). Although no homology is detected between these sequences and either Group I or Group II α -KG-dependent dioxygenases by BLAST comparisons, the motif common to this group is clearly similar to those described above (Table 2C). Again, there is a conserved H-X-D motif and two additional invariant histidines in this small set of sequences (Appendix A) and in uncharacterized homologs in other bacteria (120). A His-X₁₀-R motif (similar to Group I and Group II enzymes) identifies a good candidate for the third metal ligand; however, biochemical

studies or structural information is needed to establish the roles of these residues. In humans, non-functional phytanoyl-CoA hydroxylase results in Refsum disease due to the inability to break down phytanic acid (3,7,11,15-tetramethylhexadecanoic acid), a degradation product of chlorophyll (12). It is interesting to note that two of the disease-causing alleles of phytanoyl-CoA hydroxylase, which encode inactive enzyme, have mutations of either the conserved arginine or an invariant asparagine nearby.

Summary of α -KG-dependent dioxygenase sequence analyses

Sequence comparisons of members of the α -KG-dependent dioxygenase superfamily find three distinct subgroups of related enzymes; no overall sequence identity was detected between enzymes from different subgroups. Comparison of more closely related sequences allows for the identification of potentially important, conserved residues. The consensus motifs for the three subgroups are similar (an H-X-D motif distant from an H-X₁₀-R arrangement) and likely identify residues important for active site structure. As the number of α -KG-dependent dioxygenase sequences grows, the three groups may merge into a continuum of sequences. Alternatively, as other sequences are found, distinctions between the groups may be maintained. Differences in the arrangement of the conserved residues across the superfamily may be indicative of the mechanisms that drove the divergent evolution of these enzymes.

Biochemical and biophysical characterization of α -KG-dependent dioxygenases

Biochemistry of TfdA and related enzymes

TfdA was detected in a 2,4-D-degrading *Arthrobacter* sp. in 1967 (116). Preliminary studies on the degradation of ^{18}O -ether-labeled 2,4-D found the products to be ^{18}O -2,4-dichlorophenol and glyoxalate. Thus, it was proposed that the 2,4-D decomposition proceeds through a hemiacetal intermediate that spontaneously breaks down to yield the reaction products (Scheme 1). Almost twenty-five years later, the mechanism of purified TfdA was examined (27), proving this enzyme to be an α -KG-dependent dioxygenase.

Various characteristics of recombinant TfdA, purified from *E. coli* cells containing the *Ralstonia eutropha* JMP134 *tfdA* gene, have been elucidated over the past five years. TfdA, with a predicted subunit molecular weight of 31.7 kDa has an apparent molecular weight of 50 ± 2.5 kDa by gel filtration chromatography suggesting that the native protein exists as a homodimer. The high affinity for α -KG is demonstrated by a K_m of 3.2 ± 0.54 μM . Several different α -keto-acids, including α -ketoadipate and pyruvate, are less efficient substitutes for α -KG as the cosubstrate. The k_{cat} and K_m for 2,4-D are 529 ± 16 min^{-1} and 17.5 μM , respectively. 2,4-D can be replaced with other aromatic compounds such as phenoxyacetic acids (27), substituted cinnamic acids, naphthoxyacetic acid and benzofurancarboxylic acid (R. Padmakumar and J. Hotopp, unpublished data). TfdA enzymes from both *R. eutropha* JMP134 and *Burkholderia cepacia* RASC (112) selectively abstract the pro-R hydrogen atom from the prochiral side-chain carbon adjacent to the ether bond of 2,4-D (98). Interestingly, there is evidence

of a TfdA-like α -KG-dependent dioxygenase that has the opposite stereoselectivity from the TfdAs described above (98, 114), however, this enzyme has not been cloned or characterized (Appendix B). Distinct α -KG-dependent dioxygenases in *Sphingomonas herbicidovorans* act on each enantiomer of mecoprop ((*R,S*)-2-(4-chloro-2-methylphenoxy)-propionic acid), a chiral analog of 2,4-D (84).

Three characterized enzymes with similarity to TfdA include TauD, which releases sulfite from taurine, γ -butyrobetaine hydroxylase, which is responsible for the final step in carnitine biosynthesis, and clavamate synthase, which catalyzes three distinct transformations in the biosynthesis of the β -lactamase inhibitor clavulanic acid. The diverse substrates of these enzymes are compared in Figure 1. While all four enzymes have approximately the same apparent K_D for iron, other kinetic parameters vary significantly. The K_m for α -KG ranges from 3 μ M for TfdA to 260 μ M for clavamate synthase. TfdA and TauD are the only enzymes that can substitute other α -keto acids for α -KG. The k_{cat}/K_m ($\text{min}^{-1} \mu\text{M}^{-1}$) is 31.1, 2.0, 0.3, 0.013 for TfdA, TauD, γ -butyrobetaine hydroxylase, and clavamate synthase, respectively. The wide range of catalytic efficiencies likely reflects the diversity of substrates. In each case, the hydroxylated carbon is one or two carbons away from either a carboxylate or sulfonate group indicating that a positively charged amino acid might be involved in substrate binding. The pro-R hydrogens abstracted by γ -butyrobetaine hydroxylase (22) and clavamate synthase (5) are in similar relative positions to the carboxylate moiety, which is two carbons away from the hydroxylation site. The pro-S hydrogen removed by TfdA (98) is in the opposite position with respect to the carboxylate. The stereochemistry of TauD catalysis has not been examined.

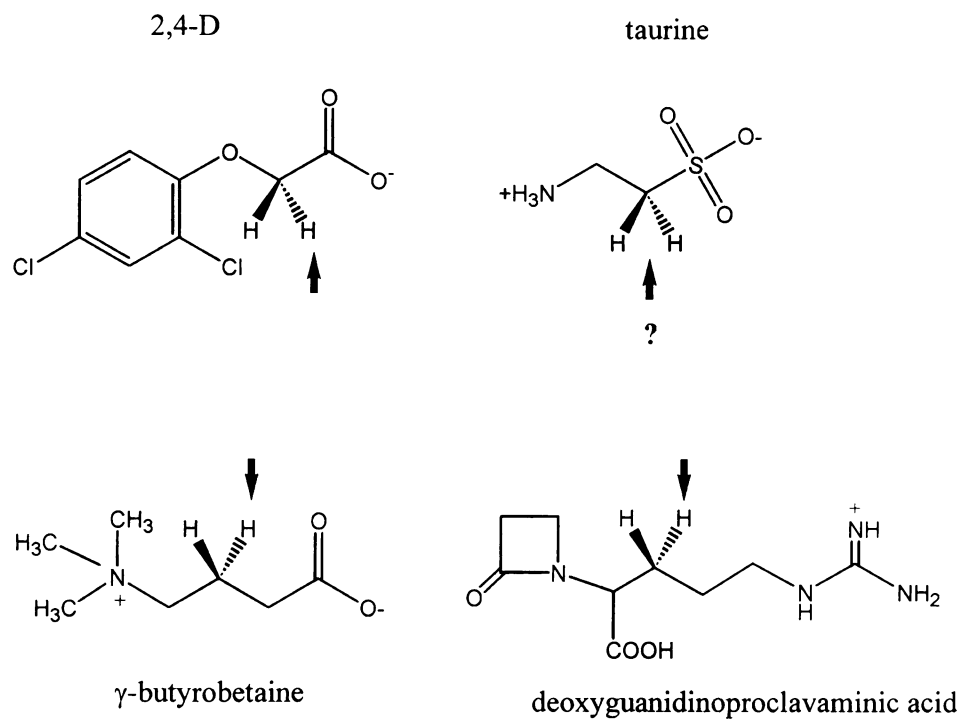


Figure 1. Substrates of TfdA-like enzymes

Structures of substrates for TfdA, TauD, γ -butyrobetaine hydroxylase, and clavamate synthase are compared. The abstracted proton is indicated by an arrow.

For maximal activity, many α -KG-dependent dioxygenases require ascorbate to reduce the iron after non-productive decarboxylation of α -KG that is uncoupled from oxidation of substrate. Although TfdA activity is stimulated by the presence of ascorbate in the reaction mix (27), TfdA does not appear to undergo uncoupled turnover of α -KG in the absence of substrate. Even with the addition of ascorbate, TfdA is inactivated in a matter of minutes in the presence of iron under oxic conditions. Inactivation of TfdA appears to occur by both turnover-dependent and a turnover-independent mechanisms (97). TauD activity is also stimulated by 50% in the presence of ascorbate at concentrations over 200 μ M. γ -Butyrobetaine hydroxylase activity is stimulated six-fold by the addition of 100 μ M potassium ions; the K_m for both substrates is also reduced in the presence of potassium (130). Without potassium present, γ -butyrobetaine hydroxylase performs the uncoupled decarboxylation of α -KG. Higher rates of uncoupling are achieved by the addition of product and its enantiomer (42). Clavamate synthase also catalyzes the uncoupled decarboxylation of α -KG, but the rate is greatly reduced (1 in 890 turnovers) in the presence of substrate (60).

Beyond the differences in kinetic parameters and activity towards α -KG in the absence of substrate, other characteristics of these enzymes can be compared. All four enzymes have a pH optimum of 6.5-7. TauD (subunit size of 37.4 kDa) and γ -butyrobetaine hydroxylase, (43 kDa) both exist as homodimers (21, 62). In contrast, gel filtration chromatography of clavamate synthase gives an estimated mass of 36 kDa indicating that the enzyme is not multimeric. Clavamate synthase is unique in that it catalyzes hydroxylation, desaturation, and cyclization reactions (Scheme 2), all coupled to α -KG decarboxylation, at the same active site (11, 60). Kinetic studies suggest that

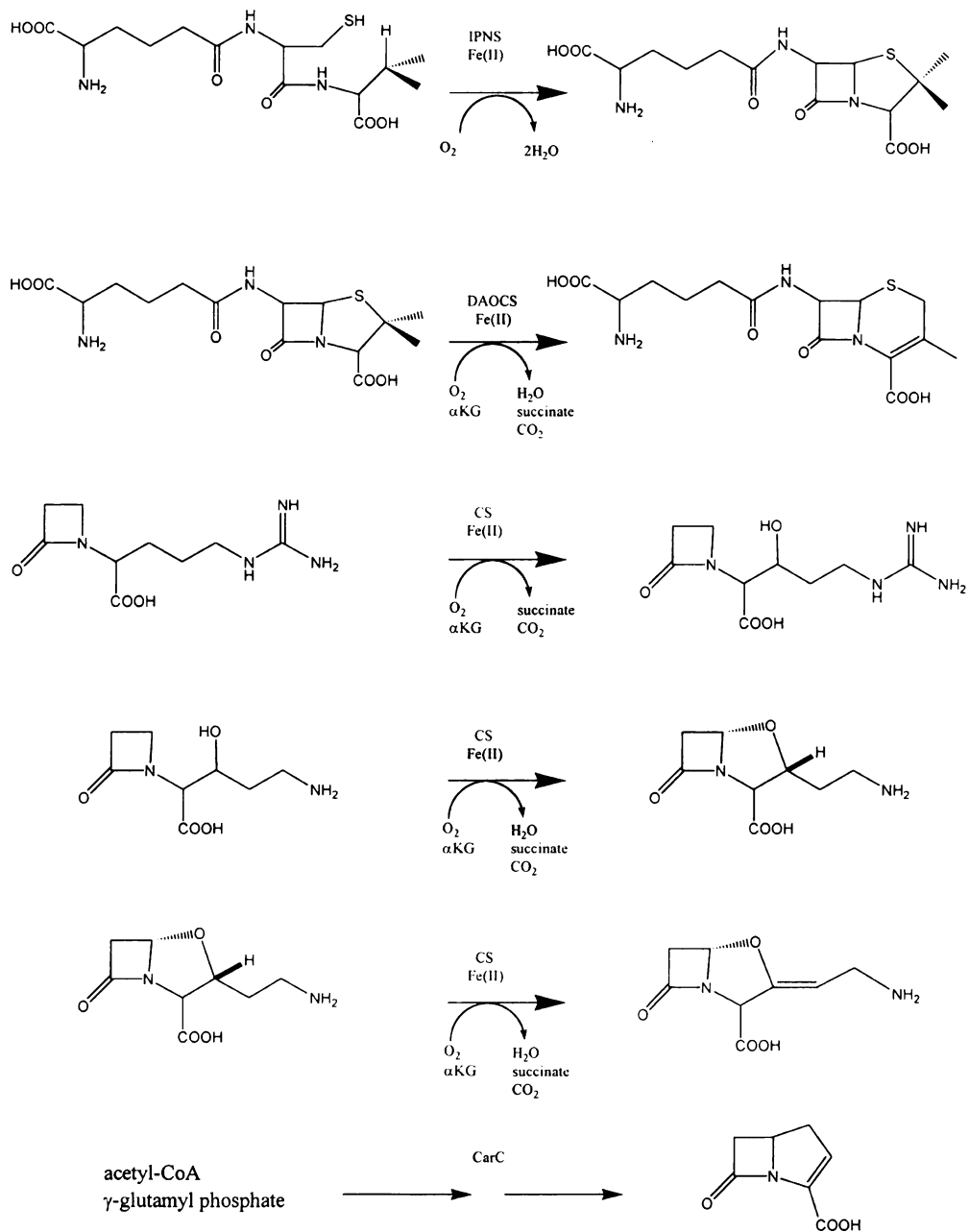
there is no release of the substrate between the desaturation and cyclization reaction. It is interesting to recognize the similarities between the substrates of clavamate synthase and those of IPNS and DAOCS. Despite a lack of sequence similarity, and all three enzymes participate in the synthesis of β -lactam antibiotics. In addition, a poorly characterized enzyme, CarC, which shows high levels of identity to TfdA over the entire sequence, is involved in formation of carbapenem, another β -lactam-containing compound (Scheme 2).

Biochemical studies of other α -KG-dependent dioxygenases

There is significant diversity in the subunit size and quaternary structure within the α -KG-dependent dioxygenase superfamily. Among the enzymes related to IPNS, most are between 38 and 45 kDa (similar in size to TfdA-like enzymes) and many (flavone synthase (9), gibberellin 3 β -hydroxylase (37), gibberellin 20-oxidase (100), hyoscyamine (34)), but not all (flavanone 3-hydroxylase (10), ACC oxidase (49), thymine hydroxylase (115)), of the enzymes in this subgroup exist in a monomeric state. Crystal structure information suggests that apo-DAOCS exists as a trimer but dissociates to a monomer upon metal binding (122). The three mammalian enzymes involved in collagen maturation, aspartyl hydroxylase, lysyl hydroxylase and prolyl hydroxylase, show additional differences from other α -KG-dependent dioxygenases. Aspartyl hydroxylase has a subunit size of 85 kDa, but a 52 kDa catalytic domain still has full catalytic activity (47). Lysyl hydroxylase has been identified as an 87 kDa monomer in chick embryos and bovine skin, and a dimer of 70 and 110 kDa subunits in porcine skin. Prolyl hydroxylase, with a subunit size of 61 kDa, forms an $\alpha_2\beta_2$ heterodimer in

mammals and an $\alpha\beta$ dimer in *C. elegans* (54). In both cases, the β subunit is protein disulfide isomerase. In all three enzymes, the C-terminal catalytic domain appears to be linked to a separate N-terminal region involved in cellular localization (52). Furthermore, a recently discovered prolyl 4-hydroxylase from *Paramecium bursaria* Chovella virus-1, an algal virus, that is 20% identical to the C-terminus of mammalian prolyl 4-hydroxylase lacks the N-terminal localization domain; thus, its subunit size is closer to that of bacterial and fungal α -KG-dependent dioxygenases (23).

Almost all α -KG-dependent dioxygenases have an apparent K_D for iron of approximately 2 μ M. The K_m for α -KG ranges from 5 μ M to between 140 μ M for different enzymes. The K_m for O_2 has been determined to be 30-40 μ M for prolyl hydroxylase (82), 60 μ M for thymine hydroxylase (41), and 45 μ M for desacetoxyvindoline 4-hydroxylase (14). Not surprisingly, the measured K_m values for the unique substrates vary from nanomolar to near millimolar concentrations. Substrate interaction kinetics and product inhibition studies in four α -KG-dependent dioxygenases, desacetoxyvindoline 4-hydroxylase (14), prolyl hydroxylase (82), lysyl hydroxylase (92), and thymine hydroxylase (41), all indicate an ordered *ter-ter* mechanism for substrate binding. Competitive inhibition studies indicated that in three of the four enzymes, α -KG binds first, followed by the appropriate substrate, then O_2 . In prolyl hydroxylase, the order of O_2 and substrate binding are reversed (82). The oxidized product, CO_2 , and succinate are then released sequentially in that order. The unproductive decarboxylation of α -KG in the absence of substrates provides additional evidence that α -KG can bind without the substrate present.



Scheme 2. Reactions catalyzed by IPNS, DAOCS, clavamate synthase and CarC.

Although in TfdA and related enzymes α -KG decarboxylation is relatively tightly coupled to substrate oxidation, prolyl 4-hydroxylase and lysyl hydroxylase (80) have a near absolute requirement for ascorbate. Early spectroscopic studies with Fe(II)-prolyl hydroxylase demonstrated that ascorbate serves to reduce the iron metallocenter which becomes oxidized to an Fe(III) form upon brief incubation with α -KG. Ascorbate is consumed stoichiometrically with respect to uncoupled decarboxylation (80). Catalysis is not as dependent on the presence of ascorbate in bacterial proline hydroxylases (78). Studies with analogs of α -KG and ascorbate suggest that both occupy a similar or overlapping site in prolyl 4-hydroxylase and both compounds chelate the metal (65).

In addition to IPNS, aminocyclopropane carboxylate (ACC) oxidase does not require α -KG for activity. ACC oxidase, responsible for the generation of ethylene in plants, requires Fe(II) and CO₂ (49). The role for CO₂ has yet to be determined, but it has been suggested that bicarbonate, a carbamylated lysine, or CO₂ itself may ligate the iron (49). Stoichiometric amounts of ascorbate are consumed during the course of the reaction, perhaps suggesting that ascorbate replaces α -KG.

Site-directed mutagenesis and chemical modification studies of α -KG-dependent dioxygenases

Mutagenesis studies of several enzymes within Group I of the α -KG-dependent dioxygenase superfamily have confirmed the importance of the conserved residues (H-X-D-X₅₅-H-X₁₀-R). In IPNS, replacement of His 214, Asp 216 or His 272 with leucine completely inactivates the enzyme (113). The crystal structure of IPNS proves these residues to be metallocenter ligands (94, 95). Although a fourth metal ligand, Gln 330, is

evident in the substrate-free structure, this residue is neither conserved nor critical for activity (101). The importance of the corresponding residues in flavanone 3 β -hydroxylase, which is 23% identical to IPNS over the entire sequence, has also been demonstrated (63). Alteration of His 220 or Asp 222 to glutamine causes a greater than 99% loss of activity but the resultant enzymes only show a modest increase in the apparent K_D for iron. Mutation of His 278 to glutamine completely abolished activity, and mutation of a conserved Arg in position 288 to lysine or glutamine corresponded to decreased affinity for α -KG (63).

Additional studies have been carried out with the enzymes that hydroxylate peptidyl substrates. Mutation of His 656, Asp 658, and His 708 rendered lysyl hydroxylase inactive (88). Likewise, alteration of the second conserved histidine in aspartate hydroxylase (His 675) completely abolishes activity (70) and appears to cause a decrease in metal and α -KG binding (47). Replacement of His 675 in aspartate hydroxylase with iron-binding amino acids restores partial activity (70). In prolyl hydroxylase, alteration His412, Asp 416, His483 and Lys493 in the human-derived enzyme had significant effects on activity. Prolyl hydroxylase variants in which either of the histidines was mutated were inactive regardless of the substitution (59). Chemically-equivalent substitutions of remaining conserved residues, Glu for Asp 414 and Arg for Lys 493, cause an increase in the K_m for iron and α -KG, respectively. Mutation of a fourth histidine in prolyl hydroxylase, His 501, leads to a 95% loss of activity, a small increase in K_m for α -KG, and an increase in the rate of uncoupled α -KG decarboxylation suggesting that this residue is also present at or near the active site (79).

Together, these studies conclusively show the importance of histidines and carboxylates in the creation of the reactive metallocenter of α -KG-dependent dioxygenases. In most enzymes, no alternative amino acids (Arg, Asp, Glu, Gln, Ala) can substitute for a metal-binding histidine, although in certain instances, low levels of activity can be seen with a His to Gln substitution. Alteration of the conserved aspartate to even the very similar glutamate cannot always retain activity, yet in clavaminic synthase and the sequence of SyrB, glutamate replaces aspartate in the metal binding motif. In the cases presented above, the conserved residues are identified through sequence comparisons to IPNS and related enzymes. To date, no mutagenesis studies on enzymes without similarity to IPNS have been published.

Spectroscopic experiments for metallocenter characterization of α -KG-dependent dioxygenases

Early insight into the metallocenter structure of enzymes in the α -KG-dependent dioxygenase superfamily came from spectroscopic studies of IPNS. Electron paramagnetic resonance (EPR) spectra of inactive Cu(II)- and Co(II)-substituted IPNS, used to model the EPR silent Fe(II) form of the enzyme, are characteristic of a five- or six-coordinate tetragonally distorted site (75). Electron spin-echo envelope modulation (ESEEM) spectroscopic data are indicative of two equatorial histidines to the Cu(II) form of the enzyme, one of which is displaced upon substrate binding (48). Extended X-ray absorption fine structure (EXAFS) (105) spectroscopy demonstrates the presence of a thiolate ligand to the metal upon substrate binding. Site-directed mutagenesis of cysteine



residues ruled out a potential role for endogenous S-containing ligands thus indicating that the metal-bound sulfur is derived from substrate (85).

Spectroscopic studies of three Group II α -KG-dependent-dioxygenases, clavamate synthase, TfdA and TauD, demonstrate common features among these three enzymes as well as similarity to IPNS. Again, initial EPR characterization was performed on the inactive Cu(II)-substituted form of the enzyme. Structural information on the Cu(II)-metallocenter is likely relevant to the Fe(II) conformation as Cu(II) binds competitively with respect to iron with an approximate K_i of 1-3 μ M (131). Later studies, using Fe(II)- nitric oxide (NO) complexes to derive an EPR signal, were also performed on TfdA (39). In the absence of substrates, EPR spectra of both Fe(II) and Cu(II)-substituted TfdA indicate the presence of two histidines bound to the metal. ESEEM studies of Cu(II)-TfdA agree with the EPR data, and also identify three metal-bound waters in the remaining coordination sites. Addition of 2,4-D to the enzyme does not affect the coordination geometry, but binding of α -KG decreases the rhombicity of the metallocenter and displaces two solvent molecules indicating direct interaction between α -KG and the metal. ESEEM studies of the Cu(II)- α -KG-2,4-D TfdA ternary complex indicated the loss or shift of a histidine ligand from the equatorial plane. Studies with the Fe(II) TfdA are consistent with the rearrangement of ligands and loss of the third water upon substrate binding to give a five-coordinate metal center. Nitric oxide, which also serves as an oxygen analog, binds reversibly to Fe-TfdA and Fe- α -KG-TfdA complexes, but shows a greatly increased affinity for the metal when both substrates are present.

The interaction between α -KG and the metal was studied in detail using UV-visible, magnetic circular dichroism (MCD) and circular dichroism (CD) spectroscopies

with clavamate synthase. These techniques revealed that upon binding of α -KG to clavamate synthase, the six-coordinate geometry is distorted. The formation of a pink intermediate arising from ligand to metal charge transfer between α -KG and the iron indicates that α -KG binds to the metal through both the C-1 carboxylate and the C-2 keto group based on comparisons to model compounds (87). A similar mode for binding of α -KG to TfdA and TauD is predicted from the results of recent experiments (39, 96).

Crystal structures of IPNS and DAOCS

IPNS has been crystallized in the presence of Mn(II) and Fe(II) (94, 95). Both structures show that the metalcenter is ligated by His 214, Asp 216, His 270, and Gln 330. The active site is buried within the hydrophobic pocket of an eight-strand “jelly-roll” motif. In the Fe(II)-IPNS structure with substrate bound, Gln 330 and one water is displaced upon addition of the tripeptide substrate, ACV. In the Fe-ACV-IPNS complex, the iron is five-coordinate which agrees with the geometry observed in the spectroscopic experiments described above. Furthermore, nitric oxide binds to the open axial coordination site forming an octahedral complex as revealed by the crystallographic studies.

The crystal structure of DAOCS is the only published structure of an α -KG dependent dioxygenase. The anaerobic addition of Fe(II) to crystals of apo-DAOCS leads to only small structural changes. In DAOCS, ferrous ion is ligated by residues corresponding to the metal ligands in IPNS, and three water molecules. As predicted by the spectroscopic experiments described above, α -KG displaces two solvent molecules to chelate the iron. The C-1 carboxylate binds opposite to His 243 (the distal histidine of the

H-X-D-X₅₅-H motif) and the C-2 keto group binds *trans* to the metal-bound aspartate. The only accessible site, located in a hydrophobic pocket, is occupied by a solvent molecule.

The crystal structures of IPNS and DAOCS lend very strong support for the models of α -KG-dependent dioxygenase metallocenter structure as deduced from sequence alignments, site-directed mutagenesis studies, and spectroscopic experiments. Although the substrate-free configuration of the two metallocenters are similar, the differences in the chemistry performed by these two enzymes, particularly the use of α -KG as a co-substrate in DAOCS and not in IPNS, is reflected in the differences in ligands and coordination geometries upon substrate binding. There is no available structure of an α -KG-dependent dioxygenase that performs hydroxylation chemistry.

Crystal structures for two additional α -KG-dependent dioxygenases, clavamate synthase (Group II) and proline 4-hydroxylase (Group III) will soon accompany the structures of IPNS and DAOCS as described in a seminar by Prof. C. Schofield. Despite the distinct differences between the three groups of sequences, these enzymes appear to fold on a similar scaffold. This exciting finding will allow us to better assimilate the large amount of spectroscopic, stereochemical, and biochemical data into a universal model for enzymes in this superfamily. Within the subgroups, information from one crystal structure will greatly aid in the prediction of substrate binding residues and potential catalytic residues in other related enzymes.

A 2-His-1-carboxylate motif is also found in other non-heme, ferrous ion dependent enzymes such as lipoxygenase, extradiol dioxygenase, and pterin-dependent tyrosine hydroxylase (38). These three ligands anchor the iron in the active sites, and, as

demonstrated by site-directed mutagenesis studies, are clearly important for establishing the proper geometry and reactivity for interaction with substrates. Thus, the three remaining coordination sites provide the opportunity for substrates to interact directly with the iron to modulate activity.

Mechanism of α -KG-dependent dioxygenases

α -KG-dependent dioxygenases perform a wide range of oxidative reactions including hydroxylations, cyclizations, ring expansions and desaturations using α -KG as a reductant of diatomic oxygen. Despite the diversity of substrates and reactions, the initial catalytic steps likely proceed in a similar fashion in these disparate enzymes. Kinetic, spectroscopic, and structural data, in addition to mutagenesis data and the studies on the behavior of model compounds, have lent support to the Hanauske-Abel and Günzler model (33) that was proposed for prolyl hydroxylase. The expanded and updated catalytic model for this superfamily of enzymes predicts the generation of the ferryl-oxo species (Fe(IV)=O) via the oxidative decarboxylation of α -KG. A summary of the steps proposed in the oxyferryl mechanism for α -KG-dependent dioxygenases are summarized in Figure 2. The iron in the resting enzyme is bound by two histidines and one carboxylate with three waters occupying the open coordination sites. Spectroscopic studies indicate that α -KG displaces at least one water molecule upon binding to the metal through the C-1 carboxylate and C-2 keto groups. Chelation of the iron by α -KG alters the coordination geometry and redox environment sufficiently to induce binding of oxygen in an axial position. In some enzymes, the presence of substrates may be necessary for oxygen to bind to the metal. During the course of oxidative decarboxylation, one oxygen atom is incorporated into succinate, the other forming an

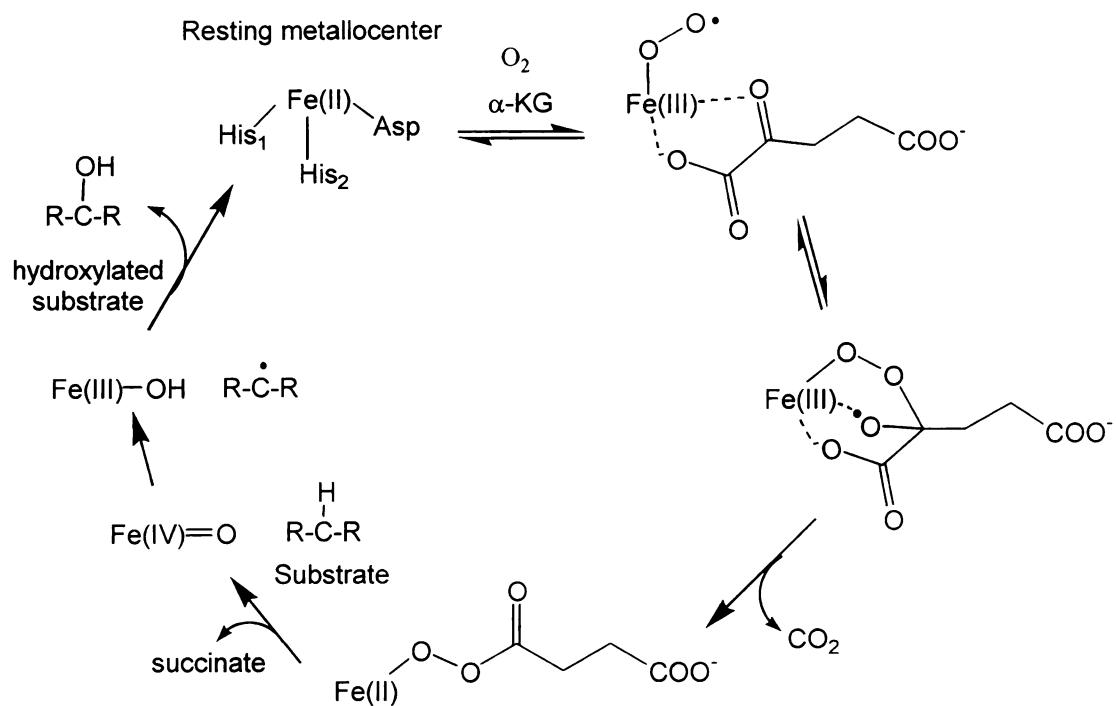


Figure 2. Oxyferryl mechanistic model for α -KG-dependent dioxygenases.

Fe(IV)-oxo species. In hydroxylation reactions (shown here), the reactive oxygen species abstracts a hydrogen atom from the substrate to yield a hydroxide radical that recombines with the substrate to give the final product. During cyclization, ring expansion, or desaturation reactions, the iron-bound oxo species is reduced by two electrons to water.

Degradation of 2,4-D and Ecology of TfdA

TfdA was initially characterized for its ability to degrade 2,4-D (110), one of the most commonly used herbicides in agriculture (121). Despite its widespread use, 2,4-D does not accumulate in the environment due to its rapid consumption by soil bacteria. The estimated half-life for 2,4-D in oxic soils is approximately seven days (132). Over the past few decades, researchers have been particularly interested the mechanism by which soil microorganisms come to exploit 2,4-D, a xenobiotic compound, as a source for carbon and energy.

The best characterized pathway for 2,4-D degradation is encoded by genes found on plasmid pJP4 isolated from *Ralstonia eutropha* (formerly *Alcaligenes eutrophus*) JMP134 (Figure 3) (17, 19). In this bacterium, 2,4-D is converted to 2,4-dichlorophenol which is then broken down by series of enzymes encoded by *tfdBCDEF* to form β -ketoadipate, a Kreb's cycle intermediate. A thorough review of the enzymes involved in 2,4-D degradation as well as an overview of other 2,4-D degradation pathways can be found in a recent chapter by Hausinger *et al.* (35) and will be only briefly summarized here. After TfdA catalyzes the initial transformation of 2,4-D, 2,4-dichlorophenol hydroxylase (TfdB) hydroxylates the aromatic ring to give dichlorocatechol. TfdB is a homotetramer with 63 kDa subunits and is similar in sequence and mechanism to

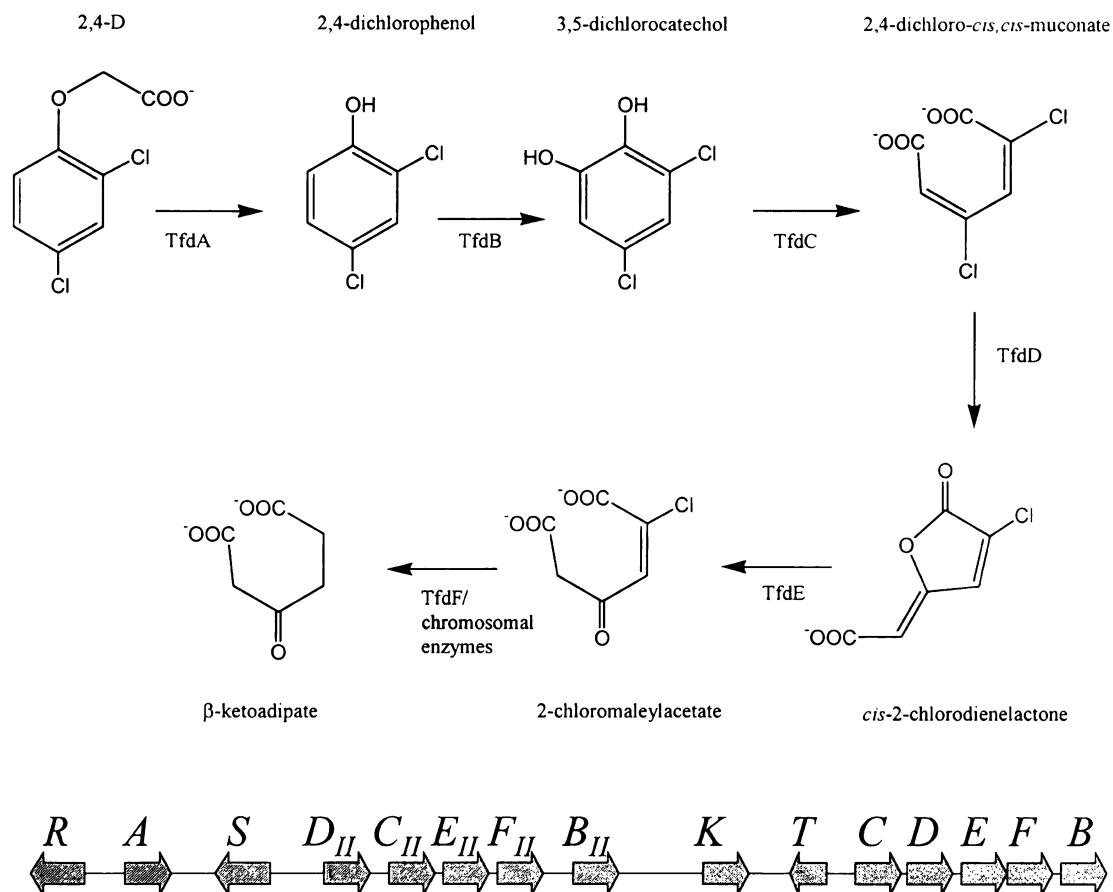


Figure 3. Pathway for the degradation of 2,4-D by *Ralstonia eutropha* JMP134(pJP4)

The enzymes involved in 2,4-D degradation include TfdA, 2,4-dichlorophenoxyacetic acid/α-KG dioxygenase; TfdB, 2,4-dichlorophenol hydroxylase; TfdC, 3,5-dichlorocatechol dioxygenase; TfdD, chloromuconate cycloisomerase; TfdE, dienelactone hydrolase; and TfdF, maleylacetate reductase. The region of the pJP4 plasmid encoding these enzymes is also shown. The *tfd* gene names in italics correspond to the enzymes defined above. *tfdK* encodes 2,4-D permease and *tfdR/S* encodes a LysR-type regulator of the *tfd* genes. The above figure is adapted from van der Meer et al. (126).

enzymes responsible for the hydroxylation of salicylate and other aromatics. Each subunit contains a molecule of FAD and activity is dependent on NAD(P)H as a cosubstrate. TfdC is an Fe(III)-dependent intradiol dioxygenase that converts 3,5-dichlorocatechol to 2,4-dichloro-*cis,cis*-muconate. The fourth enzyme involved in 2,4-D degradation, choromuconate isomerase, or TfdD, converts 2,4-dichloro-*cis,cis*-muconate to 2-chlorodienelactone which is then hydrolyzed to 2-chloromaleylacetate by dienelactone hydrolase or TfdE. The resultant chloromaleylacetate is then degraded by either a chromosomally-encoded maleylacetate reductase, which has been purified from *R. eutropha* JMP134, or by TfdF, an enzyme which, by sequence, appears to have the same activity. The genes encoding TfdC, TfdD, TfdE, and TfdF are cotranscribed and are highly similar to operons involved in the degradation of other chlorinated aromatic compounds such as chlorobenzoate and trichlorobenzene (126).

As shown in Figure 3, there are several other *tfd* genes associated with the 2,4-D degradative pathway in addition to the catabolic enzymes. The transcription of *tfdA* and the *tfdCDEFB* operon are regulated by a LysR-type regulator, TfdR/S, which activates transcription in response to the inducer 2,4-dichloro-*cis,cis*-muconate (24). There are two identical copies of the gene encoding TfdR/S. Recently, an energy-dependent protein that facilitates the uptake of 2,4-D, TfdK, was described and found to be similar to transporters for 4-hydroxybenzoate and other aromatic compounds (61). In addition, a second set of genes similar to *tfdCDEFB* and a truncated regulatory gene, *tfdT*, are located in between the two sets of *tfd* genes. Because the second set of *tfd* genes (*tfdD_{II}C_{II}E_{II}F_{II}B_{II}*) is not required for 2,4-D degradation, but is induced in the presence of

1

2,4-D, they may have resulted from a gene duplication or gene transfer event that failed to produce a functional 2,4-D degradation pathway (126).

Researchers have used the pJP4-encoded 2,4-D degradation pathway as a model to study the assembly of genes necessary to enable an organism to degrade a xenobiotic compound. Several features of the *tfd* operon, including the duplication of the regulatory element, a second copy of the *tfdCDEF* operon, and the presence of the ISJP4 insertion element sequences in *tfdT* and near *tfdS*, suggest recent evolution of the 2,4-D degradation cassette. The data presented below provide additional evidence that the necessary genes are widespread in environmental bacteria and that they have been assembled multiple times to enable single organisms to degrade 2,4-D.

Enrichments from soils ((86) and references therein), aquifers and water samples (3) readily degrade 2,4-D, although often only after an acclimation period (29, 103, 107). Soulas (107) modeled the dynamics the 2,4-D degradation as the result of competition between two populations with different 2,4-D degradation rates. In this simulation, the acclimation period reflects the time required for competitive 2,4-D degraders to achieve dominance. In support of this theory, phylogenetically diverse 2,4-D degrading isolates were obtained by directly plating soil bacteria onto 2,4-D-containing medium, but the diversity of 2,4-D degraders in liquid enrichment cultures, a more competitive environment, was greatly reduced (20). Experiments using pristine soils argue that genetic exchange may also play a role in 2,4-D degradation. Soil enrichments from six pristine locations metabolized 3-chlorobenzoate (3-CBA) and 2,4-D (29). While 3-CBA was catabolized without a lag period and 3-CBA-degrading cultures were readily isolated from these enrichments, 2,4-D was generally not consumed until the second week of

incubation and only a small number 2,4-D degrading bacteria were obtained (29). These data suggest that 2,4-D is degraded by a consortium in environments without a history of 2,4-D treatment.

Diverse bacteria capable of 2,4-D degradation have been isolated from various environmental samples and enrichments (76). Survey studies of isolates from soil, water and sewage sludge have found distinct taxa capable of growth on 2,4-D coexisting in certain environments (3, 20, 117). Over the past thirty years, many 2,4-D degrading bacteria from different genera have been characterized including strains of *Pseudomonas* (3, 31), *Bordetella* (31) and *Alcaligenes* (3, 18, 32), *Variovorax* (123), *Burkholderia* (112), *Halomonas* (66), *Flavobacterium* (13) *Sphingomonas* (50), *Acinetobacter* (6), *Arthrobacter* (116), *Corynebacterium* (3), *Nocardioides* (57), *Azotobacter* (4), *Achromobacter* (108), and *Streptomyces* (128). Further, genetic and biochemical studies of many of these strains demonstrate the pervasiveness of TfdA in these 2,4-D degradation pathways. *Sphingomonas* strains that degrade 2,4-D are commonly found in Michigan soils, but these isolates do not have a *tfdA* gene that can be detected by gene probes or a PCR-based screening method for different alleles of the *tfdA* gene (50). Nevertheless, biochemical characterization of the *Sphingomonas* isolates indicate that 2,4-D degradation is initiated by an α -KG-dependent dioxygenase (104).

The *tfd* genes often reside on mobile genetic elements. Plasmids belonging to at least two different incompatibility groups have been isolated from *Alcaligenes* species (18) and soils (118). Plasmid capture experiments were used to isolate pEMT8, a 75-kb plasmid that encodes *tfdA*. This plasmid does not appear to contain *tfdB* or *tfdCDEF* and fails to confer activities of the downstream enzymes to a 2,4-D *Ralstonia eutropha*

recipient (119). Nearly identical alleles of *tfdA* have been detected on plasmids isolated from soils (68) and on the chromosome of plasmid-cured *Burkholderia* sp. suggesting that the gene may travel on transposons as well as plasmids (112). Evidence for a conjugative plasmid capable of integration into the chromosome of different strains has also been published (51). The pJP4 plasmid can be transferred to bacteria of different genera such as *Variovorax*, *Pseudomonas*, and *Burkholderia* in soils (16, 25) and similar plasmids have been isolated from *Flavobacterium* sp. (13, 50). Different plasmids (7, 64) and putative degradative transposons, such as Tn5530 carried on pIJB1 (134) have also been purified from 2,4-D degrading strains. Additional proof of the extensive intergeneric transfer of *tfdA* is the distribution of at least three different alleles of *tfdA* across the β -Proteobacteria (71).

In addition to studies on the dispersal of 2,4-D degradative ability, much attention has been paid to the creation or assembly of this pathway. Several experiments have been designed to determine if there is one common ancestor to *tfd*-based gene cluster or if these genes were assembled multiple times from other biodegradative pathways. Xia et al. (133) reported that DNA from soils with no or low exposure to 2,4-D do not hybridize to the pJP4 *tfdA* gene probe and no 2,4-D degrading isolates could be cultured from these soils. Upon exposure to herbicide, 2,4-D degraders with different *tfdA* and *tfdB* genes become dominant in the different plots. Because there was not a major shift in the total community structure in response to 2,4-D application, based on random amplified polymorphic DNA (RAPD) fingerprint analysis, it seems that either a 2,4-D degrading organism was created from the resident community or a mobile element carrying the necessary genes was acquired and transferred among resident organisms. Phylogenetic

analyses of different 2,4-D degrading bacteria also indicate independent recruitment of the *tfd* genes into different organisms during the assembly of the 2,4-D catabolic pathway (124). Dendrograms plotting the relationships of each of three *tfd* alleles (*tfdA*, *tfdB*, and *tfdC*) from a collection of 2,4-D degraders are significantly different indicating that these three genes have not evolved together (28, 124).

The seemingly ubiquitous nature of 2,4-D degrading organisms from both agricultural and pristine soils as well as from aquatic environments argues that this metabolic characteristic is important for competitiveness in the environment. Although some bacteria can degrade 2,4-D by other means (4, 53, 57), TfdA appears to play a major role in the breakdown of 2,4-D in the environment. Of all the enzymes in the pJP4-encoded pathway, TfdA is the most unique to 2,4-D degradation. Phenols and catechols are intermediates in numerous catabolic pathways, thus different enzymes exist to catalyze their degradation. No alternative role for TfdA has been identified.

Overview of thesis

In this thesis, I present my research on the characterization of the active site of TfdA and a study of related enzymes. Chapter 2 focuses specifically on studies relating to the structure and activity of TfdA from *Ralstonia eutropha* JMP134. I describe the site-directed mutagenesis of ten residues and the characterization of the resultant enzymes to determine the role, if any, of these amino acids in TfdA structure or activity. These studies are an important contribution to research on the structure and mechanism of TfdA and the related enzyme TauD. In Chapter 3, I describe the cloning and characterization of an α -KG-dependent dioxygenase from *Saccharomyces cerevisiae* to determine if it

possesses activity similar to TfdA. Work with a strain of *S. cerevisiae* in which this gene was disrupted confirms our findings that this enzyme is a sulfonate/ α -KG dioxygenase. Chapter 4 describes my research on putative TfdA-like α -KG-dependent dioxygenases in soil bacteria. In the last chapter, I summarize my current thoughts on the role of α -KG-dependent dioxygenases in the environment and propose future directions for research on TfdA and TfdA-like enzymes.

Literature cited

1. **Altschul, S. F., W. Gish, W. Miller, E. W. Myers, and D. J. Lipman.** 1990. Basic local alignment search tool. *J Mol Biol* **215**:403-10.
2. **Altschul, S. F., T. L. Madden, A. A. Schäffer, J. Zhang, Z. Zhang, W. Miller, and D. J. Lipman.** 1997. Gapped BLAST and PSI-BLAST: a new generation of protein database search programs. *Nucleic Acids Res.* **25**:3389-3402.
3. **Amy, P. S., J. W. Schulke, L. M. Frazier, and R. J. Seidler.** 1985. Characterization of aquatic bacteria and cloning of genes specifying partial degradation of 2,4-dichlorophenoxyacetic acid. *Appl. Environ. Microbiol.* **49**:1237-1245.
4. **Balajee, S., and A. Mahadevan.** 1990. Dissimilation of 2,4-dichlorophenoxyacetic acid by *Azotobacter chroococcum*. *Xenobiotica* **20**:607-617.
5. **Baldwin, J. E., K. D. Merritt, C. J. Schofield, S. W. Elson, and K. H. Baggeley.** 1993. Studies on the stereospecificity of the clavaminic acid synthase catalyzed hydroxylation reaction. *J. Chem. Soc., Chem. Comm.*:1301-1302.
6. **Bell, G. R.** 1957. Some morphological and biochemical characteristics of a soil bacterium which decomposes 2,4-dichlorophenoxyacetic acid. *Can. J. Microbiol.* **3**:821-840.
7. **Bhat, M. A., M. Tsuda, K. Horiike, M. Nozaki, C. S. Vaidyanathan, and T. Nakazawa.** 1994. Identification and characterization of a new plasmid carrying genes for degradation of 2,4-dichlorophenoxyacetate from *Pseudomonas cepacia* CSV90. *Appl. Environ. Microbiol.* **60**:307-312.
8. **Borovok, I., O. Landman, R. Kreisberg-Zakarin, Y. Aharonowitz, and G. Cohen.** 1996. Ferrous active site of isopenicillin N synthase: genetic and sequence analysis of the endogenous ligands. *Biochemistry* **35**:1981-1987.
9. **Britsch, L.** 1990. Purification and characterization of flavone synthase I, a 2-oxoglutarate-dependent desaturase. *Arch. Biochem. Biophys.* **282**:152-160.
10. **Britsch, L., and H. Grisebach.** 1986. Purification and characterization of (2S)-flavanone 3-hydroxylase from *Petunia hybrida*. *Eur. J. Biochem.* **156**:569-577.
11. **Busby, R. W., M. D.-T. Chang, R. C. Busby, J. Wimp, and C. A. Townsend.** 1995. Expression and purification of two isozymes of clavamate synthase and initial characterization of the iron binding site. *J. Biol. Chem.* **270**:4262-4269.

12. **Chahal, A., M. Khan, S. G. Pai, E. Barbosa, and I. Singh.** 1998. Restoration of phytanic acid oxidation in Refsum disease fibroblasts from patients with mutations in the phytanoyl-CoA hydroxylase gene. *FEBS Lett.* **429**:119-122.
13. **Chaudry, G. R., and G. H. Huang.** 1988. Isolation and characterization of a new plasmid from a *Flavobacterium* sp. which carries the genes for the degradation of 2,4-dichlorophenoxyacetate. *J. Bacteriol.* **170**:3897-3902.
14. **De Carolis, E., and V. De Luca.** 1993. Purification, characterization, and kinetic analysis of a 2-oxoglutarate-dependent dioxygenase involved in vindoline biosynthesis of *Catharanthus roseus*. *J. Biol. Chem.* **268**:5504-5511.
15. **De Long, L., S. P. J. Albracht, and A. Kemp.** 1982. Prolyl 4-hydroxylase activity in relation to the oxidation state of enzyme-bound iron. *Biochim. Biophys. Acta.* **704**:326-332.
16. **DiGiovanni, G. D., J. W. Neilson, I. L. Pepper, and N. A. Sinclair.** 1996. Gene transfer of *Alcaligenes eutrophus* JMP134 plasmid pJP4 to indigenous soil recipients. *Appl. Environ. Microbiol.* **62**:2521-2526.
17. **Don, R. H., and J. M. Pemberton.** 1985. Genetic and physical map of the 2,4-dichlorophenoxyacetic acid-degrading plasmid pJP4. *J. Bacteriol.* **161**:466-468.
18. **Don, R. H., and J. M. Pemberton.** 1981. Properties of six pesticide degradation plasmids isolated from *Alcaligenes paradoxus* and *Alcaligenes eutrophus*. *J. Bacteriol.* **145**:681-686.
19. **Don, R. H., A. J. Weightman, H. J. Knackmuss, and K. N. Timmis.** 1985. Transposon mutagenesis and cloning analysis of the pathways for degradation of 2,4-dichlorophenoxyacetic acid and 3-chlorobenzoate in *Alcaligenes eutrophus* JMP134 (pJP4). *J. Bacteriol.* **161**:85-90.
20. **Dunbar, J., S. White, and L. Forney.** 1997. Genetic diversity through the looking glass: effect of enrichment bias. *Appl. Environ. Microbiol.* **63**:1326-1331.
21. **Eichhorn, E., J. R. van der Ploeg, M. A. Kertesz, and T. Leisinger.** 1997. Characterization of α -ketoglutarate-dependent taurine dioxygenase from *Escherichia coli*. *J. Biol. Chem.* **272**:23031-23036.
22. **Englard, S., J. S. Blanchard, and C. F. Midelfort.** 1985. γ -Butyrobetaine hydroxylase: stereochemical course of the hydroxylation reaction. *Biochemistry* **24**:1110-1116.
23. **Eriksson, M., J. Myllyharju, H. Tu, M. Hellman, and K. I. Kivirikko.** 1999. Evidence for 4-hydroxyproline in viral proteins. Characterization of a viral prolyl 4-hydroxylase and its peptide substrates. *J Biol Chem* **274**:22131-22134.

24. **Filer, K., and A. R. Harker.** 1997. Identification of the inducing agent of the 2,4-dichlorophenoxyacetic acid pathway encoded by plasmid pJP4. *Appl. Environ. Microbiol.* **63**:317-320.
25. **Friedrich, B., M. Meyer, and H. G. Schlegel.** 1983. Transfer and expression of the herbicide-degrading plasmid pJP4 in aerobic autotrophic bacteria. *Arch. Microbiol.* **134**:92-7.
26. **Fukumori, F., and R. P. Hausinger.** 1993. *Alcaligenes eutrophus* JMP134 "2,4-dichlorophenoxyacetate monooxygenase" is an α -ketoglutarate-dependent dioxygenase. *J. Bacteriol.* **175**:2083-2086.
27. **Fukumori, F., and R. P. Hausinger.** 1993. Purification and characterization of 2,4-dichlorophenoxyacetate/ α -ketoglutarate dioxygenase. *J. Biol. Chem.* **268**:24311-24317.
28. **Fulthorpe, R. R., C. McGowan, O. V. Maltseva, W. E. Holben, and J. M. Tiedje.** 1995. 2,4-Dichlorophenoxyacetic acid-degrading bacteria contain mosaics of catabolic genes. *Appl. Environ. Microbiol.* **61**:3274-3281.
29. **Fulthorpe, R. R., A. N. Rhodes, and J. M. Tiedje.** 1996. Pristine soils mineralize 3-chlorobenzoate and 2,4-dichlorophenoxyacetate via different microbial populations. *Appl. Environ. Microbiol.* **62**:1159-1166.
30. **Galland, S., F. Le Borgne, D. Guyonnet, P. Clouet, and J. Demarquoy.** 1998. Purification and characterization of the rat liver gamma-butyrobetaine hydroxylase. *Mol. Cell. Biochem.* **178**:163-8.
31. **Greer, L. E., J. A. Robinson, and D. R. Shelton.** 1992. Kinetic comparison of seven strains of 2,4-dichlorophenoxyacetic acid-degrading bacteria. *Appl. Environ. Microbiol.* **58**:1027-1030.
32. **Gunalan, and J. C. Fournier.** 1993. Effect of microbial competition on the survival and activity of 2,4-D degrading *Alcaligenes xylosoxidans* subsp. *denitrificans* added to soil. *Lett. Appl. Microbiol.* **16**:178-181.
33. **Hanauske-Abel, H. M., and V. Günzler.** 1982. A stereochemical concept for the catalytic mechanism of prolyl hydroxylase. Applicability to classification and design of inhibitors. *J. Theor. Biol.* **94**:421-455.
34. **Hashimoto, T., and Y. Yamada.** 1987. Purification and characterization of hyoscyamine 6 β -hydroxylase, from root cultures of *Hyoscyamus niger* L. *Eur. J. Biochem.* **164**:277-285.

35. **Hausinger, R. P., F. Fukumori, D. A. Hogan, T. M. Sassanella, Y. Kamagata, H. Takami, and R. E. Wallace.** 1996. Biochemistry of 2,4-D degradation: evolutionary implications, p. 35-51. *In* K. Horikoshi, M. Fukuda, and T. Kudo (ed.), *Microbial Diversity and Genetics of Biodegradation*. Japan Scientific Press, Tokyo.
36. **Hedden, P.** 1992. 2-Oxoglutarate-dependent dioxygenases in plants: mechanism and function. *Biochem. Soc. Trans.* **20**:373-377.
37. **Hedden, P.** 1997. The oxidases of giberellin biosynthesis: Their function and mechanism. *Physiol. Planta.* **101**:709-719.
38. **Hegg, E. L., and L. Que Jr.** 1997. The 2-His-1-carboxylate facial triad. *Eur. J. Biochem.* **250**:625-629.
39. **Hegg, E. L., A. K. Whiting, J. McCracken, R. P. Hausinger, and J. Que, L.** 1999. The herbicide-degrading α -keto acid enzyme TfdA: metal coordination environment and mechanistic insights. *Biochemistry* **In press**.
40. **Hogan, D. A., T. A. Auchtung, and R. P. Hausinger.** 1999. Cloning and characterization of a sulfonate/ α -ketoglutarate dioxygenase from *Saccharomyces cerevisiae*. *J. Bacteriol.* **181**:5876-5879.
41. **Holme, E.** 1975. A kintic study of thymine 7-hydroxylase from *Neurospora crassa*. *Biochemistry* **14**:4999-5003.
42. **Holme, E., S. Lindstedt, and I. Nordin.** 1982. Uncoupling in the γ -butyrobetaine hydroxylase reaction by D- and L-carnitine. *Biochem. Biophys. Res. Comm.* **107**:518-524.
43. **Holton, T. A., F. Brugliera, and Y. Tanaka.** 1993. Cloning and expression of flavonol synthase from *Petunia hybrida*. *Plant J* **4**:1003-10.
44. **Hulse, J. D., S. R. Ellis, and L. M. Henderson.** 1978. Carnitine biosynthesis. β -Hydroxylation of trimethyllysine by an α -ketoglutarate-dependent mitochondrial dioxygenase. *J. Biol. Chem.* **253**:1654-9.
45. **Hutton Jr., J. J., A. L. Tappel, and S. Udenfriend.** 1967. Cofactor and substrate requirements of collagen proline hydroxylase. *Arch. Biochem. Biophys.* **118**:231-240.
46. **Jansen, G. A., S. J. Mihalik, P. A. Watkins, C. Jakobs, H. W. Moser, and R. J. Wanders.** 1998. Characterization of phytanoyl-coenzyme A hydroxylase in human liver and activity measurements in patients with peroxisomal disorders. *Clin. Chim. Acta* **271**:203-11.

47. **Jia, S., K. McGinnis, W. J. VanDusen, C. J. Burke, A. Kuo, P. R. Griffin, M. K. Sardana, K. O. Elliston, A. M. Stern, and P. A. Friedman.** 1994. A fully active catalytic domain of bovine aspartyl (asparaginy)- β -hydroxylase expressed in *Escherichia coli*: characterization and evidence for the identification of an active-site region in vertebrate- α -ketoglutarate-dependent dioxygenases. *Proc. Natl. Acad. Sci.* **91**:7227-7231.
48. **Jiang, F., J. Peisach, L.-J. Ming, L. Que, Jr., and V. J. Chen.** 1991. Electron spin-echo envelope modulation studies of the Cu(II)-substituted derivative of isopenicillin N synthase: a structural and spectroscopic model. *Biochemistry* **30**:11437-11445.
49. **John, P.** 1997. Ethylene biosynthesis: The role of 1-aminocyclopropane-1-carboxylate (ACC) oxidase, and its possible evolutionary origin. *Physiologia Plantarum* **100**:583-592.
50. **Ka, J. O., W. E. Holben, and J. M. Tiedje.** 1994. Genetic and phenotypic diversity of 2,4-dichlorophenoxyacetic acid (2,4-D)-degrading bacteria isolated from 2,4-D-treated field soils. *Appl. Environ. Microbiol.* **60**:1106-1115.
51. **Ka, J. O., and J. M. Tiedje.** 1994. Integration and excision of a 2,4-dichlorophenoxyacetic acid degradative plasmid in *Alcaligenes paradoxus* and evidence of its natural intergeneric transfer. *J. Bacteriol.* **176**:5284-5289.
52. **Kellokumpu, S., R. Sormunen, J. Heikkinene, and R. Myllylä.** 1994. Lysyl hydroxylase, a collagen processing enzyme, exemplifies a novel class of lumenally-oriented peripheral membrane protein in the endoplasmic reticulum. *J. Biol. Chem.* **269**:30524-30529.
53. **Kilbane, J. J., D. K. Chatterjee, J. S. Karns, S. T. Kellogg, and A. M. Chakrabarty.** 1982. Biodegradation of 2,4,5-trichlorophenoxyacetic acid by a pure culture of *Pseudomonas cepacia*. *Appl. Environ. Microbiol.* **44**:72-78.
54. **Kivirikko, K. I., and T. Pihlajaniemi.** 1998. Collagen hydroxylases and the protein disulfide isomerase subunit of prolyl 4-hydroxylases. *Adv. Enzymol. Relat. Areas Mol. Biol.* **72**:328-398.
55. **Korioth, F., C. Gieffers, and J. Frey.** 1994. Cloning and characterization of the human gene encoding aspartyl β -hydroxylase. *Gene* **150**:395-399.
56. **Kovacevic, S., B. J. Weigel, M. B. Tobin, T. D. Ingolia, and J. R. Miller.** 1989. Cloning, characterization, and expression in *Escherichia coli* of the *Streptomyces clavuligerus* gene encoding deacetoxycephalosporin C synthetase. *J. Bacteriol.* **171**:754-60.

57. **Kozyreva, L. P., Y. V. Shurukhin, Z. I. Finkelstein, B. P. Baskunov, and L. A. Golovleva.** 1993. Metabolism of the herbicide 2,4-D by a *Nocardioides simplex* strain. *Mikrobiol.* **62**:110-119.
58. **Kreisberg-Zakarin, R., I. Borovok, M. Yanko, Y. Aharonowitz, and G. Cohen.** 1999. Recent advances in the structure and function of isopenicillin N synthase. *Antonie Van Leeuwenhoek* **75**:33-39.
59. **Lamberg, A., T. Pihlajaniemi, and K. I. Kivirikko.** 1995. Site-directed mutagenesis of the α subunit of the human prolyl 4-hydroxylase. *J. Biol. Chem.* **270**:9926-9931.
60. **Lawlor, E. J., S. W. Elson, S. Holland, R. Cassels, and J. E. Hodgson.** 1994. Expression in *Escherichia coli* of a clavaminic acid synthase isozyme: a trifunctional oxygenases involved in clavulanic acid biosynthesis. *Tetrahedron* **50**:8737-8748.
61. **Leveau, J. H., A. J. B. Zehnder, and J. R. Van der Meer.** 1998. The *tfdK* gene product facilitates the uptake of 2,4-dichlorophenoxyacetate by *Ralstonia eutropha* JMP134(pJP4). *J. Bacteriol.* **180**:2237-2243.
62. **Lindstedt, G., and S. Lindstedt.** 1970. Cofactor requirements of γ -butyrobetaine hydroxylase from rat liver. *J. Biol. Chem.* **245**:4178-4180.
63. **Lukacin, R., and L. Britsch.** 1997. Identification of strictly conserved histidine and arginine residues as part of the active site in *Petunia hybrida* flavanone 3 β -hydroxylase. *Eur. J. Biochem.* **249**:748-757.
64. **Mäe, A. A., R. O. Martis, N. R. Ausmees, V. M. Kõiv, and A. L. Heinaru.** 1993. Characterization of a new 2,4-dichlorophenoxyacetic acid degrading plasmid pEST4011: physical map and localization of catabolic genes. *J. Gen. Microbiol.* **139**:3165-3170.
65. **Majamaa, K., V. Günzler, H. M. Hanauske-Abel, R. Myllylä, and K. I. Kivirikko.** 1986. Partial identity of the 2-oxoglutarate and ascorbate binding sites of prolyl 4-hydroxylase. *J. Biol. Chem.* **261**:7819-7823.
66. **Maltseva, O. V., C. McGowan, R. Fulthorpe, and P. J. Oriel.** 1996. Degradation of 2,4-dichlorophenoxyacetic acid by haloalkaliphilic bacteria. *Microbiol.* **142**:1115-1122.
67. **Mao, Y. Q., M. Vargolu, and D. H. Sherman.** 1999. Molecular characterization and analysis of the biosynthetic gene cluster for the antitumor antibiotic mitomycin C from *Streptomyces lavendulae* NRRL2564. *Chem. Biol.* **6**:251-263.

68. **Matheson, V. G., L. F. Forney, Y. Suwa, C. H. Nakatsu, A. J. Sexstone, and W. E. Holben.** 1996. Evidence for acquisition in nature of a chromosomal 2,4-dichlorophenoxyacetic acid/ α -ketoglutarate dioxygenase gene by different *Burkholderia* spp. *Appl. Environ. Microbiol.* **62**:2457-2463.
69. **Matsuda, J., S. Okabe, T. Hashimoto, and Y. Yamada.** 1991. Molecular cloning of hyoscyamine 6 beta-hydroxylase, a 2-oxoglutarate- dependent dioxygenase, from cultured roots of *Hyoscyamus niger*. *J. Biol. Chem.* **266**:9460-9464.
70. **McGinnis, K., G. M. Ku, W. J. VanDusen, J. Fu, V. Garsky, A. M. Stern, and P. A. Friedman.** 1996. Site-directed mutagenesis of residues in a conserved region of bovine aspartyl (asparaginyl) β -hydroxylase: evidence that histidine 675 has a role in binding Fe^{+2} . *Biochemistry* **35**:3957-3962.
71. **McGowan, C., R. Fulthorpe, A. Wright, and J. M. Tiedje.** 1998. Evidence for interspecies gene transfer in the evolution of 2,4-dichlorophenoxyacetic acid degraders. *Appl. Environ. Microbiol.* **64**:4089-4092.
72. **McGowan, S. J., M. T. Holden, B. W. Bycroft, and G. P. Salmond.** 1999. Molecular genetics of carbapenem antibiotic biosynthesis. *Antonie Van Leeuwenhoek* **75**:135-141.
73. **Metcalf, W. W., and R. S. Wolfe.** 1998. Molecular genetic analysis of phosphite and hypophosphite oxidation by *Pseudomonas stutzeri* WM88. *J. Bacteriol.* **180**:5547-5558.
74. **Miller, R. L., and H. H. Varner.** 1979. Purification and enzymic properties of lysyl hydroxylase from fetal porcine skin. *Biochemistry* **18**:5928-5932.
75. **Ming, L.-J., L. Que, Jr., A. Kriauciunas, C. A. Frolik, and V. J. Chen.** 1990. Coordination chemistry of the metal binding site of isopenicillin N synthase. *Inorg. Chem.* **29**:1111-1112.
76. **Miwa, N., and S. Kuwatsuka.** 1991. Characteristics of 2,4-dichlorophenoxyacetic acid (2,4-D)-degrading microorganisms isolated from different soils. *Soil Sci. Plant Nutr.* **37**:575-581.
77. **Mori, H., T. Shiasaki, K. Yano, and A. Ozaki.** 1997. Purification and cloning of a proline 3-hydroxylase, a novel enzyme which hydroxylates free L-proline to *cis*-3-hydroxyl-L-proline. *J. Bacteriol.* **179**:5677-5683.
78. **Mori, H., T. Shibasaki, Y. Uozaki, K. Ochiai, and A. Ozaki.** 1996. Detection of novel proline 3-hydroxylase activities in *Streptomyces* and *Bacillus* spp. by regio- and stereospecific hydroxylation of L-proline. *Appl. Environ. Microbiol.* **62**:1903-1907.

79. **Myllyharju, J., and K. I. Kivirikko.** 1997. Characterization of the iron- and 2-oxoglutarate-binding sites of human prolyl 4-hydroxylase. *EMBO J.* **16**:1173-1180.
80. **Myllylä, R., K. Majamaa, V. Günzler, H. N. Hanauske-Abel, and K. I. Kivirikko.** 1984. Ascorbate is consumed stoichiometrically in the uncoupled reactions catalyzed by prolyl 4-hydroxylase and lysyl hydroxylase. *J. Biol. Chem.* **259**:5403-5405.
81. **Myllylä, R., T. Pihlajaniemi, L. Pajunen, T. Turpeenniemi-Hujanen, and K. I. Kivirikko.** 1991. Molecular cloning of chick lysyl hydroxylase. Little homology in primary structure to the two types of subunit of prolyl 4-hydroxylase. *J. Biol. Chem.* **266**:2805-2810.
82. **Myllylä, R., L. Tuderman, and K. I. Kivirikko.** 1977. Mechanism of the prolyl hydroxylase reaction: 2. Kinetic analysis of the reaction sequence. *Eur. J. Biochem.* **80**:349-357.
83. **Nagahama, K., T. Ogawa, T. Fujii, M. Tazaki, S. Tanase, Y. Morino, and H. Fukuda.** 1991. Purification and properties of an ethylene-forming enzyme from *Pseudomonas syringae* pv. *phaseolicola* PK2. *J. Gen. Microbiol.* **137**:2281-2286.
84. **Nickel, K., M. J.-F. Suter, and H.-P. E. Kohler.** 1997. Involvement of two α -ketoglutarate-dependent dioxygenases in enantioselective degradation of (R)- and (S)-mecoprop by *Sphingomonas herbicidovorans* MH. *J. Bacteriol.* **179**:6674-6679.
85. **Orville, A. M., V. J. Chen, A. Kriauciunas, M. R. Harpel, B. G. Fox, E. Münck, and J. D. Lipscomb.** 1992. Thiolate ligation of the active site Fe^{+2} of isopenicillin N synthase derived from substrate rather than endogenous cysteine: spectroscopic studies of site-specific Cys to Ser mutated enzymes. *Biochemistry* **31**:4602-4612.
86. **Ou, L.-T.** 1984. 2,4-D degradation and 2,4-D degrading microorganisms in soils. *Soil Sci.* **137**:100-107.
87. **Pavel, E. G., J. Zhou, R. W. Busby, M. Gunsior, C. A. Townsend, and E. I. Solomon.** 1998. Circular dichroism and magnetic circular dichroism spectroscopic studies of the non-heme ferrous active site in clavamate synthase and its interaction with α -ketoglutarate cosubstrate. *J. Am. Chem. Soc.* **120**:743-754.
88. **Pirskanen, A., A.-M. Kaimio, R. Myllylä, and K. I. Kivirikko.** 1996. Site-directed mutagenesis of human lysyl hydroxylase expressed in insect cells. *J. Biol. Chem.* **271**:9398-9402.

89. **Pirskanen, A., A.-M. Kaimio, R. Myllylä, and K. I. Kivirikko.** 1996. Site-directed mutagenesis of human lysyl hydroxylase expressed in insect cells. Identification of histidine residues and an aspartic acid residue critical for catalytic activity. *J. Biol. Chem.* **271**:9398-9402.
90. **Prescott, A. G.** 1993. A dilemma of dioxygenases (or where biochemistry and molecular biology fail to meet). *J. Exp. Bot.* **44**:849-861.
91. **Prescott, A. G., and P. John.** 1996. Dioxygenases: Molecular structure and role in plant metabolism. *Annu. Rev. Plant Physiol. Plant Mol. Biol.* **47**:245-271.
92. **Puistola, U., T. M. Turpeenniemi-Hujanen, R. Myllylä, and K. I. Kivirikko.** 1980. Studies on the lysyl hydroxylase reaction: II. Inhibition kinetics and the reaction mechanism. *Biochim. Biophys. Acta* **611**:51-60.
93. **Ramon, D., L. Carramolino, C. Patino, F. Sanchez, and M. A. Penalva.** 1987. Cloning and characterization of the isopenicillin N synthetase gene mediating the formation of the beta-lactam ring in *Aspergillus nidulans*. *Gene* **57**:171-81.
94. **Roach, P. L., I. J. Clifton, V. Fülöp, K. Harlos, G. J. Barton, J. Hajdu, I. Andersson, C. J. Schofield, and J. E. Baldwin.** 1995. Crystal structure of isopenicillin N synthase is the first from a new structural family of enzymes. *Nature* **375**:700-704.
95. **Roach, P. L., I. J. Clifton, C. M. H. Hensgens, N. Shibata, C. J. Schofield, J. Hajdu, and J. E. Baldwin.** 1997. Structure of isopenicillin N synthase complexed with substrate and the mechanism of penicillin formation. *Nature* **387**:827-830.
96. **Ryle, M. J., R. Padmakumar, and R. P. Hausinger.** 1999. Stopped-flow kinetic analysis of *Escherchia coli* taurine/ α -ketoglutarate dioxygenase: interactions with α -ketoglutarate, taurine, and oxygen. *Biochem.* **In press.**
97. **Saari, R. E., and R. P. Hausinger.** 1998. Ascorbic acid-dependent turnover and reactivation of 2,4- dichlorophenoxyacetic acid/ α -ketoglutarate dioxygenase using thiophenoxyacetic acid. *Biochemistry* **37**:3035-3042.
98. **Saari, R. E., D. A. Hogan, and R. P. Hausinger.** 1999. Stereospecific degradation of the phenoxypropionate herbicide dichlorprop. *J. Molec. Catalysis B: Enzymatic* **266**:421-428.
99. **Saito, K., M. Kobayashi, Z. Gong, Y. Tanaka, and M. Yamazaki.** 1999. Direct evidence for anthocyanidin synthase as a 2-oxoglutarate-dependent oxygenase: molecular cloning and functional expression of cDNA from a red form of *Perilla frutescens*. *Plant Journal* **17**:181-189.

100. **Saito, T., S. S. Kwak, Y. Kamiya, H. Yamane, A. Sakurai, N. Murofushi, and N. Takahashi.** 1991. Plant Cell. Physiol. **32**:239-245.
101. **Sami, M., T. J. N. Brown, P. L. Roach, C. J. Schofield, and J. E. Baldwin.** 1997. Glutamine--330 is not essential for activity in isopenicillin N synthase from *Aspergillus nidulans*. FEBS Lett. **405**:191-194.
102. **Samson, S. M., J. E. Dotzla, M. L. Slisz, G. W. Becker, R. M. Van Frank, L. E. Veal, W. K. Yeh, J. R. Miller, S. W. Queener, and T. D. Ingolia.** 1987. Cloning and expression of the fungal expandase/hydroxylase gene involved in cephalosporin biosynthesis. Biotechnology **5**:1207-1214.
103. **Sandmann, E. R. I. C., M. A. Loos, and L. P. van Dyk.** 1988. Microbial degradation of 2,4-dichlorophenoxyacetic acid in soil. Rev. Environ. Contamin. Tox. **101**:1-53.
104. **Sassanella, T. M., F. Fukumori, M. Bagdasarian, and R. P. Hausinger.** 1997. Use of 4-nitrophenoxyacetic acid for the detection and quantitation of 2,4-dichlorophenoxyacetic acid (2,4-D)/ α -ketoglutarate dioxygenase activity in 2,4-D degrading microorganisms. Appl. Environ. Microbiol. **63**:1189-1191.
105. **Scott, R. A., S. Wang, M. K. Eidsness, A. Kriauciunas, C. A. Frolik, and V. J. Chen.** 1992. X-ray absorption spectroscopic studies of the high-spin iron(II) active site of isopenicillin N synthase: evidence for Fe-S interaction in the enzyme-substrate complex. Biochemistry **31**:4596-601.
106. **Shibasaki, T., H. Mori, S. Chiba, and A. Ozaki.** 1999. Microbial proline 4-hydroxylase screening and gene cloning. Appl. Environ. Microbiol. **65**:4028-4031.
107. **Soulas, G.** 1993. Evidence for the existence of different physiological groups in the microbial community responsible for 2,4-D mineralization in soil. Soil Biol. Biochem. **25**:443-449.
108. **Stenson, T. I., and N. Walker.** 1957. The pathway of breakdown of 2,4-dichloro- and 4-chloro-2-methyl-phenoxyacetic acid by bacteria. J. Gen. Microbiol. **16**:146-155.
109. **Stintzi, A., Z. Johnson, M. Stonehouse, U. Ochsner, J. Meyer, M. Vasil, and K. Poole.** 1999. The *pvc* gene cluster of *Pseudomonas aeruginosa*: role in synthesis of the pyoverdine chromophore and regulation by PtxR and PvdS. J. Bacteriol. **181**:4118-4124.
110. **Streber, W. R., K. N. Timmis, and M. H. Zenk.** 1987. Analysis, cloning, and high-level expression of 2,4-dichlorophenoxyacetate monooxygenase gene *tfdA* of *Alcaligenes eutrophus* JMP134. J. Bacteriol. **169**:2950-2955.

111. **Stubbe, J.** 1985. Identification of two alpha-ketoglutarate-dependent dioxygenases in extracts of *Rhodotorula glutinis* catalyzing deoxyuridine hydroxylation. *J. Biol. Chem.* **260**:9972-9975.
112. **Suwa, Y., A. D. Wright, F. Fukumori, K. A. Nummy, R. P. Hausinger, W. E. Holben, and L. J. Forney.** 1996. Characterization of a chromosomally encoded 2,4-dichlorophenoxyacetic acid/ α -ketoglutarate dioxygenase from *Burkholderia* sp. strain RASC. *Appl. Environ. Microbiol.* **62**:2464-2469.
113. **Tan, D. S. H., and T.-S. Sim.** 1996. Functional analysis of conserved histidine residues in *Cephalosporin acremonium* isopenicillin N synthase by site-directed mutagenesis. *J. Biol. Chem.* **271**:889-894.
114. **Tett, V. A., A. J. Willetts, and H. M. Lappin-Scott.** 1997. Biodegradation of the chlorophenoxy herbicide (R)(+)-mecoprop by *Alcaligenes denitrificans*. *Biodegradation* **8**:43-52.
115. **Thornburg, L. D., M. T. Lai, J. S. Wishnok, and J. Stubbe.** 1993. A non-heme protein with heme tendencies: an investigation of the substrate specificity of thymine hydroxylase. *Biochemistry* **32**:14023-14033.
116. **Tiedje, J. M., and M. Alexander.** 1969. Enzymatic cleavage of the ether bond of 2,4-dichlorophenoxyacetate. *J. Agr. Food Chem.* **17**:1080-1084.
117. **Tonso, N. L., V. G. Matheson, and W. E. Holben.** 1995. Polyphasic characterization of a suite of bacterial isolates capable of degrading 2,4-D. *Microb. Ecol.* **3**:3-24.
118. **Top, E. M., W. E. Holben, and L. J. Forney.** 1995. Characterization of diverse 2,4-dichlorophenoxyacetic acid-degradative plasmids isolated from soil by complementation. *Appl. Environ. Microbiol.* **61**:1691-1698.
119. **Top, E. M., O. V. Maltseva, and L. J. Forney.** 1996. Capture of a catabolic plasmid that encodes only 2,4-D/ α -ketoglutarate dioxygenase (TfdA) by genetic complementation. *Appl. Environ. Microbiol.* **62**:2470-2476.
120. **Unfinished Genome Database Website.** 11 October 1999.
<http://www.ncbi.nlm.nih.gov/BLAST/unfinishedgenome.html>.
121. **United States Department of Agriculture.** 1996. Biologic and economic benefits from the use of phenoxy herbicides in the United States NAPIAP Report No. 1-PA-96.
122. **Valegård, K., A. C. T. van Scheltinga, M. D. Lloyd, T. Hara, S. Ramaswamy, A. Perrakis, A. Thompson, H.-J. Lee, J. E. Baldwin, C. J. Schofield, J. Hajdu,**

- and I. Andersson.** 1998. Structure of a cephalosporin synthase. *Nature* **394**:805-809.
123. **Vallaey, T., L. Albino, G. Soulas, A. D. Wright, and A. J. Weightman.** 1998. Isolation and characterization of a stable 2,4-dichlorophenoxyacetic acid degrading bacterium, *Variovorax paradoxus*, using chemostat culture. *Biotechnol. Lett.* **20**:1073-6.
124. **Vallaey, T., L. Courde, C. McGowan, A. D. Wright, and R. R. Fulthorpe.** 1999. Phylogenetic analyses indicate independent recruitment of diverse gene cassettes during assemblage of the 2,4-D catabolic pathway. *FEMS Microbiol. Ecology* **28**:373-382.
125. **Valtavaara, M., H. Papponene, A.-M. Pirttilä, K. Hiltunen, H. Helander, and R. Myllylä.** 1997. Cloning and characterization of a novel human lysyl hydroxylase isoform highly expressed in pancreas and muscle. *J. Biol. Chem.* **272**:6831-6834.
126. **van der Meer, J. R., W. M. de Vos, S. Harayama, and A. J. B. Zehnder.** 1992. Molecular mechanisms of genetic adaption to xenobiotic compounds. *Microbiol. Rev.* **56**:677-694.
127. **Vermeij, P., J. Hummerjohann, T. Leisinger, and M. A. Kertesz.** 1999. Unpublished.
128. **Walker, R. L., and A. S. Newman.** 1956. Microbial decomposition of 2,4-dichlorophenoxyacetic acid. *Appl. Microbiol* **4**:201-207.
129. **Wang, Q., W. J. VanDusen, C. J. Petroski, V. M. Garsky, A. M. Stern, and P. A. Friedman.** 1991. Bovine liver aspartyl β -hydroxylase. Purification and characterization. *J. Biol. Chem.* **266**:14004-14010.
130. **Wehbie, R. S., N. S. Punekar, and H. A. Lardy.** 1988. Rat liver γ -butyrobetaine hydroxylase catalyzed reaction: influence of potassium, substrates and substrate analogues on hydroxylation and decarboxylation. *Biochemistry* **27**:2222-2228.
131. **Whiting, A. K., L. Que Jr., R. E. Saari, R. P. Hausinger, M. A. Fredrick, and J. McCracken.** 1997. Metal coordination environment of a Cu(II)-substituted α -keto acid-dependent dioxygenase that degrades the herbicide 2,4-D. *J. Amer. Chem. Soc.* **119**:3413-3414.
132. **Wilson, R. D., J. Geronimo, and J. A. Armbruster.** 1997. Dissipation in field soils after application of 2,4-D dimethylamine salt and 2,4-D 2-ethylhexyl ester. *Environmental Toxicology and Chemistry* **16**:1239-1246.

133. **Xia, X., J. Bollinger, and A. Ogram.** 1995. Molecular genetic analysis of the response of three soil microbial communities to the application of 2,4-D. *Mol. Ecol.* **4**:17-28.
134. **Xia, X.-S., S. Aathithan, K. Oswiecimska, A. R. W. Smith, and I. J. Bruce.** 1998. A novel plasmid pIJB1 possessing a putative 2,4-dichlorophenoxyacetate degradative transposon TN5530 in *Burkholderia cepacia* strain 2a. *Plasmid* **39**:154-159.
135. **Zhang, Z., C. J. Schofield, J. E. Baldwin, P. Thomas, and P. John.** 1995. Expression, purification and characterization of 1-aminocyclopropane-1-carboxylate oxidase from tomato in *Escherichia coli*. *Biochem. J.* **307**:77-85.

CHAPTER 2
CHARACTERIZATION OF THE ACTIVE SITE OF 2,4-
DICHLOROPHENOXYACETIC ACID/ α -KETOGLUTARATE DIOXYGENASE

Many of the results in this chapter have been submitted for publication to the Journal of Biological Chemistry in a manuscript entitled "Site-directed mutagenesis of 2,4-dichlorophenoxyacetic acid/ α -ketoglutarate dioxygenase" by Hogan, D.A., S. R. Smith, E. A. Saari, J. McCracken, and R. P. Hausinger.

Introduction

2,4-Dichlorophenoxyacetic acid (2,4-D)/ α -ketoglutarate (α -KG) dioxygenase (TfdA) is an Fe(II)- and α -KG-dependent enzyme that catalyzes the first step in degradation of the herbicide 2,4-D. This enzyme couples the oxidative decarboxylation of α -KG to the hydroxylation of a side-chain carbon atom. The resultant hemiacetal spontaneously decomposes to form 2,4-dichlorophenol and glyoxalate (6). Mechanistically, TfdA resembles numerous other α -KG-dependent dioxygenases from plants, animals, fungi, and bacteria that catalyze similar hydroxylation reactions at unactivated carbon centers (4, 28). The best-studied α -KG-dependent hydroxylases, including prolyl and lysyl hydroxylase (14) and flavanone hydroxylase (8, 28), show sequence identity to isopenicillin *N* synthase (IPNS) and thus fall into Group I of the α -KG-dependent dioxygenase superfamily (defined in Chapter 1). These enzymes have an H-X-D-X₅₅-H-X₁₀-R motif in common (2, 18) and site-directed mutagenesis studies have confirmed the importance of these residues (15, 18, 21, 25, 27). Through various biochemical and biophysical studies of Group I enzymes, these amino acids are implicated in creating the Fe(II) and α -KG binding sites (17, 29, 30, 33). The sequence of TfdA does not have significant overall identity to the sequences of Group I enzymes.

Although TfdA is not similar in sequence to the Group I α -KG-dependent dioxygenases, it is clearly homologous to a number of other enzymes (Group II). Sequences of *Escherichia coli* taurine/ α -KG dioxygenase (TauD) (5) and sulfonate/ α -KG dioxygenase from *Saccharomyces cerevisiae* (11) have 25-30% overall identity to TfdA. Alignment of TfdA, TauD and sulfonate/ α -KG dioxygenase indicates the conservation of

an H-X-D motif (His 113 and Asp 115 in TfdA) and three other histidines (Appendix A). One invariant histidine, His 167, is positioned to create a three amino acid arrangement similar to the H-X-D-X₋₅₅-H configuration of metal ligands in Group I enzymes, but there are no good candidates for a residue corresponding to the conserved arginine in the Group I motif. In addition, sequence comparisons between TfdA and more distantly related Group II enzymes, such as γ -butyrobetaine hydroxylase and clavamate synthase, do not show conservation of a histidine corresponding to His 167. Alignment of Group II dioxygenase sequences indicates that His 262 is absolutely conserved and is in close proximity to an invariant arginine which may be analogous to the α -KG-binding arginine in deacetoxycephalosporin synthase (DAOCS) and other Group I enzymes.

In this study, we used site-directed mutagenesis methods to examine the roles of the all nine histidines and Asp 115 in TfdA. Previously published work showed that TfdA was inactivated by diethylpyrocarbonate, a histidine-selective reagent, and provided evidence consistent with the presence of multiple histidines in the active site (7). Spectroscopic studies of TfdA showed the presence of two equatorially-bound imidazole nitrogens as ligands to the active site metal, and indicated that one imidazole ligand may be displaced or shifted to an axial position upon substrate binding (3, 34). Based on analyses of different TfdA variants, I identify several likely metal-binding residues and provide evidence that another one or two histidines may aid in substrate coordination.

Experimental Procedures

Recombinant Plasmids

All plasmids were constructed from pUS311 (7), a pUC19 derivative that contains the *Ralstonia eutropha* JMP134 *tfdA* gene (Figure 4). The H8A, D115A, H213A, H216A, H235A, H245A, and H262A TfdA variants were created by direct mutation of *tfdA* in pUS311 by the Stratagene Quickchange System (Stratagene, La Jolla, CA). All mutagenic primers are listed in Table 4. Two alternative approaches were used to construct the three remaining variants. Plasmids encoding H113A and H167A TfdA variants were created by Clontech mutagenesis of pXHtfdA, a pUC19 plasmid containing the 5'-*XbaI-HindII* fragment of the *tfdA* gene (Figure 4). To create the complete gene containing the indicated mutations, the *XbaI-HindII* fragment was cloned into pHKtfdA, which contains the 3' end of the *tfdA* gene. pHKtfdA was constructed in two steps. First, the 1.4-kb *XbaI-SalI* fragment from pUS311, containing the complete *tfdA* gene, was cloned into pBC KS⁻ (Stratagene) cut with *XbaI* and *XhoI* to create pBCtfdA. This step had the benefit of eliminating a *HindII* site that interfered with further cloning steps. The 727-bp *HindII-KpnI* fragment of pBCtfdA was subcloned into pBC KS⁻ cut with the same enzymes to give pHKtfdA. Similarly, the gene encoding H200A TfdA was made by mutagenesis of pXXtfdA, a pUC19 plasmid containing the 5'-*XbaI-XhoI* fragment of *tfdA*. The altered *XbaI-XhoI* fragment was then inserted into pHKtfdA cut with *XbaI* and *XhoI* to give the complete H200A *tfdA* gene. The identity of



Figure 4. Restriction maps of the plasmids used in construction of *tfdA* mutants.

Abbreviations for the restriction enzyme sites are as follows: H, *Hind*II; X, *Xba*I; Xh, *Xho*I; Sl, *Sall*; K, *Kpn*I; Sc, *Sac*I; N, *Nru*I. The vector backbone is indicated in the box on the left. The *tfdA* open reading frame is shown as a wide, solid line.

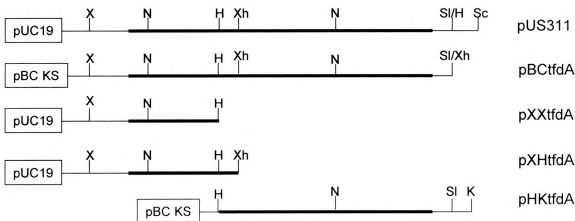


Table 4. Sequences of mutagenic primers used to create altered *tfdA* genes

Mutant	Primer Sequence ^a
H8A	5'- CGC AAA TCC CCT TGC TCC TCT TTT CGC C -3'
H113A	5'- GTC GCT GGC CCA AGC TGG-3'
D115A	5'-GCA CAG CGC CAG CTC CTT TCA-3'
H167A	5'-GCG TGC CGA GCA GTA CGC ACT G-3'
H200A	5'-GGT TCG AAC CGC CGC CGG CTC-3'
H213A	5'-GCT CGC GGC CGC GCC GAT-3'
H216A	5'-CCT TCG ACG GCG CTC GCG-3'
H235A	5'-GCT TCT CGA GGC GAC ACA G-3'
H245A	5'-GTG TAC CGG GCT CGC TGG AAC-3'
H262A	5'-CGT TCT TGC ACG CGG ACG CAG-3'
Tfda-MBPF	5'-TCT CTA GAG TGA GCG TCG TCG CAA ATC C-3'
Tfda-MBPR	5'-GTC AAG CTT GGT TGC GTA CAT CTT GTG G-3'

^aThe reverse primer used for the creation of all mutants was the complement of the forward primer.

all final constructs was confirmed by sequence analysis. To insert the genes encoding H167A and H262A variants of TfdA into a plasmid that would allow for IPTG-controlled expression, the *XbaI-SalI* fragments from the corresponding plasmids described above were cloned into pET23a (Novagen) prepared with the same enzymes.

To create the maltose-binding protein (MBP)-TfdA fusion proteins, the wild-type *tfdA* gene was amplified from pUS311 with TfdA-MBPF and TfdA-MBPR primers (Table 4) to create an *XbaI* site directly upstream of the GTG start codon of the *tfdA* gene and a *HindIII* restriction site 54 bp downstream of the stop codon. The PCR product was cloned directly into the pGEM-T vector according to the manufacturer's instructions (Promega, Madison, WI). The *XbaI-HindIII* fragment was isolated from the resulting plasmid and cloned into the pMAL-c2 vector that had been digested with the same enzymes. The identity of the newly created *malE-tfdA* gene fusion was confirmed by sequencing. Substitution of the mutation-containing internal *NruI* fragment for the same fragment of the wild-type *malE-tfdA* gene created MBP-fusion forms of altered TfdAs. First, pMAL-*tfdA* was digested with *NruI* and the vector fragment was purified and religated to create pMAL-*tfdA*Δ*NruI*. The resultant plasmid was linearized with *NruI* and dephosphorylated with calf intestine alkaline phosphatase prior to ligation with the *NruI* fragments isolated from the previously described mutant genes. Constructs were confirmed by restriction analysis.

Protein Purification

H8A, H113A, D115A, H216A, H235A and wild-type TfdA proteins were purified from *E. coli* DH5α cells carrying pUS311 and its mutated derivatives according to a previously described protocol (7). In addition, the non-mutated enzyme and the TfdA

variants H167A, H200A, H213A, H245A and H262A were purified as MBP-TfdA fusion proteins from *E. coli* DH5 α by the protocol described in the pMAL Protein Fusion and Purification System Manual (New England Biolabs, Beverly, MA).

Analysis of Kinetic Parameters

Specific activities of the wild-type and variant TfdA proteins were determined by a previously described spectrophotometric assay (7). The typical assay mixture contained 1 mM 2,4-D, 1 mM α -KG, 100 μ M $(\text{NH}_4)_2\text{Fe}(\text{SO}_4)_2$, and 100 μ M ascorbic acid in 10 mM MOPS buffer (pH 6.75) at 30°C. The reactions were quenched by the addition of EDTA to a concentration of 5 mM. 2,4-Dichlorophenol was quantified by reaction with 4-aminoantipyrene followed by measurement of the absorbance at 510 nm. One unit of activity was defined as the amount of enzyme required to produce one μ mol of dichlorophenol $\cdot\text{min}^{-1}$. Protein concentrations were determined using the BioRad Protein Assay with bovine serum albumin as a standard. For calculation of the k_{cat} values, the TfdA variants were assumed to have $M_r = 31,600$ and the MBP-TfdA variants were assigned $M_r = 74,500$.

The low K_m for α -KG (~ 2 -5 μ M for the wild-type enzyme) precluded use of the 4-aminoantipyrene assay for accurate determination of this value. The alternative method used to measure the K_m for α -KG quantified the amount of $^{14}\text{CO}_2$ liberated from α -[1- ^{14}C]-KG during the course of the reaction (7).

Native Protein Analysis by Gel Filtration

Size exclusion chromatography was used to estimate the native molecular weights of TfdA, MBP-TfdA, and mutant proteins. The proteins were chromatographed on a Superose 6 gel filtration column (1.0 x 30 cm, Pharmacia-Upjohn) in 20 mM Tris buffer (pH 7.5), 1 mM EDTA, and 200 mM NaCl at a flow rate of 0.2 ml·min⁻¹. The elution volumes were compared to those for gel filtration standards (Bio-Rad) including thyroglobulin, 670 kDa; bovine gamma globulin, 158 kDa; chicken ovalbumin, 44 kDa; myoglobin, 17 kDa; and vitamin B₁₂, 1350 Da.

Spectroscopic Analysis

Proteins for electron paramagnetic resonance (EPR) and electron spin-echo envelope modulation (ESEEM) spectroscopic analyses were exchanged into 25 mM MOPS (pH 6.75) by repeated concentration and dilution in Centricon 30 (Amicon) centrifugal concentrators. The final subunit concentration was 0.5 mM for the non-fusion forms of TfdA and 0.4 mM for the MBP-TfdA proteins. CuCl₂ was added to a concentration of 450 μM and 350 μM, respectively. Buffered solutions of α-KG and 2,4-D were added to final concentrations of 5 mM. Glycerol was present at 40% in all samples.

X-band EPR spectra were obtained at 77K on a Bruker ESP-300E spectrometer. ESEEM data were collected on a home-built spectrometer; the microwave bridge of this instrument has been previously described in detail (20). Data collection and analyses were controlled by a Power Computing model 200 Power PC using software written with LabView v. 5.01 (National Instruments). Electron spin echoes were digitized, averaged,

and integrated by a Tektronix model 620B digital oscilloscope interfaced to the spectrometer computer via an IEEE-488 bus. Two four-channel delay and gate generators (Stanford Research Systems model DG535), a Bruker BH-15 magnetic field controller, and a Hewlett-Packard model 8656B radiofrequency synthesizer were also interfaced using IEEE-488 protocol. Data were collected using a reflection cavity that employed a folded microstrip resonator (16). A three-pulse stimulated echo sequence (90° - τ - 90° -T- 90°) was used. ESEEM spectra were generated by Fourier transformation of the time-domain data using dead time reconstruction (23). Simulations of the experimental data were performed on a Sun SparcII work station. Simulation programs were written in FORTRAN and based on the density matrix formalism developed by Mims (22). Software for the frequency analysis of the experimental and simulated data was written in Matlab (Mathworks, Natick, MA).

Results

Production of the mutant TfdAs

Initially, all of the mutant genes were expressed from their pUC19-based plasmids except for *tfdA* genes encoding H113A, H167A and H200A TfdA, which were in pBC KS⁻-derived plasmids. Using the standard protocol to produce soluble, wild-type TfdA (growth at 30°C to early stationary phase), only the H8A, H113A, D115A, H216A, and H235A variants existed as soluble proteins. All of the other TfdA variants were present as inclusion bodies even when grown at lower temperatures (22°C), in M9 minimal medium, or in LB broth containing 660 mM sorbitol and 2.5 mM betaine (1). In addition,

IPTG-controlled production of H167A and H262A proteins from mutant genes cloned into pET23a did not yield soluble samples even when the harvested cell pellets were suspended in buffer containing 20% glycerol to limit protein aggregation.

To overcome the solubility problems for the five TfdA variants, MBP-TfdA fusion proteins were created. Wild-type TfdA and the MBP-TfdA fusion protein had essentially identical k_{cat} and very similar K_{m} values for α -KG and 2,4-D (Table 5). A slight increase in the apparent K_{D} Fe(II) may reflect some metal binding capacity of MBP. Since the presence of the fusion protein did not appear to greatly affect the kinetic parameters of wild-type enzyme, similar fusion proteins were created for the H167A, H200A, H213A, H245A, and H262A TfdA variants.

Kinetic analyses of altered TfdAs

Results from kinetic analyses of the four active mutant proteins are summarized in Table 5. H8A TfdA was soluble and active, but was rapidly proteolyzed to an inactive form. By electrophoretic comparisons, the cleavage site appeared to be the same as in wild-type TfdA (between Arg77 and Phe78) (7). The rate of proteolysis of H8A TfdA was enhanced compared to that seen for the wild-type enzyme despite the presence of EDTA and protease inhibitors in the purification buffer. Because purified H8A TfdA was more than 75% degraded, the catalytic rate constant was calculated on the basis of the estimated amount of intact enzyme. These calculations indicate rates and K_{m} values similar to those for the wild-type enzyme. Similarly, the kinetic parameters for H235A TfdA were comparable to the native enzyme. In contrast, two variants exhibited differences from wild-type enzyme in their kinetic parameters. The H213A MBP-TfdA

variant exhibited a twenty-fold reduction in k_{cat} and a ten-fold increase in K_m for 2,4-D. In addition, H216A TfdA had a modest (2.5-fold) increase in the K_m for 2,4-D and no change in catalytic rate. The other kinetic parameters for H213A MBP-TfdA and H216A TfdA (K_m for α -KG and K_D for ferrous ion) did not differ significantly from the wild-type values. Six soluble TfdA variants (H113A, D115A, MBP-H167A, MBP-H200A, MBP-H245A and MBP-H262A) exhibited no activity even when assayed with elevated substrate and cofactor concentrations (10 mM α -KG, 5 mM 2,4-D, 250 μ M Fe(II)).

Table 5. Summary of the kinetic parameters for active TfdA variants

TfdA Sample	k_{cat} min^{-1}	K_m α KG μM	K_m 2,4-D μM	K_D Fe(II) μM
wild-type	442 \pm 33	4.9 \pm 0.73	19.3 \pm 3.7	2.0 \pm 0.5
MBP-fusion	411 \pm 23	9.9 \pm 1.8	33.7 \pm 2.5	15.2 \pm 5.4
H8A ^a	284 \pm 6.9	6.5 \pm 1.8	17.7 \pm 3.8	1.9 \pm 0.7
MBP-H213A	22.1 \pm 2.9	8.3 \pm 2.9	318 \pm 44	27.7 \pm 9.8
H216A	474 \pm 47	6.05 \pm 2.6	52 \pm 5	2.4 \pm 1.7
H235A	284 \pm 25	9.6 \pm 1.6	34 \pm 8	1.4 \pm 1.7

^a More than 75% of the protein was present as the degradation product. The k_{cat} was estimated from the active, full-length fraction.

Evaluation of the Structural Consequences of the Mutations

To assess whether the inactive mutant proteins assumed conformations similar to the wild-type enzyme, their apparent molecular weights were estimated by gel filtration analysis. The observed size of wild-type TfdA was found to be 51 kDa by comparison to protein standards, suggesting that TfdA forms a compact dimer or an elongated monomer. The elution volume for both H113A and D115A corresponded exactly to wild-type TfdA indicating that these proteins are not significantly altered in their quaternary structure. MBP-TfdA eluted both in the void volume (approximately 25 % of the protein) and at a position corresponding to 216 kDa (roughly 75% of the protein), suggesting that

MBP-TfdA forms at least a dimer. Because each MBP-TfdA subunit is comprised of two domains separated by a thirteen amino acid linker, the resultant protein may migrate with a larger apparent molecular weight. MBP-H167A and MBP-H200A samples demonstrated the same two-peak profile as MBP-TfdA, but with larger proportions eluting in the void volume. MBP-H245A and MBP-H262A proteins were soluble, however, gel filtration analysis indicated the presence of only highly aggregated material eluting in the void volume. Because these mutant proteins exhibited aberrations in their folding properties, the catalytic role of His 245 and His 262, if any, could not be assessed.

EPR Spectroscopic Characterization of Variants with Altered Metal Sites

The TfdA metallocenter properties were examined by EPR spectroscopy. For the purposes of these experiments, the diamagnetic Fe(II) metallocenter of TfdA was substituted with spectroscopically active Cu(II) ion. Although the Cu(II) form of TfdA is inactive, Cu(II) binds competitively with respect to Fe(II) ($K_i = 1-3 \mu\text{M}$) and Cu(II)-substituted TfdA has been used previously to study the metal coordination environment of this enzyme in the presence and absence of substrates (3, 34). Spectral parameters of wild-type Cu(II)-TfdA, Cu(II)-TfdA + α -KG, and Cu(II)-TfdA + α -KG + 2,4-D (Figure 5A and Table 6), agreed well with those reported previously (34). Earlier studies of Cu(II)-substituted wild-type TfdA indicated that the metal was bound in a tetragonal environment with a mixture of O and N ligands in the equatorial plane. Upon addition of α -KG and 2,4-D, the spectral parameters were altered to a more rhombic signal with accompanying resolution of ligand hyperfine coupling (Figure 5A). These results suggest that binding of the cofactor and substrate to the enzyme leads to a better-defined copper

Figure 5. X-band CW-EPR spectra of Cu(II)-substituted TfdA variants.

EPR spectra were obtained at 77 K for the following samples (substrate concentrations were 5 mM, when present). **A**, (Top to bottom) Wild-type Cu-TfdA in the absence of substrates, with α -KG, and with α -KG + 2,4-D. **B**, H113A Cu-TfdA in the absence of substrates, with α -KG, and with α -KG + 2,4-D. **C**, D115A Cu-TfdA in the absence of substrates, with α -KG, and with α -KG + 2,4-D. **D**, MBP-H167A Cu-TfdA in the absence of substrates, with α -KG, and with α -KG + 2,4-D. **E**, MBP-H200A Cu-TfdA in the absence of substrates and in the presence of α -KG + 2,4-D. Spectral parameters are listed in Table 6.

Figure 5. X-band cw-EPR spectra of Cu(II) substituted TfdA variants

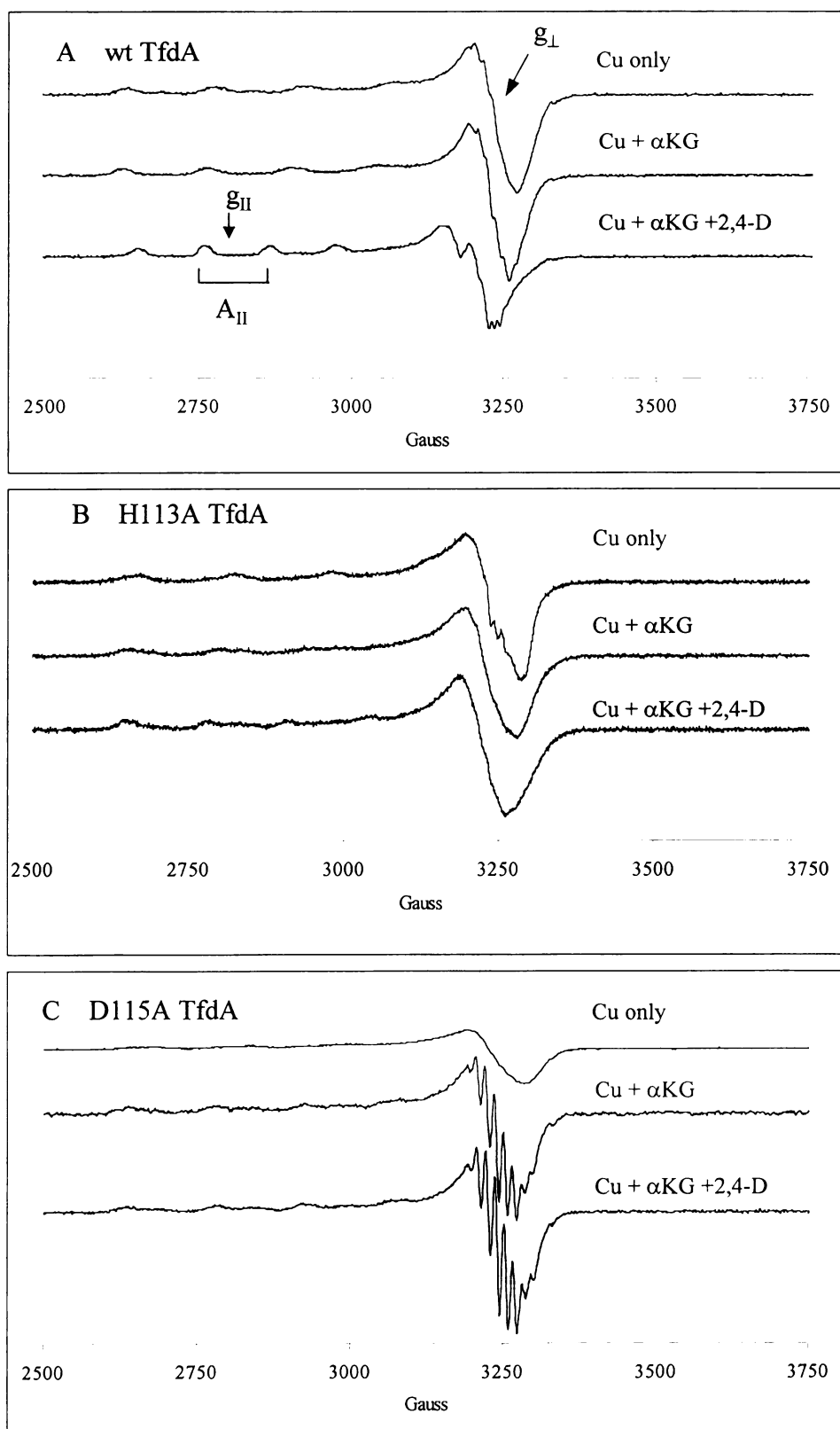


Figure 5. (con't)

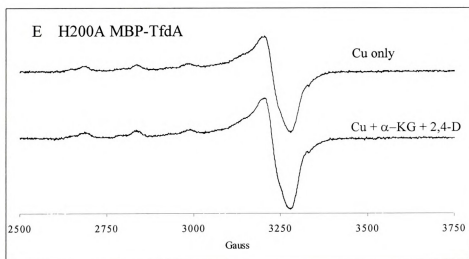
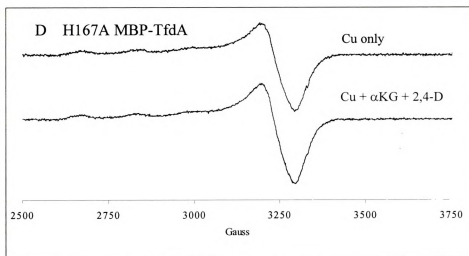


Table 6. Summary of the EPR spectral parameters for Cu(II)-substituted TfdA variants.

	g_{\parallel}	A_{\parallel} mT	g_{\perp}
wild-type TfdA	2.34	16.3	2.07
wild-type TfdA/ α -KG	2.36	15.1	2.07
wild-type TfdA/ α -KG/2,4-D	2.38	12.0	2.09
H113A	2.30	16.6	2.07
H113A/ α -KG	2.33	15.8	2.07
H113A/ α -KG/2,4-D	2.35	14.0	2.08
D115A	2.30	17.0	2.06
D115A/ α -KG	2.30	16.2	2.06
	2.34	16.8	2.06
D115A/ α -KG/2,4-D	2.30	16.2	2.06
	2.34	16.8	2.06
MBP-H167A	2.30	17.1	2.07
MBP-H167A/ α -KG/2,4-D	2.30	17.1	2.07
MBP-H200A	2.30	17.1	2.07
	2.34	16.1	2.07
MBP-H200A/ α -KG/2,4-D	2.30	17.1	2.07
	2.34	16.1	2.07



site in the enzyme (34) and the decreased values for A_{\parallel} upon addition of substrates (A_{\parallel} = 12.0 mT) indicated a significant distortion from planarity.

The effects of the amino acid substitutions on metalcenter structure in the TfdA variants with quaternary structures similar to the corresponding wild-type protein (H113A, D115A, MBP-H167A and MBP-H200A TfdA) were assessed by EPR spectroscopy. Because there were no significant differences between the spectra of MBP-TfdA and the non-fusion wild-type form of the protein (data not shown), H167A and H200A TfdA were analyzed as MBP fusion. In all cases, EPR spectra of the Cu(II)-substituted TfdA variants showed contributions from multiple copper species. The mixture of copper centers may have resulted from either copper interactions in other regions of the protein or the presence of multiple binding modes at the active site.

The EPR spectra for Cu-H113A TfdA (Figure 5B and Table 6) differed significantly from spectra of wild-type enzyme. Importantly, these spectra showed clear changes in Cu(II) g-values and hyperfine tensor principal values upon substrate additions consistent with the binding of copper to the active site pocket. The broadening of the EPR signal in the g_{\parallel} region upon addition of α -KG suggested a mixture of copper coordination environments consistent with a less tightly bound metal site.

The EPR spectrum of D115A TfdA (Figure 5C) had parameters similar to those observed in the copper-substituted wild-type protein (Table 6), although with less resolution of A_{\parallel} . Addition of α -KG (in the presence or absence of 2,4-D) had a dramatic effect on the appearance of the D115A data, enhancing resolution of the Cu hyperfine peaks at g_{\parallel} and the ligand hyperfine structure in the g_{\perp} region (Figure 5C). The appearance of these superhyperfine interactions may have resulted from a subtle shift in

the orientation of the principal g-tensor such that the imidazole ligands occupied an increasingly equatorial position (31). These results were consistent with the formation of a tighter or more regular copper binding site upon addition of the cofactor. Again, the perturbations of the spectrum upon α -KG addition were consistent with copper binding to the active site.

MBP-H167A TfdA (Figure 5D) and MBP-H200A TfdA (Figure 5E) EPR spectra were poorly resolved and showed evidence for multiple modes of copper binding. Significantly, few changes were seen upon addition of either α -KG or 2,4-D. The MBP-H200A EPR spectrum (Figure 5E) was more defined than that of H113A or MBP-H167A, and clearly showed a second set of resonances of lower amplitude with parameters identical to those observed for the copper-substituted wild-type enzyme (Table 6). The broadness of the resonances in the MBP-H167A sample suggested that a similar situation may occur in that enzyme as well.

ESEEM Spectroscopic Characterization of Variants with Altered Metal Sites

ESEEM spectroscopy was used to gain additional insight into the number of nitrogen ligands that create the copper centers in the TfdA variants. As reported previously, ESEEM analysis of wild-type Cu(II)-TfdA indicated the presence of two equatorial histidines directly coordinated to the metal (34). The Fourier transformed 3-pulse ESEEM data, collected near $g_{||}$, for wild-type Cu(II) TfdA with α -KG showed sharp peaks at 0.6, 0.9, and 1.5 MHz and a broad feature at 3.5 MHz (Figure 6). This signature is typical of copper bound by an equatorial imidazole. The narrow combination bands at 2.1, 2.5, and 3.1 MHz (Figure 6) indicated the presence of more than one histidine per

copper site (19, 20, 24). Simulations of the ESEEM data for the wild-type enzyme plus α -KG, generated with the density matrix approach of Mims (22) and the parameters for copper coordinated by two *identical* equatorial histidines, are superimposed on the experimental data in Figure 6. ESEEM data for Cu(II)-TfdA in the presence of α -KG plus 2,4-D were analyzed by a similar method (data not shown). A substantial decrease in the modulation intensity and disappearance of the combination bands (34) upon addition of both substrates is consistent with the loss of one histidine from the equatorial plane.

Similar analyses of Cu(II)-substituted TfdA variants were used to compare their metalcenter structure to that of the wild-type enzyme. Three pulse ESEEM patterns were generated for the H113A, MBP-H167A, and D115A variants of TfdA (Figure 7) as well as for the MBP-H200A samples (data not shown). To normalize the data, the amplitudes in the spectra for all four mutants were corrected to account for differences in baseline frequencies. Samples for each TfdA variant gave rise to low frequency modulations indicative of equatorially-bound histidine ligands. The ESEEM spectra from H113A (Figure 7A) and MBP-H200A (not shown) variants were nearly identical and show modulations that were considerably weaker than those measured for MBP-H167A (Figure 7B) and D115A (Figure 7C). As for wild-type spectra, the data were simulated with a program based on Mims' density matrix formalism, assuming a system of spherical symmetry. In each case, the ratio of modulated signal intensity to unmodulated signal intensity was suggestive of copper bound in more than one coordination environment. The differences in strength of copper binding to the active site can be visualized in Figure 7 by comparing of the peak heights of a given spectrum (modulated frequency) to the background signal that is observed at the end of data collection upon shift to the direct

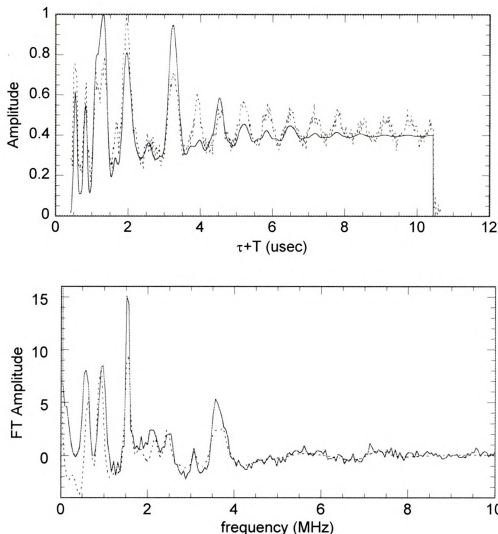


Figure 6. 3-Pulse ESEEM spectra of Cu-substituted wild-type TfdA with 2-histidine simulation data.

ESEEM spectrum of wild-type Cu(II)-TfdA + α -KG (solid) and computer-simulated data for Cu(II) bound by two identical histidines (dashed) (A) and the corresponding frequency domain spectrum (B). Parameters for data collections were magnetic field = 2800 G, $\tau = 375$ ns, $T = 50$ ns, $\nu = 8.98$ GHz; 4.2 K. Cu hyperfine parameters: $g_{xy} = 2.05$, $g_z = 2.34$, $A_{xx} = A_{yy} = 20$ MHz, $A_{zz} = 487$ MHz, Superhyperfine parameters: $g_N = 0.40347$, $A_{iso} = 1.7$ MHz, radius = 2.75 Å, $[\theta, \phi] = [2.37, 2.07]$ radians, $e^2qQ = 1.60$ MHz, $\eta = 0.75$, NQI $[\alpha, \beta, \gamma] = [0.50, 1.1, 0.1]$ radians. The simulated data were treated with an exponential decay function to give $y'_{ij} = (y_{ij} - 0.17) * \exp\left(\frac{(\tau + T)}{3500}\right)^{1.5} + 0.17$. For each simulation, a background decay function was applied to allow the amplitudes of the initial 1.5 μ sec of the simulations to match the data.

current (unmodulated frequency). Although this ratio was less than the wild-type value for all of the TfdA variants, H113A and MBP-H200A had a markedly decreased capacity to constrain copper to one geometry in the absence of substrates.

Fourier transformations of the data shown in Figure 7 yielded major features at 0.7, 1.5, and 4.0 MHz indicative of histidines equatorially coordinated to Cu(II) (24). Although Cu-bound histidines were visible in the H113A and MBP-H200A spectra, the ESEEM signals were too weak to be consistent with one dominant Cu(II) conformation, and thus were omitted from further analyses. The frequency and Fourier transformed data, with the corresponding simulations, are shown for D115A (Figure 8) and MBP-H167A TfdA (Figure 9). In both cases, the large unmodulated component of the data required a severe decay function in order to simulate the data. In addition, it was necessary to use the average of several simulation data sets with varying isotropic hyperfine coupling constants to compensate for the presence of multiple copper binding environments identified by EPR spectroscopy. Although the combination lines were weaker in the data for D115A than for wild-type TfdA, the combination line at approximately 3.0 MHz was observed and its frequency was predicted nicely by the 2 His simulation data. Thus, these data were most consistent with two histidine ligands to the Cu(II) site in this protein. The broadness of the Fourier transformed spectrum for D115A TfdA and the subsequent difficulty in observing the combination lines most likely reflects a distribution of ^{14}N superhyperfine couplings from multiple Cu(II) centers in D115A TfdA which is consistent with our use of an average of several isotropic hyperfine coupling constants to simulate the data.

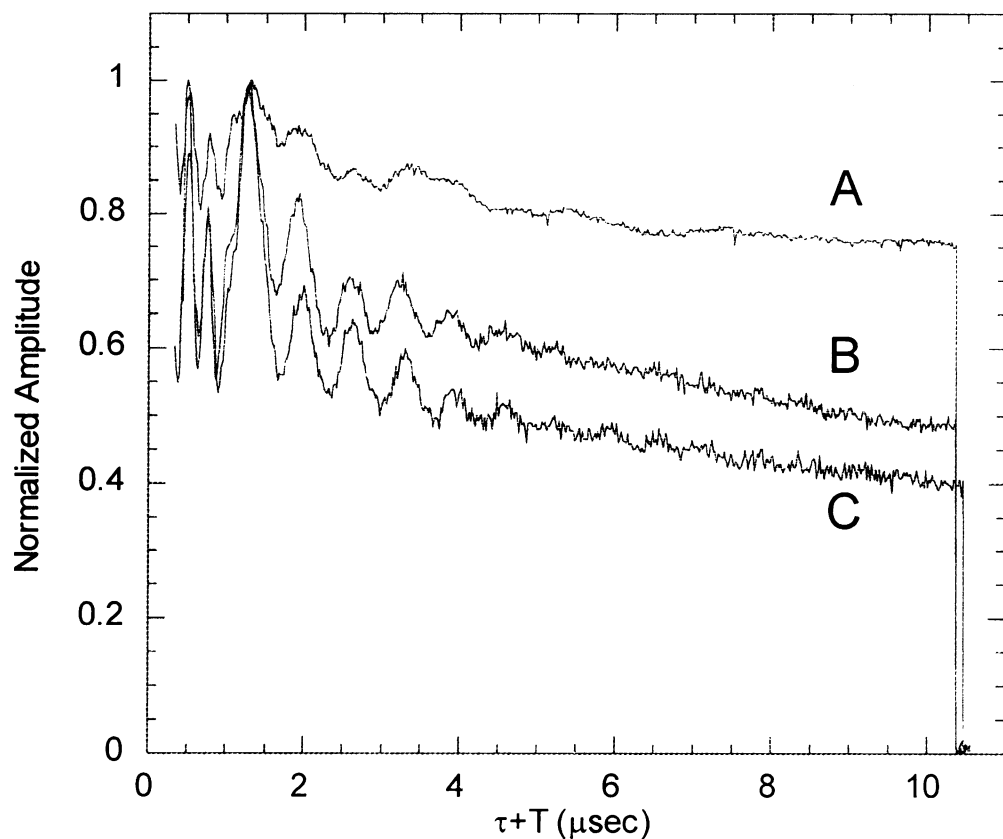


Figure 7. 3-Pulse ESEEM time-domain spectra of TfdA variants.

Spectra for H113A Cu-TfdA (A) (magnetic field = 3050 G, τ = 300 ns, T = 40 ns); MBP-H167A Cu-TfdA (B) (magnetic field = 3100 G, τ = 300 ns, T = 40 ns) and D115A Cu-TfdA (C) (magnetic field = 3050 G, τ = 385 ns, T = 55 ns, ν = 8.8 GHz) are compared. All were collected at 4.2 K.

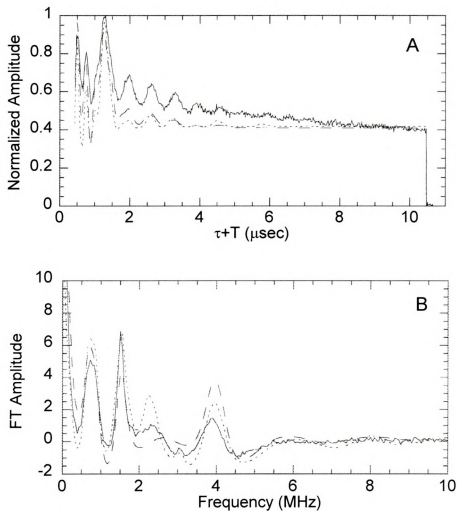


Figure 8. Spectral simulation of ESEEM data for D115A-Cu-TfdA.

Experimental (solid line), computer-simulated 1-His (dashed line), and simulated 2-His (dotted line) (A) and the corresponding time-domain spectra (B) for copper-substituted D115A TfdA are shown. Magnetic Field = 3050 G, $\tau = 230$ ns, $T = 50$ ns, $\nu = 8.8$ GHz, 4.2 K, $g_N = 0.40347$, $e^2qQ = 1.55$ MHz, $\eta = 0.87$, $A_{xx} = 1.6$ MHz, $A_{yy} = 1.9$ MHz, $A_{zz} = 2.2$ MHz. The simulated data were treated with an exponential decay function to give

$$y'_{ij} = (y_{ij} - 0.05) * \exp\left(-\frac{(\tau + T)^{0.8}}{600}\right) - 0.05.$$

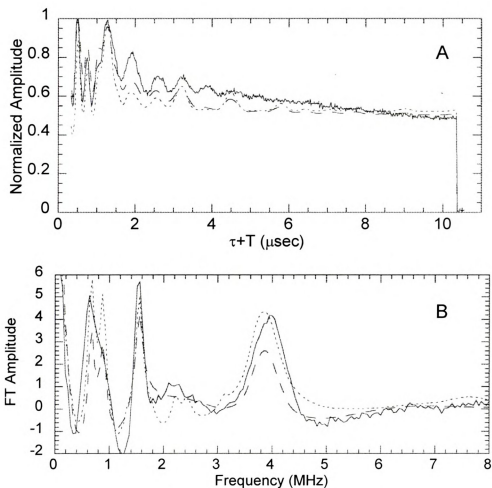


Figure 9. Spectral simulation of ESEEM data for Cu(II) MBP-H167A TfdA.

Experimental (solid line), computer-simulated 1-His (dashed line), and 2-His (dotted line) time-domain spectra (A) and the corresponding Fourier transformed data (B) are shown. Magnetic field = 3100 G, $\tau = 300$ ns, $T = 40$ ns, $\nu = 8.8$ GHz, 4.2 K, $g_N = 0.40347$, $e^2qQ = 1.60$ MHz, $\eta = 0.82$, $A_{xx} = 1.55$ MHz, $A_{yy} = 1.9$ MHz, $A_{zz} = 2.0$ MHz. The simulated data were treated with an exponential decay function to give

$$y'_{jj} = (y_{jj} - 0.03) * \exp\left(\frac{(t+T)^{0.5}}{350}\right) - 0.03.$$

Simulations of the MBP-H167A TfdA also suggested the presence of two histidines per copper (Figure 9). The peak broadness in the experimental data resulted in our inability to resolve the features at 0.6 and 0.9 MHz, indicative of a heterogeneous population of copper sites. Simulations achieved by averaging of multiple isotropic hyperfine coupling constants, as in those for D115A, predicted the coalescence of these peaks. The number of averaged data sets required to simulate the MBP-H167A spectra indicated that the copper center in this protein was more disordered than that in D115A TfdA. The increased number of unconstrained copper binding environments in MBP-H167A TfdA may have resulted from non-specific binding to the MBP domain or a small population of misfolded TfdA protein, as observed in gel filtration experiments.

The Cu-substituted forms of H113A, D115A, MBP-H167A, and MBP-H200A TfdA species were also analyzed in the presence of α -KG and 2,4-D. Although the Cu(II) site in wild-type TfdA appeared to undergo significant rearrangement upon binding of substrates, only slight variations in the lineshape of the higher frequency peak at \sim 4.0 MHz were observed for H113A, MBP-H167A, and MBP-His 200A. The substrate-dependent changes in the copper site of H113A TfdA upon substrate addition that were observed by EPR spectroscopy were not well defined in the ESEEM spectra, again indicating a less constrained copper site. Addition of α -KG and 2,4-D to D115A TfdA led to enhanced definition of the D115A copper site similar to what was observed by EPR analysis (Figure 5). The ternary complex of Cu(II)-D115A TfdA exhibited coherence in the frequency data at longer times with a slightly increased depth of modulation. These changes were *not* accompanied by a significant increase in unmodulated intensity (Figure 10) indicating that the copper was predominantly found in



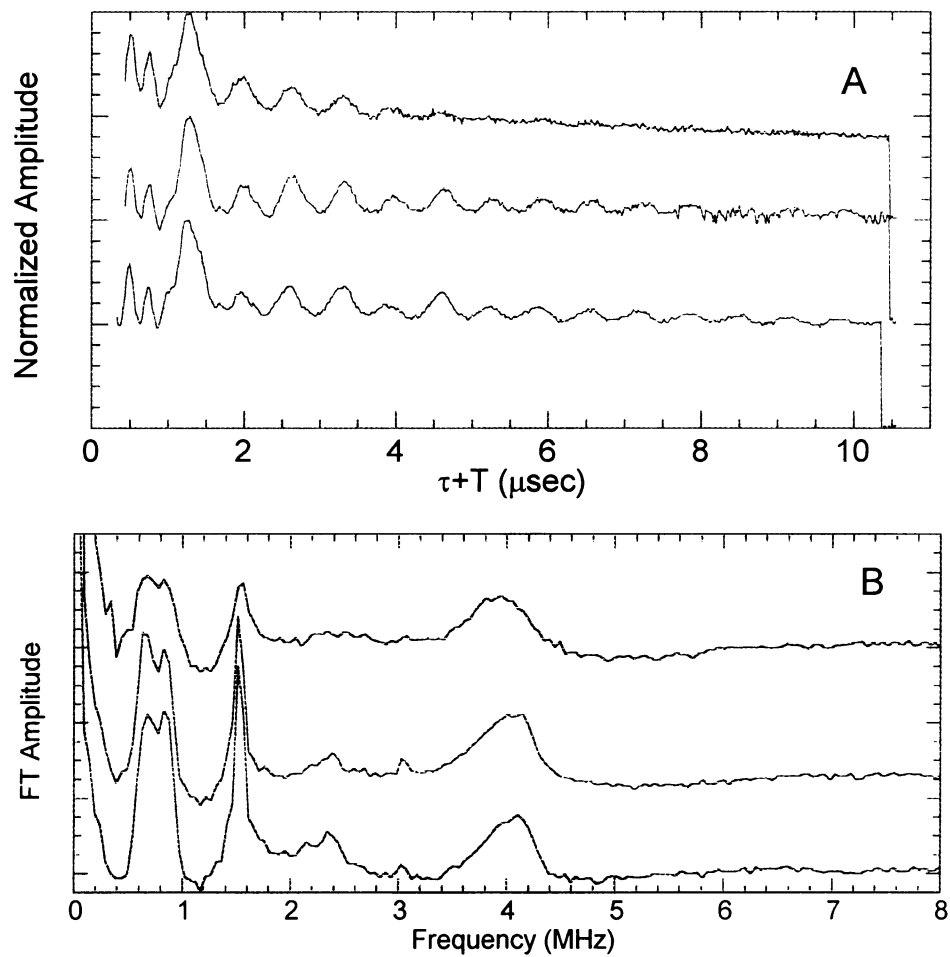


Figure 10. 3-pulse ESEEM of Cu(II) D115A TfdA (4.2K).

(Top to bottom) ESEEM spectra for Cu(II) D115A TfdA in the absence of substrate, with 5 mM α -KG, and with 5 mM α -KG + 5 mM 2,4-D (A) and the corresponding Fourier transformed data (B) are shown. Conditions for these measurements were identical to those of Figure 6.

a single environment. ESEEM spectra of the D115A TfdA ternary complex showed resolution of all three combination lines from the electron spin manifold that gave rise to the intense low-frequency peaks (Figure 10B). These data provided convincing evidence for two equatorial histidine ligands to the copper in D115A TfdA in the presence of substrates and supported the conclusions drawn from substrate-free Cu (II)-D115A TfdA ESEEM spectra. The enhanced intensity and definition upon substrate binding suggested that α -KG constrained the geometry of the copper at the active site.

Discussion

Our results demonstrate the importance of multiple histidines and one aspartate for TfdA activity. EPR, ESEEM, and extended x-ray absorption fine structure spectroscopies of both the Fe(II)- and Cu(II)-forms of wild-type TfdA had previously indicated that the resting enzyme has two imidazoles and a mixture of bound nitrogens and oxygens as ligands to the metal (3, 34). Changes in the Cu-EPR spectral parameters upon addition of α -KG are consistent with an increased number of oxygen ligands to the metal, but ESEEM and X-ray absorption data indicated that both imidazole ligands are retained. Addition of 2,4-D, however, leads to the displacement or g-tensor reorientation of a histidine out of the equatorial plane (3, 34).

Mutation of His 113 or Asp 115 to alanine both eliminates activity and greatly alters the structure of Cu(II) metallocenter site. Significantly, however, substrate binding perturbs the spectra of these sites consistent with the metal binding to the active site pocket. These residues comprise the H-X-D motif which is conserved in enzymes related to TfdA (Appendix A) and common to all other known α -KG-dependent dioxygenases

(2) (Chapter 1). Site-directed mutagenesis studies analogous to those described here demonstrated the importance of this motif in a number of Group I enzymes including aspartyl, lysyl, prolyl, and flavanone hydroxylases (15, 18, 21, 25, 27). Crystal structures of IPNS and DAOCS established these residues as ligands to the metal. My studies support the proposal that residues in the H-X-D motif are ligands to the metal in TfdA and, most likely, other Group II enzymes.

Cu(II)-D115A TfdA ESEEM spectra indicate the presence of two imidazole ligands, whereas similar analyses of the H113A proteins shows evidence of multiple copper binding environments. Clearly, the absence of the aspartate ligand results in a significantly altered binding site, producing a less structurally-defined copper geometry, and contributes to the increased damping of the ESEEM. Addition of α -KG to this mutant, however, results in increased resolution in the EPR spectrum and ESEEM pattern, indicating that the binding of this cofactor locks the geometry of the active site into place. Together, these data may suggest that the histidines are primarily responsible for Cu(II) binding, and Asp 115 may contribute more to the orientation of the metal. The properties of copper predict a much stronger interaction with nitrogen rather than oxygen ligands; in fact, there are no mononuclear copper enzymes known to have a carboxylate metal ligands (13). Because of differences in the preferred environments of Fe(II) and Cu(II), it is difficult to draw conclusions about the specific electronic role of Asp 115 in the native Fe(II) TfdA based on these observations.

The identity of the second metal binding histidine, predicted by various spectroscopic studies, is less clear. A previously described motif (H-X-D-X₋₅₅-H-X₁₀-R-X-S) common to IPNS and related enzymes (2, 18) would best match His 167 in TfdA

except that the terminal arginine is displaced. Spectral simulations of H167A, however, are consistent with the presence of two imidazole nitrogens per copper in this protein. Furthermore, His 167 is replaced with an arginine in the TfdA sequence from pLJB in *Burkholderia cepacia* (Appendix A). Thus, it is unlikely that His 167 is one of the three metal ligands necessary to create the metallocenter. EPR and ESEEM analyses of H200A TfdA suggest that His 200 is important for creation of the metallocenter. Although His 200 is conserved among the enzymes with high identities to TfdA, such as TauD from *E. coli* and sulfonate/ α -KG dioxygenase from yeast, a corresponding histidine is not found in more distantly related Group II enzymes such as γ -butyrobetaine hydroxylase or clavamate synthase (Appendix A). Mutational analysis of prolyl 4-hydroxylase (25) provided evidence for a non-ligand histidine at active site that is important for α -KG binding and controlling the decarboxylation of α -KG in the absence of substrate. Perhaps His 200 serves a similar function in TfdA providing an explanation for the changes in active site structure upon its alteration. Sequence comparisons of all Group II enzymes reveal that His 262 in TfdA is the only other invariant histidine and I suggest that this is most likely the third metal-binding residue. Supporting my assessment of His 262 as a metal ligand, this residue lies ten amino acids away from Arg 273 creating an H-X₁₀-R motif similar to that in DAOCS and related enzymes (18). It is surprising, however, that the H262A variant cannot fold properly and forms inclusion bodies when overproduced in *E. coli*. For comparison, wild-type TfdA is routinely purified in its apo-enzyme form and TfdA activity is immediately detected upon addition of Fe (II). Together, these data suggest a more general motif for α -KG-dependent dioxygenases, H-X-D/E-X_n-H-X₁₀₋₁₃-R (the carboxylate occurs as a glutamate in clavamate synthase, see Appendix A),



where X_n varies with the different subgroups within the superfamily (Group I, $n=44-65$; Group II $n=123-153$; Group III, $n=74-104$).

His 213 and His 216 may also be present at or near the TfdA active site. MBP-H213A and H216A TfdA variants had increased K_m values for 2,4-D and the former enzyme also demonstrated a decreased catalytic rate. These data may indicate that His 213 (perhaps also assisted by His 216) facilitates 2,4-D binding by electrostatic interactions between the imidazole nitrogen and the substrate carboxylate group; however, additional studies are required to test this hypothesis. The importance of the 2,4-D carboxylate for binding to TfdA is indicated by the inability of phenoxyethanol to serve as a substrate (7). Neither His 213 nor His 216 are conserved among other related α -KG-dependent dioxygenases. The divergence of sequences in this region may reflect differences in the residues required to bind substrates unique to each enzyme.

Our results provide no evidence to indicate that His 8, His 235, or His 245 are critical for catalysis. The H8A variant exhibits enhanced protease sensitivity, but the full-length protein possesses near wild-type activity. Similarly, the H235A protein is nearly unaffected in its activity. Neither of these residues is conserved in homologous sequences. As described for the H262A TfdA variant, His 245 appears to be structurally important. Because H262A and H245A derivatives of TfdA exist in non-native, highly aggregated conformations, we were unable to assess whether these residues may also play a catalytic role. Although His 245 is not conserved in these sequences, it is in the C-terminal half of the protein which in other α -KG-dependent dioxygenases show a higher level of similarity than the overall sequence comparisons (12). This region might be more constrained for structural reasons.

The H-X-D/E-X_n-H motif, which is found in all known α -KG dependent dioxygenases, is an example of the more general structural arrangement (2- His-1- carboxylate) found in non-heme Fe (II) enzymes including extradiol dioxygenases and pterin-dependent hydroxylases (9). It is proposed that these three ligands anchor the iron in the active site of the enzyme while leaving three open coordination sites available for the binding of substrate, cofactor and oxygen. Several studies suggest that O₂ reacts much more readily with such iron centers after the displacement of solvent molecules by more electronegative substrate molecules (9). In addition, it is the diversity of exogenous ligands that enable non-heme Fe(II)-dependent oxygenases to catalyze such a wide range of reactions.

Our proposed model of the active site of TfdA is shown in Figure 11. His 113, Asp 115 and a third histidine tentatively identified as His 262 are shown as ligands to the metal. As in the crystal structures of both DAOCS and IPNS, water molecules are thought to occupy the three remaining coordination sites in substrate-free enzyme. The model includes a likely binding mode for α -KG based on the DAOCS crystal structure (33). Recent spectroscopic studies of clavaminic synthase (26), TauD (32) and TfdA (10) are consistent with a similar mode of α -KG binding in these enzymes. We have no evidence to suggest direct binding of 2,4-D to the metal center, and indicate the presence of a separate 2,4-D binding site adjacent to the metal in the model. Mutation of His 213 affects both substrate binding and the rate of catalysis so I show this residue at the active site to indicate potential substrate interaction, but its precise role is still to be defined. In the absence of a crystal structure, the site-directed mutagenesis, metalcenter spectroscopy, and kinetic analysis studies described here provide the most complete

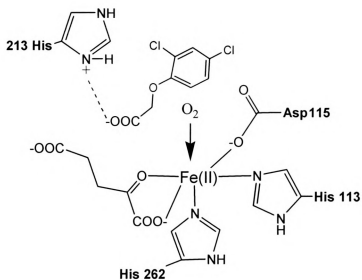


Figure 11. Model for the active site of TfdA.

The three residues proposed to ligate the ferrous ion of TfdA are shown along with a possible coordination mode for the substrates, α -KG and 2,4-D. His 213, implicated in binding 2,4-D, is also illustrated.



working model of the TfdA active site. This model begins to define the necessary elements for catalysis in Group II α -KG-dependent dioxygenases and finds similarities between these enzymes and other well-studied representatives of this superfamily.

Literature Cited

1. **Blackwell, J. R., and R. Horgan.** 1991. A novel strategy for the production of a highly expressed recombinant protein in an active form. *FEBS* **295**:1-12.
2. **Borovok, I., O. Landman, R. Kreisberg-Zakarin, Y. Aharonowitz, and G. Cohen.** 1996. Ferrous active site of isopenicillin N synthase: genetic and sequence analysis of the endogenous ligands. *Biochemistry* **35**:1981-1987.
3. **Cosper, N. J., C. M. V. Stålhandske, R. E. Saari, R. P. Hausinger, and R. A. Scott.** 1999. X-Ray absorption analysis of Fe(II) and Cu(II) forms of an herbicide-degrading α -ketoglutarate dioxygenase. *J. Biol. Inorg. Chem.* **4**:122-129.
4. **De Carolis, E., and V. De Luca.** 1994. 2-Oxoglutarate-dependent dioxygenases and related enzymes: biochemical characterization. *Phytochem.* **36**:1093-1107.
5. **Eichhorn, E., J. R. van der Ploeg, M. A. Kertesz, and T. Leisinger.** 1997. Characterization of α -ketoglutarate-dependent taurine dioxygenase from *Escherichia coli*. *J. Biol. Chem.* **272**:23031-23036.
6. **Fukumori, F., and R. P. Hausinger.** 1993. *Alcaligenes eutrophus* JMP134 "2,4-dichlorophenoxyacetate monooxygenase" is an α -ketoglutarate-dependent dioxygenase. *J. Bacteriol.* **175**:2083-2086.
7. **Fukumori, F., and R. P. Hausinger.** 1993. Purification and characterization of 2,4-dichlorophenoxyacetate/ α -ketoglutarate dioxygenase. *J. Biol. Chem.* **268**:24311-24317.
8. **Hedden, P.** 1992. 2-Oxoglutarate-dependent dioxygenases in plants: mechanism and function. *Biochem. Soc. Trans.* **20**:373-377.
9. **Hegg, E. L., and L. Que Jr.** 1997. The 2-His-1-carboxylate facial triad. *Eur. J. Biochem.* **250**:625-629.
10. **Hegg, E. L., A. K. Whiting, J. McCracken, R. P. Hausinger, and J. Que, L.** 1999. The herbicide-degrading α -keto acid enzyme TfdA: metal coordination environment and mechanistic insights. *Biochemistry In press*.
11. **Hogan, D. A., T. A. Auchtung, and R. P. Hausinger.** 1999. Cloning and characterization of a sulfonate/ α -ketoglutarate dioxygenase from *Saccharomyces cerevisiae*. *J. Bacteriol.* **181**:5876-5879.
12. **Jia, S., K. McGinnis, W. J. VanDusen, C. J. Burke, A. Kuo, P. R. Griffin, M. K. Sardana, K. O. Elliston, A. M. Stern, and P. A. Friedman.** 1994. A fully

active catalytic domain of bovine aspartyl (asparaginy)- β -hydroxylase expressed in *Escherichia coli*: characterization and evidence for the identification of an active-site region in vertebrate- α -ketoglutarate-dependent dioxygenases. *Proc. Natl. Acad. Sci.* **91**:7227-7231.

13. **Karlin, S., Z. Y. Zhu, and K. D. Karlin.** 1997. The extended environment of mononuclear metal centers in protein structures. *Proc. Natl. Acad. Sci. U S A* **94**:14225-14230.
14. **Kivirikko, K. I., and T. Pihlajaniemi.** 1998. Collagen hydroxylases and the protein disulfide isomerase subunit of prolyl 4-hydroxylases. *Adv. Enzymol. Relat. Areas Mol. Biol.* **72**:328-398.
15. **Lamberg, A., T. Pihlajaniemi, and K. I. Kivirikko.** 1995. Site-directed mutagenesis of the α subunit of the human prolyl 4-hydroxylase. *J. Biol. Chem.* **270**:9926-9931.
16. **Lin, C. P., M. K. Bowman, and J. R. Norris.** 1985. *J. Mag. Res.* **65**:369-374.
17. **Lloyd, M. D., H. J. Lee, K. Harlos, Z. H. Zhang, J. E. Baldwin, C. J. Schofield, J. M. Charnock, C. D. Garner, T. Hara, A. C. Terwisscha van Scheltinga, K. Valegard, J. A. Viklund, J. Hajdu, I. Andersson, A. Danielsson, and R. Bhikhabhai.** 1999. Studies on the active site of deacetoxycephalosporin C synthase. *J. Mol. Biol.* **287**:943-960.
18. **Lukacin, R., and L. Britsch.** 1997. Identification of strictly conserved histidine and arginine residues as part of the active site in *Petunia hybrida* flavanone 3β -hydroxylase. *Eur. J. Biochem.* **249**:748-757.
19. **McCracken, J., J. B. Cornelius, and J. Peisach.** 1989. Quantitative aspects of nitrogen-14 electron spin-echo envelope modulation in Cu(II)-proteins, p. 155-161. *In* C. P. Keijzers, E. J. Riejerse, and J. Schmidt (ed.), *Pulsed EPR: A New Field of Applications*. North Holland Publishers, Amsterdam.
20. **McCracken, J., D.-H. Shin, and J. L. Dye.** 1992. Pulsed EPR studies of polycrystalline cesium hexamethyl hexacyclen sodide. *Appl. Mag. Res.* **3**:305-316.
21. **McGinnis, K., G. M. Ku, W. J. VanDusen, J. Fu, V. Garsky, A. M. Stern, and P. A. Friedman.** 1996. Site-directed mutagenesis of residues in a conserved region of bovine aspartyl (asparaginy)- β -hydroxylase: evidence that histidine 675 has a role in binding Fe^{+2} . *Biochemistry* **35**:3957-3962.
22. **Mims, W. B.** 1972. *Phys. Rev. B: Solid State* **5**:2409-2419.

23. **Mims, W. B.** 1984. Elimination of the dead-time artifact in electron spin-echo envelop spectra. *J. Magn. Res.* **59**:291-306.
24. **Mims, W. B., and J. Peisach.** 1978. The nuclear modulation affect in electron spin echoes for complexes of Cu^{2+} and imidazole with ^{14}N and ^{15}N . *J. Chem. Phys.* **69**:4921-4930.
25. **Myllyharju, J., and K. I. Kivirikko.** 1997. Characterization of the iron- and 2-oxoglutarate-binding sites of human prolyl 4-hydroxylase. *EMBO J.* **16**:1173-1180.
26. **Pavel, E. G., J. Zhou, R. W. Busby, M. Gunsior, C. A. Townsend, and E. I. Solomon.** 1998. Circular dichroism and magnetic circular dichroism spectroscopic studies of the non-heme ferrous active site in clavaminic synthase and its interaction with α -ketoglutarate cosubstrate. *J. Am. Chem. Soc.* **120**:743-754.
27. **Pirkanen, A., A.-M. Kaimio, R. Myllylä, and K. I. Kivirikko.** 1996. Site-directed mutagenesis of human lysyl hydroxylase expressed in insect cells. *J. Biol. Chem.* **271**:9398-9402.
28. **Prescott, A. G., and P. John.** 1996. Dioxygenases: Molecular structure and role in plant metabolism. *Annu. Rev. Plant Physiol. Plant Mol. Biol.* **47**:245-271.
29. **Roach, P. L., I. J. Clifton, V. Fülöp, K. Harlos, G. J. Barton, J. Hajdu, I. Andersson, C. J. Schofield, and J. E. Baldwin.** 1995. Crystal structure of isopenicillin N synthase is the first from a new structural family of enzymes. *Nature* **375**:700-704.
30. **Roach, P. L., I. J. Clifton, C. M. H. Hensgens, N. Shibata, C. J. Schofield, J. Hajdu, and J. E. Baldwin.** 1997. Structure of isopenicillin N synthase complexed with substrate and the mechanism of penicillin formation. *Nature* **387**:827-830.
31. **Rotilio, G., A. F. Agrò, L. Calabrese, F. Bossa, P. Guerrieri, and B. Mondovì.** 1971. Studies on the metal sites of copper proteins: ligands of copper in hemocuprein. *Biochemistry* **10**:616-621.
32. **Ryle, M. J., R. Padmakumar, and R. P. Hausinger.** 1999. Stopped-flow kinetic analysis of *Escherichia coli* taurine/ α -ketoglutarate dioxygenase: interactions with α -ketoglutarate, taurine, and oxygen. *Biochem. In press.*
33. **Valegård, K., A. C. T. van Scheltinga, M. D. Lloyd, T. Hara, S. Ramaswamy, A. Perrakis, A. Thompson, H.-J. Lee, J. E. Baldwin, C. J. Schofield, J. Hajdu, and I. Andersson.** 1998. Structure of a cephalosporin synthase. *Nature* **394**:805-809.

34. **Whiting, A. K., L. Que Jr., R. E. Saari, R. P. Hausinger, M. A. Fredrick, and J. McCracken.** 1997. Metal coordination environment of a Cu(II)-substituted α -keto acid-dependent dioxygenase that degrades the herbicide 2,4-D. *J. Amer. Chem. Soc.* **119**:3413-3414.

CHAPTER 3
CLONING AND CHARACTERIZATION OF A SULFONATE/ α -
KETOGLUTARATE DIOXYGENASE FROM *Saccharomyces cerevisiae*

This chapter is based largely on the published article: Hogan, D.A., T.A. Auchtung, and R. P. Hausinger (1999) "Cloning and characterization of a sulfonate/ α -ketoglutarate dioxygenase from *Saccharomyces cerevisiae*." J. Bacteriol. 181:5876-5879.



Introduction

The *Saccharomyces cerevisiae* genome sequence project revealed an open reading frame, YLL057c, that encodes a protein with 27 % identity to the herbicide-degrading enzyme TfdA (5) and 31.5 % identity to taurine/ α -KG dioxygenase, TauD (4). The product of YLL057c has lower levels of amino acid sequence identity to other α -KG-dependent dioxygenases such as γ -butyrobetaine hydroxylase and clavamate synthase. Alignment of the deduced amino acids from YLL057c to these four sequences shows conservation of the H-X-D and H-X-R motifs that are signatures for the Group II subset of the α -KG-dependent dioxygenase superfamily that I defined in the Introduction of this thesis. The presence of these residues, which were proven to be important in the site-directed mutagenesis studies of TfdA described in Chapter 2, provides strong evidence that the product of YLL057c is an α -KG-dependent dioxygenase.

Given the nearly equivalent levels of identity between TfdA, TauD, and the putative yeast dioxygenase, it is impossible to predict the natural substrate for the yeast enzyme. Although there are no reports of 2,4-D degradation in *S. cerevisiae*, yeast may contain an enzyme involved in the decomposition of other naturally occurring aromatic compounds such as aromatic amino acids or lignin degradation products. Alternatively, the YLL057c product may resemble TauD in its ability to decompose taurine, a naturally occurring sulfonate (6). A number of yeast can use aliphatic sulfonates, such as taurine, cysteate and isethionate, as alternative sulfur sources (17). Sulfonate utilization by *S. cerevisiae* only occurs under aerobic conditions, is independent of sulfate utilizing enzymes, and requires sulfite reductase, consistent with the formation of sulfite prior to assimilation. This pattern of sulfonate utilization is similar to that in *Escherichia coli* and



other enteric bacteria (16, 18), suggesting the presence of a common pathway in these diverse organisms. In *E. coli*, TauD hydroxylates the carbon atom in the C-S bond of taurine to give an unstable intermediate that spontaneously decomposes to sulfite and aminoacetaldehyde (4). There are no reports of an analogous enzyme in fungi.

In this chapter, I report both the characterization of the *S. cerevisiae* YLL057c gene product and studies with the YLL057c deletion mutant to determine whether this enzyme plays a role that is analogous to TfdA in 2,4-D degrading microorganisms or to TauD in *E. coli*.

Materials and Methods

Cloning and expression of YLL057c.

Open reading frame YLL057c (Genbank Accession # Z73162) was PCR amplified and cloned into pET23a for expression in *E. coli*. The 1236-bp YLL057c sequence, which contains no introns, was amplified from λ PM-5392 (ATCC) containing a 30-kb fragment of *S. cerevisiae* chromosome XII, with primers 5'-CAT ATG TAC AGA GGA CGT CGT CGA G -3' and 5'-CTA CAA CAC TTT TCG TCT CCG AGG-3'. The forward primer contained a 5' extension that introduced an *NdeI* restriction site directly upstream of the start ATG codon. Template DNA was added by transferring a small amount of material from a λ PM-5392 plaque, obtained by plating on *E. coli* Y1090 (13), directly to the PCR reaction mix. The PCR reaction mix included 20 mM Tris-HCl (pH 8.4), 50 mM KCl, 1.5 mM MgCl₂, 25 μ M dNTPs (Gibco), 1 μ M of each primer and 0.05 U Taq polymerase (Gibco). The temperature program was comprised of an initial denaturation step at 95°C for 2 min 10 sec, 35 cycles of a denaturation step at 95°C for 1

min, an annealing step at 55°C for 1 min, a 2 min 10 sec extension step at 68°C, and a final extension at 68°C for 6 min. The resulting 1734-bp PCR product (which included additional downstream sequence) was cloned into pCR2.1 TOPO vector (Invitrogen) according to the manufacturer's instructions to give plasmid pCR2.1-YDO. The cloned gene was cut from pCR2.1-YDO with *NdeI* and *SacI* and inserted into pET23a cut with the same enzymes to create pB10. To create an *N*-terminal fusion of the YLL057c gene product to the maltose-binding protein (MBP), YLL057c was amplified from pB10 using the protocol described above with primers 5'-TCT CTA GAA TGT CTC CTG CAG CAG C -3' and 5'-GTC AAG CTT AAA GAA GTG TTG TCG CCG -3'. The forward primer introduced an *XbaI* site directly upstream of the start site for in-frame insertion into pMAL-c2 (New England Biolabs). The amplification product was directly cloned into pGEM-T (Promega) to give pGTYDO16. YLL057c was cut from pGTYDO16 with *XbaI* and *HindIII*, and ligated to pMAL-c2 prepared with the same enzymes to create pMBPYDO, a fusion of the *malE* gene to YLL057c.

Production and purification of YLL057c gene product.

Various efforts to directly express the yeast gene in *E. coli* DH5 α from pB10 failed to achieve high level production of the desired protein. In contrast, a MBP fusion of this product was produced in *E. coli* DH5 α (pMBPYDO), consistent with an increased stability and decreased toxicity imparted by the *N*-terminal extension. Cultures were grown to an A_{600} of 0.4-0.6 at 30 °C in LB containing 100 μ g/ml ampicillin, induced with 0.3 mM IPTG, and incubated for three hours. Harvested cells were suspended 20 mM Tris buffer (pH 7.5) containing 1 mM EDTA, 200 mM NaCl, and 1 mM

dithiothreitol, and lysed by two passages through a French pressure cell at 120 MPa. The cell lysates were spun at 100,000 x g to yield the clarified cell extracts. The 89.7 kD fusion protein was readily purified by passing cell extracts over an amylose column according to manufacturer's instructions followed by elution in the above buffer amended with 10 mM maltose.

Characterization of MBP-dioxygenase fusion protein.

The MBP-dioxygenase fusion protein was assayed for activity towards 2,4-D using the 4-aminoantipyrene assay described previously (5). Activity towards sulfonate-containing compounds was determined by quantifying the amount of sulfite released using Ellman's reagent (5,5'-dithiobis(2-nitrobenzoic acid)) (4). Standard assay conditions were defined as 10 mM dimethylglutarate (pH 7.0), 1 mM α -KG, and 50 μ M Fe(II)-ascorbic acid salt (Sigma) for 5 min at 30°C in the presence of varied substrate concentrations. Consumption of α -[14 C-1]-KG was determined using a previously described method (5). One unit is defined as one μ mol of product formed per min using the standard assay conditions.

Studies with the YLL057c deletion mutant

The *S. cerevisiae* YLL057c deletion mutant, BY4742-11545 and the corresponding wild type strain, BY4742, were obtained from Research Genetics (Huntsville, AL). Overnight cultures for inoculation of sulfur limited media were grown in yeast peptone dextrose (YPD) broth. Mutant cultures were amended with 50 μ g/ml geneticin sulfate antibiotic. To assess the growth of *S. cerevisiae* BY4742-11545 and

BY4742 with alternative sulfur sources, strains were grown aerobically in defined medium (3) with isethionate (250 μM), taurine (250 μM), sulfate (250 μM) or with no sulfur source added. Since geneticin, is sold as a sulfate salt, the antibiotic was omitted from experiments using low sulfur medium.

Results and Discussion

The product of YLL057c was found to be an Fe(II)- and α -KG-dependent dioxygenase capable of utilizing a variety of sulfonates (Figure 12, Scheme 3) but was inactive on 2,4-D. Maximum rates (V_{max}), affinities (K_{M}), and catalytic efficiencies ($k_{\text{cat}}/K_{\text{M}}$) for various substrates are compared in Table 7. Whereas taurine was a relatively poor substrate for the yeast sulfonate/ α -KG dioxygenase (with a moderate reaction rate and high K_{M}), isethionate (2-hydroxy-ethanesulfonate) and taurocholate were turned over more rapidly and bound with much higher affinity by the enzyme. According to their catalytic efficiencies, the best substrates were the synthetic compounds MOPS and *N*-phenyltaurine. Several of the better substrates for this enzyme had large adducts on the amino group, indicating a relaxed substrate specificity for this portion of the molecule. Of the substrates listed in Table 7, only taurine, MOPS (4) and taurocholate (1) were also substrates of *E. coli* TauD. Notably, TauD activity toward taurine exhibits a k_{cat} of 133 min^{-1} , which is the same order of magnitude as found here for the yeast enzyme. While taurine utilization followed simple Michaelis-Menten kinetics



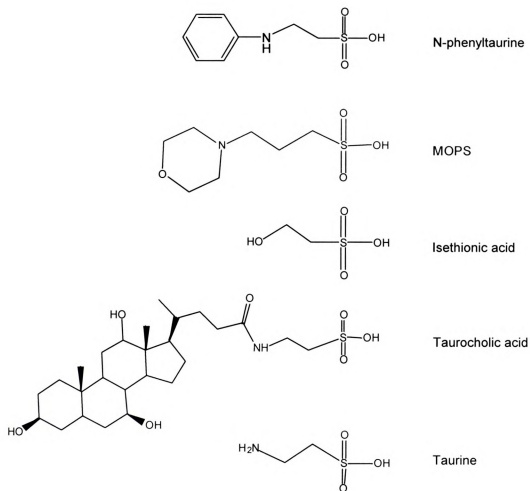
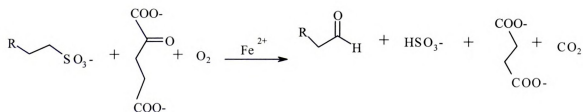


Figure 12. Structures of substrates for *S. cerevisiae* sulfonate/ α -KG dioxygenase.



Scheme 3. Reaction mechanism of *S. cerevisiae* sulfonate/ α -KG dioxygenase.



(Figure 13A), the kinetic properties for several other substrates were complicated by apparent inhibition of the enzyme at elevated substrate concentrations (Figure 13B and C). In those cases, the data were fit to the standard equation for substrate inhibition (**Equation 1**).

$$\text{Equation 1} \quad v = V_{\max}[S]/([S] + K_m + [S]^2/K_i)$$

Inhibition constants (K_i) are listed in Table 7. TauD exhibited similar substrate inhibition profiles for certain substrates other than taurine (1). High concentrations of substrate are also inhibitory to γ -butyrobetaine hydroxylase (K_i is approximately 1 mM) (19), an enzyme that catalyzes the conversion of γ -butyrobetaine to carnitine and to prolyl hydroxylase (10). In γ -butyrobetaine hydroxylase researchers demonstrated that the uncoupled decarboxylation of α -KG at high substrate concentrations did not explain the apparent inhibition. The peptide substrate of prolyl hydroxylase is a competitive inhibitor with respect to iron and α -KG for that enzyme (10). Sulfonate/ α -KG dioxygenase activity was not detected towards the following compounds: cysteate, aniline-2-sulfonic acid, homotaurine, picrylsulfonic acid, sulfosalicylic acid, 3-[(3-cholamidopropyl) dimethylammonio] propanesulfonic acid (CHAPS), 4-(2-hydroxyethyl)piperazine-1-propanesulfonic acid (EPPS), piperazine-N,N'-bis(2-ethanesulfonic acid) (PIPES), and 3-(cyclohexylamino)-1-propanesulfonic acid (CAPS).

Table 7. Sulfonate specificity and kinetic parameters for sulfonate/ α -KG dioxygenase.

Substrate ^a	V_{\max} ($\mu\text{mol}/\text{min}/\text{mg}$)	K_m (mM)	k_{cat}/K_m ($\text{min}^{-1}/\text{mM}$)	K_i (mM)
3- <i>N</i> -Morpholino- propanesulfonic acid (MOPS) [0-20 mM]	1.80 ± 0.06	0.24 ± 0.02	670.9	34.3 ± 5.8^b
<i>N</i> -Phenyltaurine [0-3 mM]	0.81 ± 0.03	0.12 ± 0.01	606.4	1.5 ± 0.1^b
2-Hydroxyethanesulfonate (Isethionate) [0-20 mM]	1.26 ± 0.05	0.27 ± 0.05	418.4	20.3 ± 2.5^b
3-Morpholino-2-hydroxy- propanesulfonic acid (MOPSO) [0-20 mM]	1.51 ± 0.03	0.33 ± 0.02	411.2	28.4 ± 2.4^b
Taurocholate [0-10 mM]	0.99 ± 0.05	0.42 ± 0.05	210.7	8.2 ± 1.1^b
2-(4-Morpholino)- ethanesulfonic acid (MES) [0-20 mM]	1.48 ± 0.05	1.94 ± 0.14	68.4	45.2 ± 6.6^b
2-(Cyclohexylamino) ethanesulfonic acid (CHES) [0-20 mM]	0.56 ± 0.02	2.57 ± 0.34	19.6	--- ^c
<i>N</i> -(Tris[hydroxymethyl] methyl)-2-amino- ethanesulfonic acid (TES) [0-15 mM]	0.75 ± 0.01	3.60 ± 0.12	18.7	--- ^c
<i>N</i> -[2-Hydroxyethyl] piperazine- <i>N'</i> -[2-hydroxy- propanesulfonic acid] (HEPPSO) [0-20 mM]	1.01 ± 0.08	5.04 ± 1.07	18.0	--- ^c
<i>N</i> -(Tris(hydroxymethyl)- methyl)-3-aminopropane- sulfonic acid (TAPS) [0-20 mM]	1.61 ± 0.06	$10.38 \pm .80$	13.9	--- ^c
4-(2-Hydroxyethyl)-1- piperazineethanesulfonic acid (HEPES) [0-20 mM]	0.82 ± 0.02	16.62 ± 0.80	4.4	--- ^c
2-Aminoethanesulfonic acid (Taurine) [0-20 mM]	0.46 ± 0.04	10.37 ± 1.82	4.0	--- ^c

^a The concentrations of substrate examined are shown in brackets

^b Data for these substrates were fit to Equation 1

^c No inhibition was detected. Kinetic parameters were fit to the Michaelis-Menten equation.

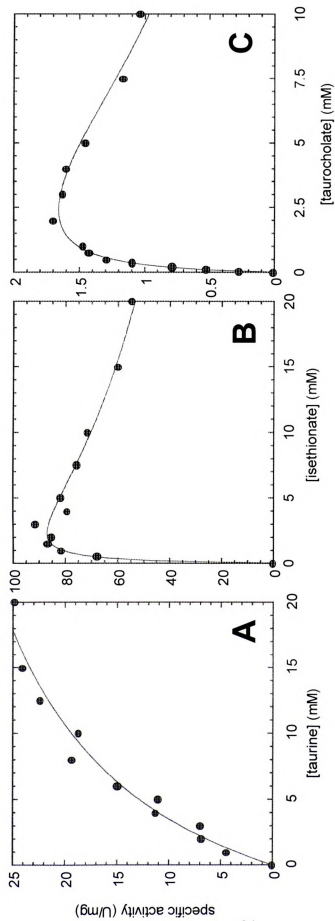


Figure 13. Substrate concentration dependence of sulfonate/α-KG dioxygenase activity. Enzyme was assayed with (A) taurine, (B) isethionate, and (C) taurocholate. The data were fit to standard Michaelis-Menten kinetics for taurine and to the standard equation for substrate inhibition (Eq. 1) for the other substrates.



Additional properties of *S. cerevisiae* sulfonate dioxygenase

Several additional properties of the MBP-dioxygenase fusion protein were characterized. The K_m for α -KG was determined to be $30 \pm 16 \mu\text{M}$. The approximate K_D for Fe(II) was found to be $44 \pm 5 \mu\text{M}$ which is ten-fold higher than the value observed for other α -KG-dependent dioxygenases (see Chapter 1). The increase in apparent K_D for iron may reflect non-specific metal binding by MBP. Temperature stability experiments, conducted by incubating the protein at varying temperatures for 1 hr prior to measuring activity at 30 °C, showed that the enzyme lost 77% of its activity after incubation at 37°C and was completely inactivated at higher temperatures. The fusion protein was shown to be cleaved by Factor Xa (New England Biolabs) to yield active 47 kDa enzyme. There was no significant difference in k_{cat} towards MOPS for the fusion protein and the free enzyme.

Phenotype of *S. cerevisiae* YLL057c deletion mutant

Studies with a *S. cerevisiae* YLL057c deletion mutant, BY4742-11545 (Research Genetics, Huntsville, AL), demonstrated the importance of sulfonate/ α -KG dioxygenase for growth on alternative sulfur sources. Comparison of the growth profiles for these two strains clearly showed that deletion of the sulfonate/ α -KG dioxygenase gene decreased the extent to which *S. cerevisiae* could use taurine and isethionate as the sole source of sulfur (Figure 14). The rate at which BY4742 grew in medium with isethionate was also affected (data not shown). The growth rate and final yield was identical for the two strains in medium containing sulfate.



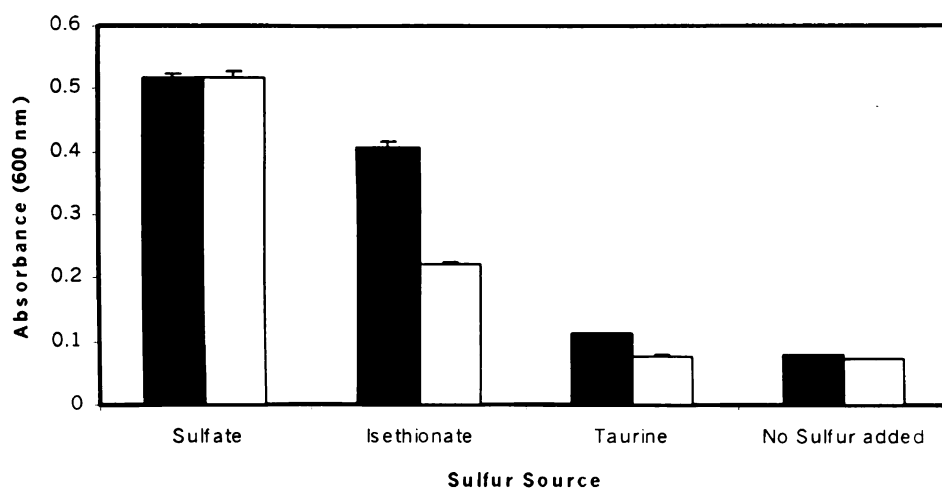


Figure 14. Role of YLL057c in the utilization of different sulfur sources. Growth of *S. cerevisiae* BY4742 (solid bars) and the YLL057c deletion strain BY4742-11545 (open bars) in medium containing either sulfate, isethionate, taurine, or no added sulfur source was measured as absorbance at 600 nm of stationary phase cultures. Error bars represent the standard deviation between replicate cultures.

Role of sulfonate/ α -KG dioxygenase in *S. cerevisiae*

The yeast sulfonate/ α -KG dioxygenase may allow cells to exploit one or more of the many naturally occurring sulfonates. Some studies suggest that sulfonate sulfur is the major form of organic sulfur in soils (2). Specific examples of environmental sources of sulfonates include the sulfonolipids of gliding bacteria, the capsules of some Gram positive bacteria (11), and the taurine produced in all vertebrates and invertebrates (6). In addition, common oxidation products of cysteine and other S-containing amino acids include sulfoacetaldehyde (9, 14), sulfopyruvate, sulfolactate, cysteate (20), and taurine (20). In mice, the gut microflora have been shown to convert taurine and taurocholate to isethionate (20). Perhaps significantly, a taurocholate transporter (YBT1) (12) resides on the same segment of chromosome XII as YLL057c. The bile acid transporter has been localized to the vacuolar membrane and efficiently imports taurocholate into the vacuole. Sulfonate/ α -KG dioxygenase may play an additional role in the degradation of taurine-conjugated compounds *in vivo*.

Candida albicans, another fungus, contains a hypothetical protein sequence with more than 50% amino acid identity to the sulfonate/ α -KG dioxygenase suggesting that other fungi have similar pathways to take advantage of these alternative sources of sulfur (15). The fact that *S. cerevisiae* BY4742-11545 could grow to some degree on isethionate suggests that an additional pathway exists for sulfonate utilization. Examples of enzymes capable of the liberation of sulfite from sulfonates include a flavin mononucleotide-dependent monooxygenase from *Pseudomonas aeruginosa* (7) and a sulfo-lyase from an *Acinetobacter* isolate (8). Redundancy of sulfonate catabolic pathways accentuates the importance of these compounds as sources of cell sulfur.

Literature cited

1. **Auchtung, T. A.** 1999. Unpublished observations.
2. **Autry, A. R., and J. W. Fitzgerald.** 1990. Sulfonate S: A major form of forest soil organic sulfur. *Biol. Fertil. Soils* **10**:50-56.
3. **Cherest, H., and Y. Surdin-Kerjan.** 1992. Genetic analysis of a new mutation conferring cysteine auxotrophy in *Saccharomyces cerevisiae*: updating of the sulfur metabolism pathway. *Genetics* **130**:51-58.
4. **Eichhorn, E., J. R. van der Ploeg, M. A. Kertesz, and T. Leisinger.** 1997. Characterization of α -ketoglutarate-dependent taurine dioxygenase from *Escherichia coli*. *J. Biol. Chem.* **272**:23031-23036.
5. **Fukumori, F., and R. P. Hausinger.** 1993. Purification and characterization of 2,4-dichlorophenoxyacetate/ α -ketoglutarate dioxygenase. *J. Biol. Chem.* **268**:24311-24317.
6. **Huxtable, R. J.** 1992. Physiological actions of taurine. *Physiol. Rev.* **72**:101-143.
7. **Kertesz, M., K. Schmidt-Larbig, and T. Wüest.** 1999. A novel reduced flavin mononucleotide-dependent methanesulfonate sulfonatase encoded by the sulfur regulated *msu* operon of *Pseudomonas aeruginosa*. *J. Bacteriol.* **181**:1464-1473.
8. **King, J. E., R. Jaouhari, and J. P. Quinn.** 1997. The role of sulfoacetaldehyde sulfo-lyase in the mineralization of isethionate by an environmental *Acinetobacter* isolate. *Microbiology* **143**:2339-2343.
9. **Kondo, H., H. Anada, K. Ohsawa, and M. Ishimoto.** 1971. Formation of sulfoacetaldehyde from taurine in bacterial extracts. *J. Biochem.* **69**:621-623.
10. **Myllylä, R., L. Tuderman, and K. I. Kivirikko.** 1977. Mechanism of the prolyl hydroxylase reaction: 2. Kinetic analysis of the reaction sequence. *Eur. J. Biochem.* **80**:349-357.
11. **Ohtomo, T., K. Yoshida, and C. L. San Clemente.** 1981. Effect of bile acid derivatives on taurine biosynthesis and extracellular slime production in encapsulated *Staphylococcus aureus* S-7. *Infect. Immun.* **31**:798-807.
12. **Ortiz, D. F., M. V. St. Pierre, A. Abdulmessih, and I. M. Arias.** 1997. A yeast ATP-binding cassette-type protein mediating ATP-dependent bile acid transport. *J. Biol. Chem.* **272**:15358-15365.

13. **Sambrook, J., E. F. Fritsch, and T. Maniatis.** 1989. Molecular cloning: a laboratory manual, 2nd ed. Cold Spring Harbor Laboratory Press, Cold Spring Harbor, NY.
14. **Shimamoto, G., and R. S. Berk.** 1979. Catabolism of taurine in *Pseudomonas aeruginosa*. *Biochim. Biophys. Acta.* **569**:287-292.
15. **Unfinished Genome Database Website.** 11 October 1999.
<http://www.ncbi.nlm.nih.gov/BLAST/unfinishedgenome.html>.
16. **Uria-Nickelsen, M. R., E. R. Leadbetter, and W. Godchaux III.** 1994. Comparative aspects of utilization of sulfonate and other sulfur sources by *Escherichia coli* K12. *Arch. Microbiol.* **161**:434-438.
17. **Uria-Nickelsen, M. R., E. R. Leadbetter, and W. Godchaux III.** 1993. Sulfonate-sulfur assimilation by yeasts resembles that of bacteria. *FEMS Microbiol. Letts* **114**:73-78.
18. **Uria-Nickelsen, M. R., E. R. Leadbetter, and W. Godchaux III.** 1993. Sulphonate utilization by enteric bacteria. *J. Gen. Microbiol.* **139**:203-208.
19. **Wehbie, R. S., N. S. Punekar, and H. A. Lardy.** 1988. Rat liver γ -butyrobetaine hydroxylase catalyzed reaction: influence of potassium, substrates and substrate analogues on hydroxylation and decarboxylation. *Biochemistry* **27**:2222-2228.
20. **Weinstein, C. L., and O. W. Griffith.** 1988. Cysteinesulfonate and β -sulfoypyruvate metabolism. *J. Biol. Chem.* **263**:3735-3743.

CHAPTER 4

DISTRIBUTION OF *tfdA* IN THE ENVIRONMENT

Many of these results have been published in the article: Hogan, D. A., D. H. Buckley, C. H. Nakatsu, T. M. Schmidt, and R.P. Hausinger (1997). "Distribution of the *tfdA* gene in soil bacteria that do not degrade 2,4-dichlorophenoxyacetic acid (2,4-D)." Microb. Ecol. 34:90-96.

Introduction

The *tfdA* gene (30) encodes 2,4-D/ α -KG dioxygenase (TfdA) (9), an enzyme that catalyzes removal of the acetate side chain of 2,4-D yielding 2,4-dichlorophenol. Thus far, *tfdA* is uniquely associated with 2,4-D catabolism, and is most often found with the other *tfd* genes necessary to complete the degradation of 2,4-D. While *tfdA* is unlike any previously characterized genes involved in aromatic compound decomposition, the other *tfd* genes are similar to components of a number of different catabolic pathways. For instance, genes similar in sequence to *tfdB* encode hydroxylases that act on various substituted or unsubstituted phenols in a variety of microorganisms (15, 39). Likewise, the *tfdCDEF* operon is homologous to other catechol degradation genes involved in many different aromatic degradative pathways (39). Because the downstream *tfd* genes are closely related to common bacterial genes, it is likely that homologs to *tfdA* can also be identified.

Several pieces of evidence suggest that the assembly of the *tfd* genes to form 2,4-D degradation plasmids has occurred numerous times. First, the 2,4-D degradative genes are found in different arrangements on a variety of different plasmid backbones (35, 37). Second, plasmids within the same incompatibility group can have different alleles of the genes that encode the first three enzymes of the 2,4-D degradative pathway (10, 36). Third, on some plasmids, *tfdA* is physically distant from the *tfdCDEFB* gene cluster (7). For there to be a “source” of *tfd* genes in the environment prior to their incorporation in 2,4-D degradative pathways, these genes must either be maintained without selection or serve an alternative purpose. Consistent with a widespread availability of *tfdA* homologs,

evidence for TfdA or TfdA-like activity has been found in diverse phylogenetic groups including the γ -(21) and β -Proteobacteria (2, 6, 10, 32), a member of the Flexibacter-Cytophaga- Bacteroides phylum (3), and *Arthrobacter* sp. in the High G+C Subdivision of the Gram-positive phylum (34).

To assess the natural distribution of *tfdA*, I used PCR primers internal to the *tfdA* gene to screen a collection of soil microorganisms, isolated on a non-selective medium, for the presence of *tfdA* or *tfdA*-like genes. In this chapter, I provide evidence that *tfdA*-like sequences are present in phylogenetically diverse soil microbes that do not degrade 2,4-D. These data suggest that *tfdA* is maintained in natural bacterial populations, possibly for a purpose other than 2,4-D degradation.

Materials and Methods

Bacterial strains

Bacterial strains were isolated from soils obtained from a Long Term Ecological Research (LTER) plot (24) at the Kellogg Biological Research Station in Hickory Corners, MI, USA which had been managed as a single cropping system to produce grain. Soil extracts were serially diluted in 50 mM phosphate buffer (pH 7), then plated on R2A medium (Difco, Detroit, MI) and incubated at 28°C for 10 days. Plates with 30 to 150 colonies were divided into quadrants. All colonies from one quadrant were purified on R2A agar and incubated at 28°C for three to four days. Additional colonies were chosen on the basis of colony morphology to include several groups of similar isolates as well as a representation of distinctive colony morphologies. The origins of *Alcaligenes eutrophus*

JMP134 (pJP4) (6), JMP228 (30), and *Burkholderia* sp. RASC (32) have been described previously.

16S rDNA partial sequence analyses

Total DNA was obtained from these isolates by detergent lysis (1) and 16S rDNA was amplified by PCR using the eubacterial primers complementary to *Escherichia coli* nucleotide positions 8-27 and 1510-1492 (8). Amplified rDNA was purified with Ultra-free MC (30,000 MWCO) centrifugal filter units (Millipore, Bedford, MA), then sequenced with primers complementary to *E. coli* positions 536-519 or 8-27 (27). The rDNA sequence was determined by automated fluorescent sequencing performed by the MSU-DOE-PRL Plant Biochemistry Facility using an ABI Catalyst 800 for Taq cycle sequencing and the ABI 373A Sequencer for the analysis of products. Partial 16S rDNA sequences were aligned manually against a collection of 16S rRNA sequences (18) on the basis of conserved regions of sequence and secondary structure of 16S rRNA. Regions of ambiguous alignment were omitted from the subsequent analysis. Phylogenetic trees were generated using the Neighbor Joining method and the topology was confirmed by Parsimony and Maximum Likelihood analyses (33).

*PCR Amplification of the *tfdA* gene*

Total DNA samples were isolated from each of the LTER strains (1). Primers were derived from conserved regions of sequence in the *tfdA* genes of pJP4 and *Burkholderia* strain RASC (79% identical to *tfdA*-pJP4). The sequence of the forward

primer, TVU, was 5'-ACG GAG TTC TG(C/T) GA(C/T) ATG-3'; the sequence of the reverse primer, TVL, was 5'-AAC GCA GCG (G/A)TT (G/A)TC CCA-3'(38). The PCR mix contained 5 µl 10X PCR buffer (Gibco, Gaithersburg, MD), 1.5 mM MgCl₂, 1 µM primer TVU, 1 µM primer TVL, 1 mM dNTPs (Boehringer Mannheim, Indianapolis, IN), 1.5 units of Taq polymerase (Gibco), 10-100 ng template DNA, and distilled water to bring the final volume to 50 µl. The PCR amplification protocol consisted of thirty five cycles with a one min denaturation at 94°C, one min annealing at 55°C and one min extension at 72°C. The predicted product size was 360 bp. Amplified products were separated on a 1% agarose gel and compared to PCR products generated from JMP134 and RASC genomic DNA as template. Generation of PCR products was confirmed by at least one additional PCR amplification reaction. Products were purified with Promega PCR mini-prep columns (Promega, Madison, WI). Selected PCR products were sequenced with either primer TVL or TVU by the method described for 16S rDNA above.

Dot Blot of PCR products

PCR products (~50 ng) were applied to a Hybond N nylon membrane (Amersham, Arlington Heights, IL) in 1 µl aliquots and UV cross-linked to the membrane with a Stratalinker (Stratagene, La Jolla, CA). To create probes, PCR products obtained using DNA from JMP134 and RASC were labeled with digoxigenin using the DIG High Prime labeling mix (Boehringer Mannheim) according to the manufacturer's instructions. Hybridization, detection, and probe removal were performed according to protocols in the Genius Detection System manual (Boehringer Mannheim). To assure high stringency, the

hybridization solution contained 50% formamide and hybridizations and stringency washes were at 68°C. Hybridization signals were detected by the colorimetric detection system (Boehringer Mannheim).

Analysis of 2,4-D degradation and TfdA activity

Isolates were streaked on R2A agar and incubated at 30°C for three days to allow for growth of all cultures. Isolated colonies were transferred to tubes containing 3 ml of A+N medium (41) amended with 0.1% yeast extract and 1 mM 2,4-D. Cultures were incubated for two weeks at 30°C on a shaker. After incubation, cells were removed by centrifugation and the supernatant was filtered (0.45 µm) into an autosampler vial. Duplicate samples of each culture were either analyzed immediately or frozen for later analysis. 2,4-D and 2,4-dichlorophenol concentrations were determined by HPLC with 70/30 methanol-0.1% phosphoric acid as eluent, with a Lichosorb RP-18 column (EM Separations, Gibbstown, NJ) and monitored with a UV detector at 230 nm. For induction experiments, cells were grown on MMO medium (29) with 5 mM succinate, harvested and washed in phosphate-buffered saline, then resuspended in medium with phenoxyacetic acid, 3-chlorobenzoate, 3-chlorocatechol, catechol, succinate (all 1 mM final concentration), or with no carbon source. TfdA activity was measured by detection of 2,4-dichlorophenol with 4-aminoantipyrene (9).

Incorporation of radiolabel from ^{14}C -2,4-D

Single colonies from cultures grown on R2A plates were transferred to sterile nylon membranes overlaid on R2A agar. After overnight incubation at 30°C, all cultures had visible growth. Each filter was replicated (25), then both master and replica filters

were transferred to minimal agar containing either ^{14}C -ring-labeled or chain-labeled 2,4-D and incubated for three days at room temperature. The filters were exposed to X-ray film (Kodak, Rochester, NY) for 18 hours to detect incorporation of radiolabeled carbon.

Results

Composition of the LTER collection

The analysis of 16S rDNA partial sequence from strains in the LTER collection showed that these isolates represent diverse phylogenetic divisions (Figure 15, Table 8). The taxonomic divisions used to describe the isolates are defined in the Ribosomal Database Project (18). Among the seventy-six isolates analyzed, twenty seven were found to cluster within the Bacillus-Lactobacillus-Streptococcus subdivision and thirteen strains fall within the High G+C Subdivision of the Gram-positive phylum. The remaining isolates included five α -Proteobacteria, two β -Proteobacteria, eleven γ -Proteobacteria, and eighteen members of the Cytophaga group. In a polyphasic taxonomy study, more than 95% of these isolates were found to be distinct taxa based on BIOLOG analyses (Biolog, Hayward, CA), fatty acid methyl ester (FAME) profiles (13), and genomic fingerprints from rep-PCR analyses (40). The polyphasic taxonomy study of the LTER isolates, including refined phylogenetic analyses based on complete 16S rDNA sequence is underway and will be presented elsewhere. Because the LTER collection includes both closely related isolates as well as organisms from several different phyla, this collection provides a good opportunity to test for the dispersion of *tfdA* between distantly related bacteria as well as for the presence of *tfdA* in similar strains within a bacterial species.

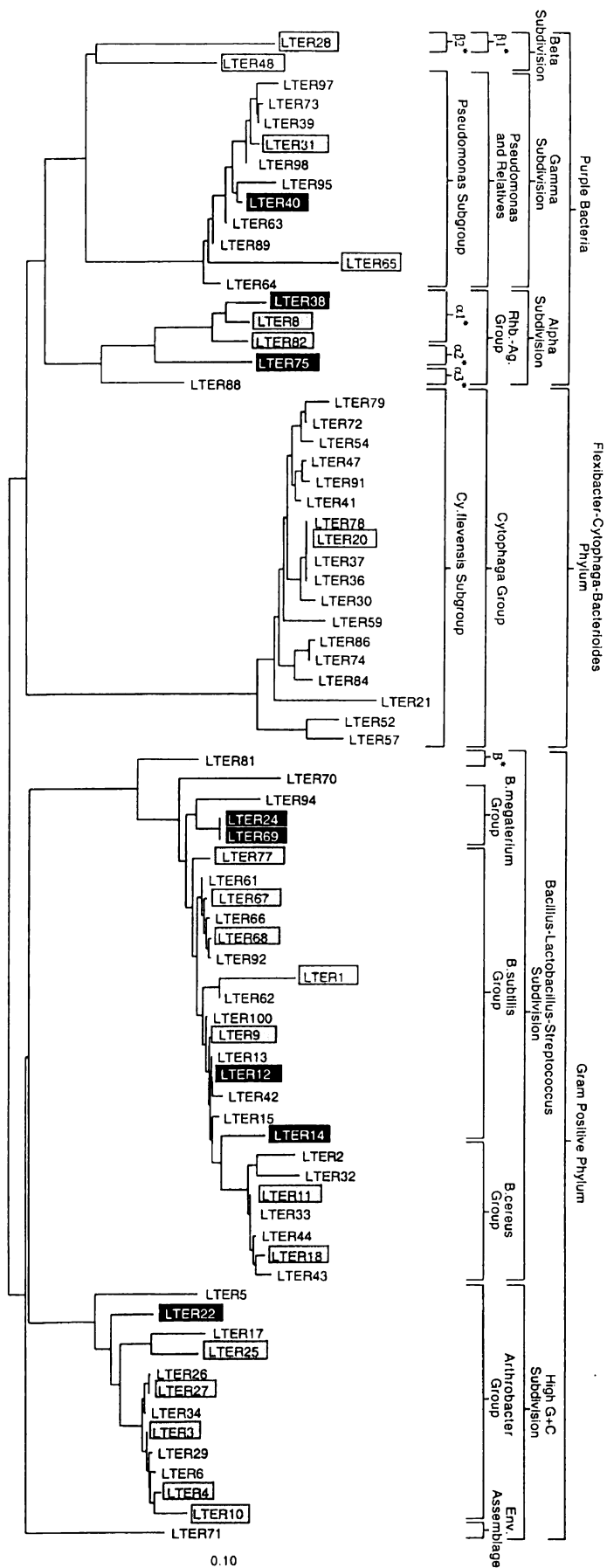
Identification of tfdA in LTER collection

PCR amplification with internal *tfdA* primers generated products using genomic DNA from twenty eight of the seventy six isolates. The products were similar in size to the *tfdA* product amplified from JMP134 and RASC (360 bp), and hybridized at high stringency to labeled products from PCR amplification of *tfdA* from JMP134 (Figure 16) and *Burkholderia* RASC. Amplification product from each isolate was assigned to either the *tfdA*_{pJP4} or *tfdA*_{RASC} hybridization group. When primers TVU and TVL were applied directly to the membrane, hybridization to the probe was not detected.

Amplified PCR products from four isolates were sequenced to assess the similarity of the *tfdA*-like gene in organisms from different phylogenetic divisions to each other and to previously characterized *tfdA* genes. Three of the isolates, LTER 1 and LTER 11 from the Bacillus-Lactobacillus-Streptococcus subdivision as well as LTER 8 from the Rhizobium-Agrobacterium group were identical to the *tfdA* partial sequence (Genbank U22499) from *Halomonas* sp. I-18, a moderate halophile (21) and to the *tfdA* sequence identified on plasmid pEMT8 (36) (Dr. Terrence Marsh, unpublished data). Although pEMT8 does not confer the ability to degrade 2,4-D to its host, it can complement *R. eutropha*(pBH501aE) (36), a *tfdA*⁻ derivative of pJP4, to restore the 2,4-D degradation phenotype (37) suggesting that it does encode a functional TfdA. The sequence of the PCR product from LTER 40, a member the β -Proteobacteria division, was identical to the sequence of *tfdA* found on pJP4.

Figure 15. 16S rDNA phylogeny of the LTER isolates

Phylogeny is based on partial sequences corresponding to *E. coli* rDNA sequence between positions 27 and 519. Names of phylogenetic divisions are derived from the RDP 5.0 release (18). The scale bar indicates the number of nucleotide changes per base position analyzed. Isolates that produce a PCR amplification product with primers internal to the *tfdA* gene are enclosed in boxes. The abbreviation Rub. indicates *Rubrivivax*, Rhb. indicate *Rhizobium*, and Ag. signifies *Agrobacterium*. LTER isolates in dark boxes yielded a PCR product belonging to *tfdA*_{JP4} hybridization group; grey boxes indicate *tfdA*-like genes more similar to *tfdA*_{RASC}.



2,4-D degradation by LTER isolates

HPLC analyses showed that 2,4-D was not degraded to a significant extent by any of the LTER isolates after a two week incubation. In contrast, JMP134 (pJP4) or *Burkholderia* sp. RASC completely consumed the 2,4-D during this time period. Uptake experiments provided additional evidence that none of the LTER isolates utilized 2,4-D for cellular carbon. Neither ring- nor chain-labeled ^{14}C -2,4-D was incorporated into the LTER cultures after a three day incubation period while JMP134(pJP4) produced a strong positive signal after incubation on medium with either radiolabeled substrate.

Experiments to determine if the tfdA-like gene encodes a functional TfdA

To determine if the *tfdA*-like genes encode functional enzymes, selected isolates from different phylogenetic groups were tested for TfdA activity and the presence of a TfdA-like protein in cell extracts. Ten isolates from different phylogenetic groups were selected for further study including: LTER 28 (β -Proteobacterium); LTER 38 and LTER 82 (α -Proteobacteria); LTER 40 (γ -Proteobacterium); LTER 20 (Cytophaga Group); LTER 1, LTER 11 and LTER 24 (*Bacillus* group); and LTER 3 and LTER 5 (*Arthrobacter* group). While JMP134 and RASC had high levels of TfdA activity after induction with 2,4-D, none of the cell lysates from the above LTER strains exhibited any activity after induction with 2,4-D, phenoxyacetic acid, 3-chlorobenzoate (3-CBA), catechol, 3-chlorocatechol, succinate or with no added carbon source. JMP134 was the only strain that degraded 3-CBA, as determined by HPLC analysis. Western blot analysis with anti-TfdA(pJP4) antibodies did not indicate the presence of a cross-reacting TfdA in

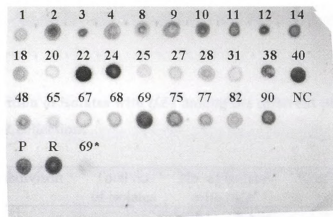


Figure 16. Hybridization of amplified products from LTER isolates to a digoxigenin-labeled fragment internal to the *tfiA* gene.

The numbers correspond to the LTER isolates that yielded the template DNA for the PCR reaction; 69* is an amplified product that is 40 bp longer than the predicted product size; as a negative control, NC, PCR primers were applied directly to the membrane; P is the amplified product from JMP134 (pJP4); R, amplified product from *Burkholderia* strain RASC. Results from hybridization to RASC probe not shown.

Table 8. Distribution of isolates with *tfdA* among the different phylogenetic groups within the LTER collection.

Phylogenetic subdivison	Total no. of isolates	No. of isolates with <i>tfdA</i> ^a		% of isolates with <i>tfdA</i>
		<u>pJP4</u>	<u>RASC</u>	
α-Proteobacteria	5	2	2	60
β-Proteobacteria	2	0	2	100
γ-Proteobacteria	11	1	2	27
Cytophaga	18	0	1	6
High G+C Gram-positives	13	1	5	46
Bacillus-Lactobacillus-Streptococcus	27	5	7	40
Total	76	9	19	37

^a Amplified PCR products were categorized into hybridization groups based on the strength of the hybridization signal to the pJP4 and RASC probe.

lysates from any of the LTER isolates. In a separate experiment, cell extracts of *Halomonas* sp. I-18 grown on 2,4-D possessed a band of approximately 32 kDa (similar in size to pJP4 and the predicted MW of pEMT8 TfdA) that cross reacted with the anti-TfdA (pJP4) antibody, however, RASC, grown with 2,4-D as the sole source of carbon, did not.

Mating experiments similar to those published by Top *et al.* (36) were also performed to determine if any of the LTER isolates could transfer a functional *tfdA* to a recipient strain. No 2,4-D⁺ transconjugants were generated after incubation of the LTER isolates with *R. eutropha* JMP228 carrying pBH501aE (a *tfdA*⁺ pJP4-derived plasmid) or plasmid-free *R. eutropha* JMP228 (Nal^R) (36).

Discussion

A significant percentage (37%) of organisms in this collection of soil isolates contains *tfdA* or *tfdA*-like genes. Two aspects of these data are particularly interesting. First, the *tfdA*-like genes are found in very phylogenetically diverse taxa (Figure 15, Table 8) including both Gram positive and Gram negative bacteria. Second, isolates within the same phylogenetic division contain *tfdA*-like genes from different hybridization groups (Table 8). Previous research provides evidence for *tfdA* in only a small number of Gram-positive 2,4-D-degraders, such as *Arthrobacter* sp. (34), compared to a vast collection of *tfdA*-containing Gram-negative bacteria (2, 6, 21, 32, 35). This is the first report of a *tfdA*-like gene in *Bacillus* or *Cytophaga*.

Despite the fact that 2,4-D is readily degraded by many different microbial communities (26), the isolation of axenic cultures that degrade 2,4-D has proven to be

more difficult (11, 17). These data suggest that, in many instances, 2,4-D is not degraded by individual organisms, but by the concerted activities of several different bacteria. The presence of *tfdA* in isolates that do not degrade 2,4-D may indicate the source of the 2,4-D-degradation potential of microbial communities. Perhaps prolonged exposure to 2,4-D is necessary to select for organisms or plasmids that contain both *tfdA* and the *tfdBCDEF* genes. If *tfdA* is present in bacteria lacking the additional genes needed for 2,4-D mineralization, TfdA activity may be difficult to detect in pure culture due to the accumulation of toxic products, such as 2,4-dichlorophenol, or lack of the proper inducer molecule (19).

The high identity of the partial *tfdA*-like sequences, amplified from the DNA of phylogenetically diverse bacteria, to previously characterized *tfdAs* suggests extensive horizontal transfer of these genes. The *tfdA* gene is most often found on self-transmissible, broad host-range plasmids that confer the ability to degrade 2,4-D (2, 6, 36). Several studies (4-6) have shown that plasmid pJP4, which encodes all of the enzymes necessary for 2,4-D degradation, can be maintained in a number of different bacteria. It is worth noting, however, that not all organisms containing pJP4 express the 2,4-D-degrading phenotype (6).

Genetic characterization of plasmid-encoded 2,4-D degradation pathways indicate that *tfdA* most often resides on transposable elements. Plasmids that confer the 2,4-D⁺ phenotype are often unstable. Multiple researchers have reported that growth on non-selective media induces the loss of a 20- to 40-kb fragment from a plasmid concurrent with the inability to degrade 2,4-D (2, 7, 20, 42). A plasmid isolated from Michigan soils, pEMT8, (37) contains *tfdA* but does not have the other genes required for 2,4-D

degradation. The pEMT8 *tfdA*, which is identical to the partial sequences amplified from three of the LTER isolates, is adjacent to a transposase of the IS1111/IS1328/IS1533 family of elements (Dr. Terrence Marsh, unpublished data). Similar transposable elements have been found in diverse organisms including strains of *Streptomyces* (16), *Mycobacterium* (16), *Pseudomonas* (Genbank # AF052750) and *Rhizobium* (Genbank# P55615). With this, it is reasonable to hypothesize that the *tfdA*-like genes in the LTER isolates are associated with a similar transposable element. Consistent with this hypothesis is the observation that the *tfdA*-like gene can be lost, as evidenced by the inability to amplify the 360 bp product (data not shown), upon multiple transfers of the isolates on rich medium.

The wide spread presence of *tfdA*, even on a transposon, in organisms that do not degrade 2,4-D may indicate that these genes serve an important metabolic purpose apart from herbicide degradation. There are several examples of genes that reside primarily on mobile elements, including those encoding virulence factors (14), plant-microbe symbiosis functions (31), and antibiotic resistance (23). The strategy of maintaining important genes in only a fraction of the population by use of mobile genetic elements is poorly understood, but may prove to be important to microbial ecology. Naturally-occurring compounds with structural similarities to 2,4-D that are potential substrates of native TfdA include the numerous aryl-ether compounds that are released during fungal degradation of lignin (22) or the different halogenated aromatic metabolites produced by fungi and bacteria (12, 28). Alternatively, it is possible that the natural substrate for TfdA shows little resemblance to 2,4-D and the ability to degrade this compound is fortuitous.

Acknowledgements.

I am grateful to Helen Corlew-Newman and Frank Lowes for providing the LTER strains and the past and present members of the Research on Microbial Evolution (ROME) Laboratory for helpful suggestions and discussions. Particular thanks go to Terry Marsh for providing the unpublished pEMT8 *tfdA* and transposase sequences and to Olga Maltseva for providing DNA and cell material from *Halomonas* strain I-18.

Literature cited

1. **Ausubel, F. M., R. Brent, R. E. Kingston, D. D. Moore, J. G. Seidman, J. A. Smith, and K. Struhl.** 1987. Current protocols in molecular biology. John Wiley and Sons, New York.
2. **Bhat, M. A., M. Tsuda, K. Horiike, M. Nozaki, C. S. Vaidyanathan, and T. Nakazawa.** 1994. Identification and characterization of a new plasmid carrying genes for degradation of 2,4-dichlorophenoxyacetate from *Pseudomonas cepacia* CSV90. Appl. Environ. Microbiol. **60**:307-312.
3. **Chaudry, G. R., and G. H. Huang.** 1988. Isolation and characterization of a new plasmid from a *Flavobacterium* sp. which carries the genes for the degradation of 2,4-dichlorophenoxyacetate. J. Bacteriol. **170**:3897-3902.
4. **Daane, L. L., J. A. E. Molina, E. C. Berry, and M. J. Sadowsky.** 1996. Influence of earthworm activity on gene transfer from *Pseudomonas fluorescens* to indigenous soil bacteria. Appl. Environ. Microbiol. **62**:515-521.
5. **DiGiovanni, G. D., J. W. Neilson, I. L. Pepper, and N. A. Sinclair.** 1996. Gene transfer of *Alcaligenes eutrophus* JMP134 plasmid pJP4 to indigenous soil recipients. Appl. Environ. Microbiol. **62**:2521-2526.
6. **Don, R. H., and J. M. Pemberton.** 1981. Properties of six pesticide degradation plasmids isolated from *Alcaligenes paradoxus* and *Alcaligenes eutrophus*. J. Bacteriol. **145**:681-686.
7. **Don, R. H., A. J. Weightman, H. J. Knackmuss, and K. N. Timmis.** 1985. Transposon mutagenesis and cloning analysis of the pathways for degradation of 2,4-dichlorophenoxyacetic acid and 3-chlorobenzoate in *Alcaligenes eutrophus* JMP134 (pJP4). J. Bacteriol. **161**:85-90.
8. **Eden, P. A., T. M. Schmidt, R. P. Blakemore, and N. R. Pace.** 1991. Phylogenetic analysis of *Aquaspirillum magnetotacticum* using polymerase chain reaction-amplified 16S rRNA-specific DNA. Int. J. Syst. Bacteriol. **42**:166-170.
9. **Fukumori, F., and R. P. Hausinger.** 1993. Purification and characterization of 2,4-dichlorophenoxyacetate/ α -ketoglutarate dioxygenase. J. Biol. Chem. **268**:24311-24317.
10. **Fulthorpe, R. R., C. McGowan, O. V. Maltseva, W. E. Holben, and J. M. Tiedje.** 1995. 2,4-Dichlorophenoxyacetic acid-degrading bacteria contain mosaics of catabolic genes. Appl. Environ. Microbiol. **61**:3274-3281.

11. **Fulthorpe, R. R., A. N. Rhodes, and J. M. Tiedje.** 1996. Pristine soils mineralize 3-chlorobenzoate and 2,4-dichlorophenoxyacetate via different microbial populations. *Appl. Environ. Microbiol.* **62**:1159-1166.
12. **Gribble, G. W.** 1992. Naturally occurring organohalogen compounds-a survey. *J. Nat. Prod.* **55**:1353-1395.
13. **Haack, S. K., H. Garchow, D. A. Odelson, L. J. Forney, and M. J. Klug.** 1994. Accuracy, reproducibility, and interpretation of fatty acid methyl ester profiles of model bacterial communities. *Appl. Environ. Microbiol.* **60**:2483-2493.
14. **Hacker, J., G. Blum-Oehler, I. Muhldorfer, and H. Tschape.** 1997. Pathogenicity islands of virulent bacteria: structure, function and impact on microbial evolution. *Mol. Microbiol.* **23**:1089-1097.
15. **Häggblom, M. M.** 1992. Microbial breakdown of halogenated aromatic pesticides and related compounds. *FEMS Microbiol. Rev.* **103**:29-72.
16. **Hoover, T. A., M. H. Vodkin, and J. C. Williams.** 1992. A *Coxiella burnetti* repeated DNA element resembling a bacterial insertion sequence. *J. Bacteriol.* **174**:5540-5548.
17. **Ka, J. O., W. E. Holben, and J. M. Tiedje.** 1994. Use of gene probes to aid in recovery and identification of functionally dominant 2,4-dichlorophenoxyacetic acid-degrading populations in soil. *Appl. Environ. Microbiol.* **60**:1116-1120.
18. **Larsen, N., G. J. Olsen, B. L. Maidak, M. J. McCaughey, R. Overbeek, T. J. Macke, T. L. Marsh, and C. R. Woese.** 1993. The ribosomal database project. *Nucl. Acids Res.* **21**:3021-3023.
19. **Leveau, J. H., F. König, H. Fuchslin, C. Werlen, and J. R. Van Der Meer.** 1999. Dynamics of multigene expression during catabolic adaptation of *Ralstonia eutropha* JMP134 (pJP4) to the herbicide 2, 4- dichlorophenoxyacetate. *Mol. Microbiol.* **33**:396-406.
20. **Mäe, A. A., R. O. Martis, N. R. Ausmees, V. M. Kõiv, and A. L. Heinaru.** 1993. Characterization of a new 2,4-dichlorophenoxyacetic acid degrading plasmid pEST4011: physical map and localization of catabolic genes. *J. Gen. Microbiol.* **139**:3165-3170.
21. **Maltseva, O. V., C. McGowan, R. Fulthorpe, and P. J. Oriel.** 1996. Degradation of 2,4-dichlorophenoxyacetic acid by haloalkaliphilic bacteria. *Microbiol.* **142**:1115-1122.

22. **Ribbons, D. W.** 1987. Presented at the Technology in the 1990s: Utilization of lignocellulosic wastes, London, U.K.
23. **Roberts, M. C.** 1996. Tetracycline resistance determinants: mechanisms of action, regulation of expression, genetic mobility, and distribution. *FEMS Microbiol. Rev.* **19**:1-24.
24. **Robertson, G. P., and D. W. Freckman.** 1995. The spatial distribution of nematode trophic groups across a cultivated ecosystem. *Ecology* **76**:1425-1432.
25. **Sambrook, J., E. F. Fritsch, and T. Maniatis.** 1989. Molecular cloning: a laboratory manual, 2nd ed. Cold Spring Harbor Laboratory Press, Cold Spring Harbor, NY.
26. **Sandmann, E. R. I. C., M. A. Loos, and L. P. van Dyk.** 1988. Microbial degradation of 2,4-dichlorophenoxyacetic acid in soil. *Rev. Environ. Contamin. Tox.* **101**:1-53.
27. **Schmidt, T. M., E. F. DeLong, and N. R. Pace.** 1991. Analysis of a marine picoplankton community by 16S rRNA gene cloning and sequencing. *J. Bacteriol.* **173**:4371-4378.
28. **Siuda, J. F., and J. F. deBernardis.** 1973. Naturally occurring halogenated compounds. *Lloydia* **36**:107-143.
29. **Stanier, R. Y., N. J. Palleroni, and M. Doudoroff.** 1966. The aerobic pseudomonads: a taxonomic study. *J. Gen. Microbiol.* **43**:159-271.
30. **Streber, W. R., K. N. Timmis, and M. H. Zenk.** 1987. Analysis, cloning, and high-level expression of 2,4-dichlorophenoxyacetate monooxygenase gene *tfdA* of *Alcaligenes eutrophus* JMP134. *J. Bacteriol.* **169**:2950-2955.
31. **Sullivan, J. T., and C. W. Ronson.** 1998. Evolution of rhizobia by acquisition of a 500-kb symbiosis island that integrates into a phe-tRNA gene [published erratum appears in *Proc Natl Acad Sci U S A* 1998 Jul 21;95(15):9059]. *Proc. Natl. Acad. Sci. U S A* **95**:5145-9.
32. **Suwa, Y., A. D. Wright, F. Fukumori, K. A. Nummy, R. P. Hausinger, W. E. Holben, and L. J. Forney.** 1996. Characterization of a chromosomally encoded 2,4-dichlorophenoxyacetic acid/a-ketoglutarate dioxygenase from *Burkholderia* sp. strain RASC. *Appl. Environ. Microbiol.* **62**:2464-2469.
33. **Swofford, D. L., and G. J. Olsen.** 1990. Phylogeny reconstruction. *In* D. Hillis and C. Moritz (ed.), *Molecular Systematics*. Sinaur Associates, Sunderland, MA.

34. **Tiedje, J. M., and M. Alexander.** 1969. Enzymatic cleavage of the ether bond of 2,4-dichlorophenoxyacetate. *J. Agr. Food Chem.* **17**:1080-1084.
35. **Tonso, N. L., V. G. Matheson, and W. E. Holben.** 1995. Polyphasic characterization of a suite of bacterial isolates capable of degrading 2,4-D. *Microb. Ecol.* **3**:3-24.
36. **Top, E. M., W. E. Holben, and L. J. Forney.** 1995. Characterization of diverse 2,4-dichlorophenoxyacetic acid-degradative plasmids isolated from soil by complementation. *Appl. Environ. Microbiol.* **61**:1691-1698.
37. **Top, E. M., O. V. Maltseva, and L. J. Forney.** 1996. Capture of a catabolic plasmid that encodes only 2,4-D/ α -ketoglutarate dioxygenase (TfdA) by genetic complementation. *Appl. Environ. Microbiol.* **62**:2470-2476.
38. **Vallaes, T., R. R. Fulthorpe, A. M. Wright, and G. Soulas.** 1996. The metabolic pathway of 2,4-dichlorophenoxyacetic acid degradation involves different families of *tfdA* and *tfdB* genes according to PCR-RFLP analysis. *FEMS Microbiol. Lett.* **20**:163-172.
39. **van der Meer, J. R., W. M. de Vos, S. Harayama, and A. J. B. Zehnder.** 1992. Molecular mechanisms of genetic adaption to xenobiotic compounds. *Microbiol. Rev.* **56**:677-694.
40. **Versalovic, J., M. Schneider, F. J. de Bruijn, and J. R. Lupski.** 1994. Genomic fingerprinting of bacteria using repetitive sequence-based polymerase chain reaction. *Methods Mol. Cell Biol.* **5**:25-40.
41. **Wyndham, R. C.** 1986. Evolved aniline catabolism in *Acinetobacter calcoaceticus* during continuous culture of river water. *Appl. Environ. Microbiol.* **51**:781-789.
42. **Xia, X.-S., S. Aathithan, K. Oswiecimska, A. R. W. Smith, and I. J. Bruce.** 1998. A novel plasmid pIJB1 possessing a putative 2,4-dichlorophenoxyacetate degradative transposon TN5530 in *Burkholderia cepacia* strain 2a. *Plasmid* **39**:154-159.

CHAPTER 5
CONCLUSIONS AND FUTURE RESEARCH

In this dissertation, I presented my research on TfdA as both a model enzyme for the α -KG-dependent dioxygenase superfamily and as an enzyme with a unique catalytic activity in nature. The concluding chapter reviews the model for activity in α -KG-dependent dioxygenases and highlights three major questions that need to be addressed to understand the catalytic cycle of these enzymes. Although it is hardly necessary to justify the study of enzymes so critical to different areas of biology, some potential applications of the research on different α -KG-dependent dioxygenases in medicine, industry and agriculture are discussed. Lastly, I describe the ongoing efforts in our laboratory to find the role of TfdA or a similar enzyme in catabolic pathways other than those for the decomposition of 2,4-D.

Understanding the mechanism of α -KG-dependent dioxygenases

Although the α -KG-dependent dioxygenases are not unified by similarities in primary structure, data from spectroscopic and biochemical experiments suggest that these enzymes share many common elements. Thus, the three groups of enzymes, defined by their amino acid sequences (Chapter 1), are likely derived from a common enzyme ancestor that underwent rearrangements, insertions or deletions during the evolution of novel catabolic activities. The similarities in tertiary structure between seemingly unrelated members of the superfamily is revealed by recent X-ray crystallographic characterizations (Prof. C. Schofield, unpublished data). Information taken from the examination of multiple α -KG-dependent dioxygenases has been incorporated into a general mechanistic model for enzymes in this superfamily.

The overall reaction catalyzed by α -KG-dependent dioxygenases can be distilled down to three major steps. In this discussion, the proposed α -KG-dependent dioxygenase mechanism is compared to that for IPNS, a related enzyme that does not use an α -keto acid as a co-substrate, to illustrate the common elements in the mechanisms of these disparate enzymes. The three stages of the reactions (A-C) are described below and depicted in Figure 17.

(A) Substrate binding to the active site alters the coordination environment of the iron center to enable oxygen binding and formation of the first reactive oxygen species.

The coordination geometry and electronic nature of ligand donors act in concert to control the reaction between iron and oxygen (19). In enzymes that use α -KG as a co-substrate, the α -keto acid chelates the metal through the C-1 carboxylate and the C-2 keto group (11, 25, 28, 36). The replacement of neutral solvent ligands with anionic species is proposed to cause a shift in the iron's redox potential that may be necessary for subsequent steps in the reaction. In TfdA (4, 42), clavamate synthase (25), and DAOCS (36), the unique substrate is not thought to interact directly with the metal, but rather induces a change in the metalcenter geometry from six- to five-coordinate. Together, the altered geometry and changes in redox potential promote O₂ binding to the iron and generation of an Fe(III)-superoxide intermediate. Although IPNS does not bind α -KG, a similar shift to five-coordinate geometry is brought about by direct ligation of a substrate thiol to the iron center (26, 27), thus enabling the binding of oxygen and formation of the proposed Fe(III)-superoxide species.

(B) The first oxidation reaction generates an Fe(IV)-oxo intermediate. Iron-containing model compounds with ligands resembling the 2 His-1-carboxylate facial triad

and a bound α -keto acid moiety have been used to study the initial steps in catalysis (10). Upon exposure to diatomic oxygen, the synthesized compound undergoes oxidative decarboxylation concomitant with the hydroxylation of an adjacent aromatic ring. Comparison of the rate for dioxygenase-like activity for this compound to the decreased rates with other model compounds suggests that the decarboxylation of α -KG provides a large driving force for cleavage of the oxygen-oxygen bond (10). This portion of the reaction catalyzed by α -KG-dependent enzymes is analogous to the first two-electron oxidation reaction in IPNS where a new nitrogen-carbon bond is created upon ring closure and two electrons are transferred from the substrate to oxygen to form a molecule of water.

(C) *The reactive Fe(IV)-oxygen species participates in a hydroxylation reaction or alternative oxidation (desaturation, ring expansion, cyclization) regenerating the Fe(II) center.* In hydroxylating enzymes, a specific hydrogen atom is abstracted from the substrate to form an Fe(III)-OH species. The iron-oxygen bond breaks, yielding a hydroxyl radical which recombines with the substrate to give the hydroxylated product (32). In IPNS, a series of bonds are cleaved homolytically to generate a ring via a new carbon-sulfur bond. Again two electrons are transferred from substrate to reduce the second atom of oxygen to water, thus restoring the iron to its Fe(II) oxidation state.

Additional research is needed in three particular areas to provide experimental evidence and additional information for several of elements of the above model. First, the ligands to the metal during different stages of catalysis must be identified and other

Figure 17. Comparison of the proposed reaction mechanisms for an α -KG-dependent hydroxylase and IPNS.

Both resting enzymes possess an Fe(II) that is bound by a facial triad of residues in an H-X-D-X_n-H motif. (A) In the α -KG-dependent hydroxylases (left branch), two water molecules are displaced upon binding of anionic α -KG to the metal and a third is lost upon binding of a second substrate (S-H) nearby. The activated metal reacts with O₂ to form Fe(III)-superoxide. A similar intermediate is generated in IPNS by stepwise binding of the substrate and oxygen (right branch). (B) An Fe(IV)-oxo species is generated by a reaction driven by α -KG decarboxylation (left) or by oxidative cyclization of the lactam ring (right). (C) The highly reactive Fe(IV)-oxo species catalyzes further oxidative chemistry and the metal returns to its resting Fe(II) state as products dissociate.

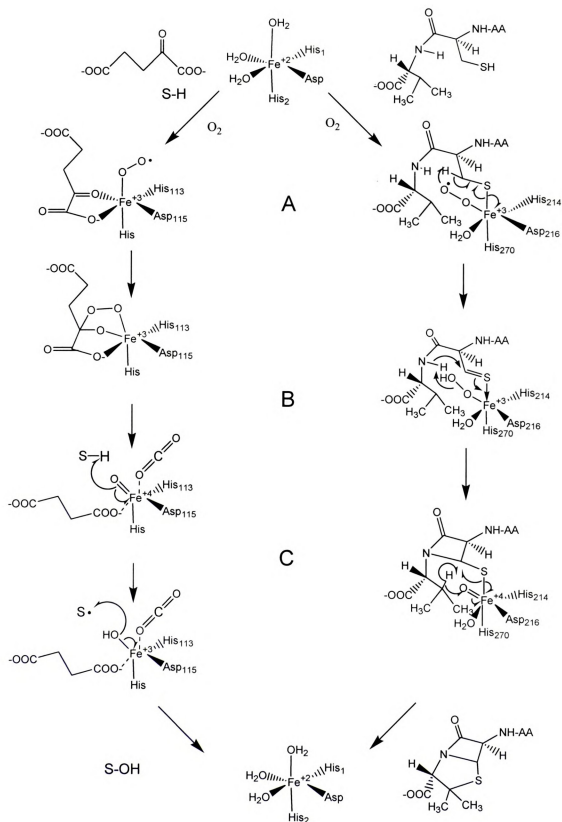


Figure 17. Comparison of the proposed mechanisms for an α -KG-dependent hydroxylase and IPNS

essential residues defined. Multiple studies of several enzymes have thoroughly characterized the iron ligands in the resting enzyme (2 His, 1 Asp, 3 waters). The identity and geometry of the ligands to the metal during the course of the reaction, however, have not been characterized. The order of dissociation of succinate and CO_2 (or bicarbonate) suggests that these products remain in the active site until after the second oxidation reaction occurs, however, no role for either product has been identified. The bicarbonate dependence of ACC oxidase, an enzyme related to IPNS that does not use α -KG as a co-substrate, may indicate the involvement of bicarbonate in the catalytic cycle of other enzymes. In addition, mutagenesis studies suggest that other amino acids present at the active site participate in the reaction; these residues need to be identified and characterized.

The second set of critical experiments needed to support the proposed model is detection of the oxygen intermediates to confirm their identity. Researchers in our lab and others have proposed experiments that may detect Fe(III)-containing intermediates (e.g. with bound superoxide or peroxide species) that may be generated during catalysis. Fe(III) is paramagnetic and therefore can be detected by EPR spectroscopy of freeze-quenched samples. Alternatively, stopped-flow UV-visible spectroscopy can also be used to detect reactive intermediates by their characteristic chromophores. Although detection of an Fe(IV)-oxo species may be difficult due to its high reactivity, model compound studies or the use of non-reactive substrate analogs might trap the reactive oxygen intermediate and aid in its identification.

The third area of study that is important for the creation of a robust model involves the interactions between the unique substrate and the Fe(IV)-oxo species. Apart

from IPNS, which has been structurally characterized with different substrate analogs, little is known about the positioning of the substrate or its interaction with the metal in other enzymes. α -KG-dependent dioxygenases demonstrate an amazing flexibility in the number and types of substrates that can be oxidized in a single catalytic center. For example, thymine 7-hydroxylase, which catalyzes the hydroxylation of methyl group of thymine, can also epoxidize olefins, oxidize thiol ethers to sulfones and sulfoxides, and demethylate the 1-methyl group of 1-methyl thymine (35). Similarly, clavamate synthase catalyzes a hydroxylation, a desaturation and a ring expansion on three different, though related substrates (Figure 2) (20). In this enzyme, the regio- and stereospecificity of the three reactions suggest significant differences in the binding modes for the structurally similar substrates (20). Alternatively, it has been proposed that clavamate synthase may modulate its reactivity by altering the position of the Fe(IV) oxo-intermediate in response to different compounds. These experiments clearly show that the substrates themselves play a significant role in influencing the aspects of the reaction; however, the rules governing these interactions are not known. Information about the importance of different substrate characteristics can be obtained by studying the products of alternative substrates, spectroscopic characterization of the enzyme in the presence of different compounds, and ultimately by crystal structure studies of enzyme-substrate complexes.

The site-directed mutagenesis studies described in Chapter 2 lay the foundation for examination of some of the questions outlined above. Knowledge of the metalcenter ligands are not only important in the design of model compounds, but are necessary for the interpretation of spectroscopic data and ultimately for our understanding of the

catalytic chemistry. For example, with both metal-bound histidines identified, we can now learn more about the rearrangements that occur upon substrate binding and how the substrate is positioned with respect to the metal. Furthermore, the ligands also play a crucial role in controlling the reactivity of the metal. For example, enzymes with heme-bound iron, such as cytochrome P450s, stabilize their iron(IV)-oxo intermediate with the porphyrin ring. In the absence of such a cofactor, α -KG-dependent dioxygenases may rely on histidines to delocalize the charge on the metal. This potential role for histidines may explain why glutamine or carboxylates are poor substitutes, and may suggest that other amino acid substitutions (His to Tyr or Cys) may be capable of sustaining activity. Continuing efforts to spectroscopically characterize TfdA (and the related enzyme TauD) with different amino acid substitutions or different substrates and substrate analogs will address some of these important questions. In addition, for the past four years, I have supplied our collaborator Peter Roach at Oxford University with purified TfdA for use in crystallization studies. Although crystals were obtained, crystallization conditions are still being optimized. Structural characterization has not yet been successful. If a crystal structure of TfdA or a closely related enzyme becomes available, more specific experiments can be designed to probe the catalytic mechanism.

Biological significance and potential applications of α -KG-dependent dioxygenases

Several α -KG-dependent dioxygenases are already being studied for their potential applications to the fields of medicine, industry, and agriculture. Prolyl and lysyl hydroxylases have long been studied for their role in collagen formation. Hydroxylated proline and lysine residues, which comprise between 0.5-5% of the amino acids in collagen or collagen-like proteins, are necessary to stabilize its triple helical structure

under physiological conditions (18). People with defects in lysyl hydroxylase suffer from Ehlers-Danlos syndrome, which is characterized by hypermobility of the joints, hyperextensibility of the skin, and other traits indicative of a connective tissue disorder (18). The excessive accumulation of collagen, termed fibrosis, can also impair function in a variety of tissues including the liver, lungs, and kidneys. Although several different inhibitors and inactivators of collagen hydroxylases prevent collagen formation in cultured human skin fibroblasts, none are currently in clinical use (18). In industry, the enzymes involved in the synthesis of β -lactam antibiotics are being scrutinized for opportunities to improve the large-scale synthesis of these complex molecules. Due to their intricate structure which defies chemical synthesis, all penicillin and cephalosporin antibiotics are still produced as natural fermentation products (31). Research on IPNS, DAOCS and related enzymes has focused on improving the specificity, rate and range of precursor substrates in hopes of optimizing steps in the synthesis and purification of these chemicals in addition to creating additional derivatives with different biological properties. Finally, in agriculture, TfdA has already been used to create transgenic plants that are resistant to the broad-leaf herbicide 2,4-D and related phenoxyacetic acids (1). It has also been proposed that TfdA could be used in the preparation and processing of phenoxy herbicides (29). Since only one isomer of chiral 2,4-D derivatives, such as mecoprop, is biologically active, TfdA-containing microorganisms or immobilized enzyme could be used to remove the inactive isomer from a chemically-synthesized racemic mixture, thus reducing the load of xenobiotics to soils.

Role of TfdA in the environment

Enzymes involved in the degradation of xenobiotic compounds are generally derived from proteins that act on chemically-similar, natural compounds. For example, benzoate and chlorobenzoate dioxygenases are related in both sequence and mechanism but have differing reactivities towards chlorinated and unsubstituted substrates (24). Similar examples include phenol hydroxylases (9), catechol dioxygenases (8), and benzene dioxygenases (2). TfdA acts on a variety of natural and synthetic substrates (Figure 18), but none with kinetic parameters approaching those for 2,4-D (R. Padmakumar, J. Hotopp, R. P. Hausinger, unpublished data). One abundant source of natural compounds that resemble known substrates of TfdA is lignin (9). This compound, the second most abundant polymer on earth, is an assemblage of aromatic units joined primarily through ether linkages. The aerobic degradation of lignin begins with “combustion” of the polymer to its constituent subunits by the action of fungal peroxidases to release a variety of monomeric and dimeric compounds. The types and relative percentages of the different intermonomer linkages found in native lignin are shown in Figure 19, and indicate the range of monomeric and dimeric compounds that are liberated during lignin decomposition. Three types of compounds in particular, β -aryl ethers, derivatives of cinnamic acids (including the corresponding alcohol (coumaryl alcohol) and cinnamic acid esters through the side-chain carboxylate), and phenoxyacetic acids bear particular resemblance to known substrates of TfdA (17).

One approach to determining if TfdA-like enzymes are involved in alternative degradative pathways, such as lignin degradation, is to examine the roles of proteins

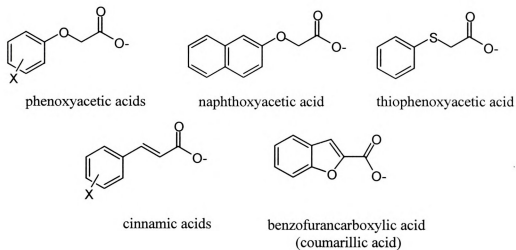


Figure 18. Structures of various substrates of TfdA

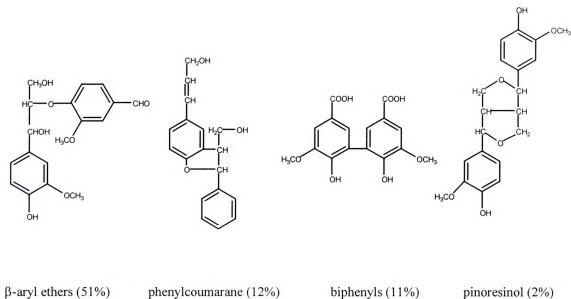
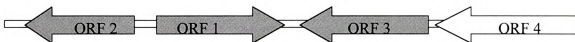


Figure 19. Representative structures of the major intermonomeric linkages in lignin. The relative percentages of these linkages are shown in parentheses (17, 22).

encoded by nearby genes. Efforts are currently underway in our laboratory to clone a *tfdA*-like gene, described in Chapter 4, from isolates that do not appear to degrade 2,4-D. The extragenic sequence of these elements may provide clues about the *in vivo* role of this gene. Alternatively, the surrounding regions of sequences encoding proteins with high identities to TfdA may indicate their potential functions in nature. In *Bordetella pertussis*, the causative agent of whooping cough, there is a hypothetical protein with 42% identity to TfdA over the entire amino acid sequence (Figure 20). Interestingly, the adjacent open reading frame, which is divergent from the *tfdA*-like gene, is 37% identical in amino acid sequence to a glutathione-S-transferase (GST) from *Sphingomonas* (formerly *Pseudomonas*) *paucimobilis* SYK-6 strain cleaves the β -aryl ether linkage of dimeric lignin components (Figure 21) (22, 23). Other open reading frames adjacent to the putative dioxygenase gene in *B. pertussis* are also homologous to enzymes involved in aromatic degradation (Figure 20), including a LysR-type transcriptional regulator (37) and a sequence homologous to *clcE*, which encodes maleyl acetate reductase (16). Although *B. pertussis* has not been found in the environment, *Bordetella* spp. have been isolated from soils (7, 33) and paper effluents (6), and at least one of these strains degrades 2,4-D (7).

Apart from lignin degradation, GSTs are associated with a number of other pathways involved in degradation of aromatics. Genes encoding GSTs are found in degradative pathways for biphenyl (BphK) in *Burkholderia* sp. LB400 (12), 2,4,5-trichlorophenoxyacetic acid (the product of *orf3*) in *Burkholderia cepacia* AC1100 (5), and polycyclic aromatic hydrocarbons (XylK) in *Cycloclasticus oligotrophicus* (41). Although gene disruption studies demonstrate that these enzymes are not required for



ORF1-putative α -KG-dependent dioxygenase (287 aa) with 42% identity to TfdA (M16730)
 ORF2-putative glutathione S-transferase (203 aa) with 37% identity β -etherase, LigE
 ORF3-putative LysR-type transcriptional regulator with 29% identity to N-terminus of SalR(316 aa).
 ORF4-putative maleyl acetate reductase with 37% identity to ClcE (329 aa) (Q47100)

Figure 20. Open reading frames adjacent to a putative α -KG-dependent dioxygenase in *Bordetella pertussis*. Genbank accession numbers are shown in parentheses.

activity, the multiple occurrences of GST-encoding genes in aromatic degradation operons suggest that they do serve a purpose. Based on the activities observed for other GSTs, proposed functions for the above enzymes include double bond isomerization, dehalogenation, and epoxide cleavage (40), but none of these activities have been demonstrated.

Despite the prevalence of lignin and its degradation products in soils, bacterial decomposition of these compounds has not been well studied due to the difficulties in working with such a large, heterogeneous substrate. The scheme for the degradation of lignin-derived aromatics in *S. paucimobilis* SYK-6 demonstrates the number and diversity of pathways and intermediates involved in this process (Figure 21) (22), but certainly does not represent the only means for lignin mineralization (17). Of the few previously characterized lignin-degrading isolates, most have generally belonged to the Actinomycete group (3, 21, 34, 39). Although not enriched in cultures with polymeric lignin as a substrate, a vast number of isolates including α -, β -, and γ -Proteobacteria and numerous Gram positive bacteria degrade a variety of aromatic compounds, including

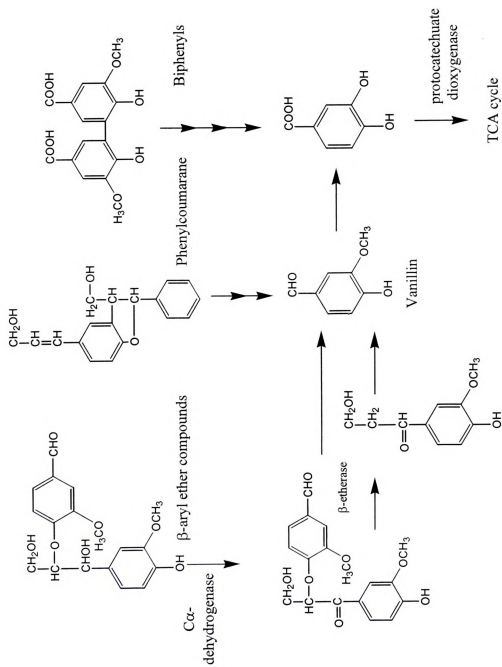


Figure 21. Degradation pathways of numerous dimeric lignin degradation products in *Sphingomonas paucimobilitis* SYK-6 (adapted from Masai et al.(22)).

biphenyls and aromatic acids (38, 39). Thus, it is not unlikely that more of these organisms possess the ability to degrade at least a fraction of the available lignin degradation products. As an aside, different *S. paucimobilis* strains are commonly isolated from 2,4-D enrichment cultures (13-15), have TfdA activity (30), but lack a *tfdA* gene with enough sequence identity to be picked up by gene hybridization methods (13).

When I began this research, there were no known enzymes with obvious sequence similarity to TfdA. Thus, little could be said about important or conserved residues or active site structure. Five years later, TfdA is related in sequence to a growing number of characterized and putative dioxygenases (Chapter 1). Sequence alignments of TfdA to two related sulfonate/ α -KG dioxygenases indicated a number of conserved residues that proved to be important for activity (Chapter 2). Comparison of these findings to studies of other enzymes in the superfamily shows both similarities in metallocenter ligands and differences in overall protein structure among the α -KG-dependent dioxygenases. In Chapter 4, I reported the intriguing presence of a *tfdA*-like gene in diverse soil isolates that do not degrade 2,4-D suggesting that this gene is maintained for a function other than in herbicide degradation. Although no alternative substrate for TfdA in soil microorganisms has been identified, there is circumstantial evidence for its involvement in the degradation of plant-synthesized ether- and cinnamic acid-containing products derived possibly from lignin. Further biochemical characterization of pJP4-derived TfdA and dioxygenases from other environmental bacteria are ongoing in the continued search for other α -KG-dependent dioxygenases with activity similar to that of TfdA.

Literature cited

1. **Bayley, C., N. Trolinder, C. Ray, M. Morgan, J. E. Quisenberry, and D. W. Ow.** 1992. Engineering 2,4-D resistance into cotton. *Theor. Appl. Gen.* **83**:645-649.
2. **Beil, S., K. N. Timmis, and D. H. Pieper.** 1999. Genetic and biochemical analyses of the *tec* operon suggest a route for evolution of chlorobenzene degradation genes. *J. Bacteriol.* **181**:341-346.
3. **Cespedes, R., L. Salas, I. Calderon, B. Gonzales, and R. Vicuna.** 1992. Microbial and biochemical-characterization of a bacterial consortium isolated from decaying wood by growth on a β -O-4 lignin-related dimeric compound. *Arch. Microbiol.* **158**:162-170.
4. **Cosper, N. J., C. M. V. Stålhandske, R. E. Saari, R. P. Hausinger, and R. A. Scott.** 1999. X-Ray absorption analysis of Fe(II) and Cu(II) forms of an herbicide-degrading α -ketoglutarate dioxygenase. *J. Biol. Inorg. Chem.* **4**:122-129.
5. **Daubaras, D. L., C. D. Hershberger, K. Kitano, and A. M. Chakrabarty.** 1995. Sequence-analysis of a gene-cluster involved in metabolism of 2,4,5-trichlorophenoxyacetic acid by *Burkholderia cepacia* AC1100. *Appl. Environ. Microbiol.* **61**:1279-1289.
6. **Foss, S., U. Heyen, and J. Harder.** 1998. *Alcaligenes defragrans* sp. nov., description of four strains isolated on alkenoic monoterpenes ((+)-menthene, alpha-pinene, 2-carene, and alpha-phellandrene) and nitrate. *Syst. Appl. Microbiol.* **21**:237-244.
7. **Greer, L. E., J. A. Robinson, and D. R. Shelton.** 1992. Kinetic comparison of seven strains of 2,4-dichlorophenoxyacetic acid-degrading bacteria. *Appl. Environ. Microbiol.* **58**:1027-1030.
8. **Häggbloom, M. M.** 1992. Microbial breakdown of halogenated aromatic pesticides and related compounds. *FEMS Microbiol. Rev.* **103**:29-72.
9. **Hausinger, R. P., F. Fukumori, D. A. Hogan, T. M. Sassanella, Y. Kamagata, H. Takami, and R. E. Wallace.** 1996. Biochemistry of 2,4-D degradation: evolutionary implications, p. 35-51. *In* K. Horikoshi, M. Fukuda, and T. Kudo (ed.), *Microbial Diversity and Genetics of Biodegradation*. Japan Scientific Press, Tokyo.

10. **Hegg, E. L., R. Y. N. Ho, and L. Que Jr.** 1999. Oxygen activation and arene hydroxylation by functional mimics of α -keto acid-dependent iron(II) dioxygenases. *J. Am. Chem. Soc.* **121**:1972-1973.
11. **Hegg, E. L., A. K. Whiting, J. McCracken, R. P. Hausinger, and J. Que, L.** 1999. The herbicide-degrading α -keto acid enzyme TfdA: metal coordination environment and mechanistic insights. *Biochemistry In press*.
12. **Hofer, B., S. Backhaus, and K. N. Timmis.** 1994. The biphenyl polychlorinated biphenyl-degradation locus (Bph) of *Pseudomonas* Sp. LB400 encodes four additional metabolic enzymes. *Gene* **144**:9-16.
13. **Ka, J. O., W. E. Holben, and J. M. Tiedje.** 1994. Genetic and phenotypic diversity of 2,4-dichlorophenoxyacetic acid (2,4-D)-degrading bacteria isolated from 2,4-D-treated field soils. *Appl. Environ. Microbiol.* **60**:1106-1115.
14. **Ka, J. O., W. E. Holben, and J. M. Tiedje.** 1994. Use of gene probes to aid in recovery and identification of functionally dominant 2,4-dichlorophenoxyacetic acid-degrading populations in soil. *Appl. Environ. Microbiol.* **60**:1116-1120.
15. **Ka, J. O., and J. M. Tiedje.** 1994. Integration and excision of a 2,4-dichlorophenoxyacetic acid degradative plasmid in *Alcaligenes paradoxus* and evidence of its natural intergeneric transfer. *J. Bacteriol.* **176**:5284-5289.
16. **Kasberg, T., D. L. Daubaras, A. M. Chakrabarty, D. Kinzelt, and W. Reineke.** 1995. Evidence that Operon-*Tcb*, operon-*Tfd*, and operon-*Clc* encode maleylacetate reductase, the fourth enzyme of the modified ortho pathway. *J. Bacteriol.* **177**:3885-3889.
17. **Kirk, T. K., and R. L. Farrell.** 1987. Enzymatic combustion - the microbial-degradation of lignin. *Ann. Rev. Microbiol.* **41**:465-505.
18. **Kivirikko, K. I., and T. Pihlajaniemi.** 1998. Collagen hydroxylases and the protein disulfide isomerase subunit of prolyl 4-hydroxylases. *Adv. Enzymol. Relat. Areas Mol. Biol.* **72**:328-398.
19. **Lippard, S. J., and J. M. Berg.** 1994. Principles of bioinorganic chemistry. University Science Books, Mill Valley, CA.
20. **Lloyd, M. D., K. D. Merritt, V. Lee, T. J. Sewell, B. Wha-Son, J. E. Baldwin, C. J. Schofield, S. W. Elson, K. H. Baggaley, and N. H. Nicholson.** 1999. Product-substrate engineering by bacteria: Studies on clavamate synthase, a trifunctional dioxygenase. *Tetrahedron* **55**:10201-10220.

21. **Lodha, S. J., R. A. Korus, and D. L. Crawford.** 1991. Synthesis and properties of lignin peroxidase from *Streptomyces viridosporus* T7a. *Appl. Biochem. Biotechnol.* **28-9**:411-420.
22. **Masai, E., Y. Katayama, S. Kawai, S. Nishikawa, M. Yamasaki, and N. Morohoshi.** 1991. Cloning and sequencing of the gene for a *Pseudomonas paucimobilis* enzyme that cleaves β -Aryl ether. *J. Bacteriol.* **173**:7950-7955.
23. **Masai, E., Y. Katayama, S. Kubota, S. Kawai, M. Yamasaki, and N. Morohoshi.** 1993. A bacterial enzyme degrading the model lignin compound β -etherase is a member of the glutathione-S-transferase superfamily. *FEBS Lett.* **323**:135-140.
24. **Nakatsu, C. H., N. A. Straus, and R. C. Wyndham.** 1995. The nucleotide-sequence of the Tn5271 3-chlorobenzoate 3,4-dioxygenase genes (*cbaAB*) unites the class Ia oxygenases in a single lineage. *Microbiol. UK* **141**:485-495.
25. **Pavel, E. G., J. Zhou, R. W. Busby, M. Gunsior, C. A. Townsend, and E. I. Solomon.** 1998. Circular dichroism and magnetic circular dichroism spectroscopic studies of the non-heme ferrous active site in clavamate synthase and its interaction with α -ketoglutarate cosubstrate. *J. Am. Chem. Soc.* **120**:743-754.
26. **Roach, P. L., I. J. Clifton, V. Fülöp, K. Harlos, G. J. Barton, J. Hajdu, I. Andersson, C. J. Schofield, and J. E. Baldwin.** 1995. Crystal structure of isopenicillin N synthase is the first from a new structural family of enzymes. *Nature* **375**:700-704.
27. **Roach, P. L., I. J. Clifton, C. M. H. Hensgens, N. Shibata, C. J. Schofield, J. Hajdu, and J. E. Baldwin.** 1997. Structure of isopenicillin N synthase complexed with substrate and the mechanism of penicillin formation. *Nature* **387**:827-830.
28. **Ryle, M. J., R. Padmakumar, and R. P. Hausinger.** 1999. Stopped-flow kinetic analysis of *Escherchia coli* taurine/ α -ketoglutarate dioxygenase: interactions with α -ketoglutarate, taurine, and oxygen. *Biochem.* **In press.**
29. **Saari, R. E., D. A. Hogan, and R. P. Hausinger.** 1999. Stereospecific degradation of the phenoxypropionate herbicide dichlorprop. *J. Molec. Catalysis B: Enzymatic* **266**:421-428.
30. **Sassanella, T. M., F. Fukumori, M. Bagdasarian, and R. P. Hausinger.** 1997. Use of 4-nitrophenoxyacetic acid for the detection and quantitation of 2,4-dichlorophenoxyacetic acid (2,4-D)/ α -ketoglutarate dioxygenase activity in 2,4-D degrading microorganisms. *Appl. Environ. Microbiol.* **63**:1189-1191.

31. **Schofield, C. J., J. E. Baldwin, M. F. Byford, I. Clifton, J. Hajdu, C. Hensgens, and P. Roach.** 1997. Proteins of the penicillin biosynthesis pathway. *Curr Opin Struct Biol* 7:857-864.
32. **Shilov, A. E., and A. A. Shteinman.** 1999. Oxygen atom transfer into C-H bond in biological and model chemical systems. Mechanistic aspects. *Accounts of Chemical Research* 32:763-771.
33. **Sturz, A. V., B. R. Christie, B. G. Matheson, and J. Nowak.** 1997. Biodiversity of endophytic bacteria which colonize red clover nodules, roots, stems and foliage and their influence on host growth. *Biol. Fert. Soil* 25:13-19.
34. **Thomas, L., and D. L. Crawford.** 1998. Cloning of clustered *Streptomyces viridosporus* T7A lignocellulose catabolism genes encoding peroxidase and endoglucanase and their extracellular expression in *Pichia pastoris*. *Can. J. Microbiol.* 44:364-372.
35. **Thornburg, L. D., M. T. Lai, J. S. Wishnok, and J. Stubbe.** 1993. A non-heme protein with heme tendencies: an investigation of the substrate specificity of thymine hydroxylase. *Biochemistry* 32:14023-14033.
36. **Valegård, K., A. C. T. van Scheltinga, M. D. Lloyd, T. Hara, S. Ramaswamy, A. Perrakis, A. Thompson, H.-J. Lee, J. E. Baldwin, C. J. Schofield, J. Hajdu, and I. Andersson.** 1998. Structure of a cephalosporin synthase. *Nature* 394:805-809.
37. **van der Meer, J. R., A. C. J. Frijters, J. J. Leveau, R. I. L. Eggen, A. J. B. Zhender, and W. M. De Vos.** 1991. Characterization of the *Pseudomonas* sp. strain P51 *tcbR*, a LysR-type transcriptional activator of the *tcbCDEF* chlorocatechol oxidative operon, and analysis of the regulatory region. *J. Bacteriol.* 173:3700-3708.
38. **Vicuña.** 1988. Bacterial degradation of lignin. *Enzyme Microb. Technol.* 10:646-655.
39. **Vicuna, R., B. Gonzalez, D. Seelenfreund, C. Ruttimann, and L. Salas.** 1993. Ability of natural bacterial isolates to metabolize high and low-molecular-weight lignin-derived molecules. *J. Biotechnol.* 30:9-13.
40. **Vuilleumier, S.** 1997. Bacterial glutathione S-transferases: What are they good for? *J. Bacteriol.* 179:1431-1441.
41. **Wang, Y., P. C. K. Lau, and D. K. Button.** 1996. A marine oligobacterium harboring genes known to be part of aromatic hydrocarbon degradation pathways of soil pseudomonads. *Appl. Environ. Microbiol.* 62:2169-2173.

42. **Whiting, A. K., L. Que Jr., R. E. Saari, R. P. Hausinger, M. A. Fredrick, and J. McCracken.** 1997. Metal coordination environment of a Cu(II)-substituted α -keto acid-dependent dioxygenase that degrades the herbicide 2,4-D. *J. Amer. Chem. Soc.* **119**:3413-3414.

APPENDIX A

AMINO ACID SEQUENCE ALIGNMENTS

Amino acid sequence alignments for Group II (Figure 22) and Group III (Figure 23) enzyme and different TfdAs (Figure 24) are shown. Alignments were performed using either the PIMA (3) or CLUSTAL (5) algorithms, which are available through the Baylor College of Medicine (BCM) Search Launcher (4). Figures were generated using GeneDoc software (1, 2).

Figure 22. Alignment of Group II α -KG-dependent dioxygenases

The accession numbers and sequence identifiers are as described in the legend of Table 3 (Chapter 1). Highly conserved residues (black boxes), residues conserved in more than 75% of the sequences (dark gray boxes), and TfdA residues targeted in site-directed mutagenesis studies (arrows) are shown.

	*	20	*	40	*	60	*	
TfdA	:	---	---	---	---	---	---	:
TauD	:	---	---	---	---	---	---	:
AtsK	:	---	---	---	---	---	---	:
YSD	:	MSPAAQTALPLP	STDL	PKII	TNGL	KNLNTSKQGYGNFT	HFYDGD	VSPGGLLKIRKSYREKSKYDYLPT : 75
CatC	:	---	---	---	---	---	---	---
PvCB	:	---	---	---	---	---	---	---
GBBH	:	---	---	---	---	---	---	---
GBBH_CEL	:	---	---	---	---	---	---	---
SYF	:	---	---	---	---	---	---	---
SYF_B	:	---	---	---	---	---	---	---
CS2	:	---	---	---	---	---	---	---
CS1	:	---	---	---	---	---	---	---
	80	*	100	*	140	*	140	*
TfdA	:	---	---	---	---	---	---	---
TauD	:	---	---	---	---	---	---	---
AtsK	:	---	---	---	---	---	---	---
YSD	:	WDPTKEYGP	LEFHYD	FDAL	RADGNF	SLFA	KNVGG	LKVKKITP
CatC	:	---	---	---	---	---	---	---
PvCB	:	---	---	---	---	---	---	---
GBBH	:	---	---	---	---	---	---	---
GBBH_CEL	:	---	---	---	---	---	---	---
SYF	:	---	---	---	---	---	---	---
SYF_B	:	---	---	---	---	---	---	---
CS2	:	---	---	---	---	---	---	---
CS1	:	---	---	---	---	---	---	---

Figure 22 (continued)

```

160      : IERIDEKSVLVRGQPI-----SQQQIA-----FARNCP-----LEGGFIKVNQRES-----VKYA- : 82
      : LYHALRRHVVLRDQAI-----TQQQRA-----LAQRCP-----ELHIHP-----FYPHA- : 76
      : IQAAVRHKVIFRGQTHI-----DQSQEG-----FALKCP-----EVAHP-----TPVVP- : 87
      : LALIVRQGVVVRFNQ-----NFADEGPD-YVEYGRHCP-----LHIHQTSGHQNNPE-----LHITFRP- : 199
      : CArC : KNLVRMRQGVVVRKN--L-----DIDSDT--FRDIYSARCP-----TIVEAD-----EKIGV- : 74
      : PvcB : FGLVREPGRPG-MH-VGELP-----AQWLKGLARSHHLLLRCF-----AAFDAESLTRYCHDFGVMHD- : 82
      : GBBB : IYELWNSKSL-KD-VPRI-----SKSTLSQSTFSKNLVKYF-----IIVDVEGTSSEATEKLCOSLVPHD- : 162
      : GBBB_CEL : HRVVOGLSLVPYD-HGAVL-----MODDDTLLEMLLAVRVCF-----TOLHCVPTPEGALILAKRISFIRE- : 181
      : SVYB : LPVRIETADGLD-PVQWASARBEATIELCRHGAVRVCF-----DLPSVAAEGEFA-----EALSP- : 98
      : CS2 : HGLVRDEAKTLAASLPEGRAA-LDTFNAGSEDGYLLLRCF-----LPVD-DSELPETPTSTPADRKRLVMEMRALA : 102
      : CS1 : -YALVRDAANTAAASLPGATA-LDTFNAGSEDGYLLLRCF-----LPVEADADLTFTSTPTAPEDRSLTMEANLGLV : 101

160      : IERIDEKSVLVRGQPI-----SQQQIA-----FARNCP-----LEGGFIKVNQRES-----VKYA- : 220
      : LYHALRRHVVLRDQAI-----TQQQRA-----LAQRCP-----ELHIHP-----FYPHA- : 76
      : IQAAVRHKVIFRGQTHI-----DQSQEG-----FALKCP-----EVAHP-----TPVVP- : 87
      : LALIVRQGVVVRFNQ-----NFADEGPD-YVEYGRHCP-----LHIHQTSGHQNNPE-----LHITFRP- : 199
      : CArC : KNLVRMRQGVVVRKN--L-----DIDSDT--FRDIYSARCP-----TIVEAD-----EKIGV- : 74
      : PvcB : FGLVREPGRPG-MH-VGELP-----AQWLKGLARSHHLLLRCF-----AAFDAESLTRYCHDFGVMHD- : 82
      : GBBB : IYELWNSKSL-KD-VPRI-----SKSTLSQSTFSKNLVKYF-----IIVDVEGTSSEATEKLCOSLVPHD- : 162
      : GBBB_CEL : HRVVOGLSLVPYD-HGAVL-----MODDDTLLEMLLAVRVCF-----TOLHCVPTPEGALILAKRISFIRE- : 181
      : SVYB : LPVRIETADGLD-PVQWASARBEATIELCRHGAVRVCF-----DLPSVAAEGEFA-----EALSP- : 98
      : CS2 : HGLVRDEAKTLAASLPEGRAA-LDTFNAGSEDGYLLLRCF-----LPVD-DSELPETPTSTPADRKRLVMEMRALA : 102
      : CS1 : -YALVRDAANTAAASLPGATA-LDTFNAGSEDGYLLLRCF-----LPVEADADLTFTSTPTAPEDRSLTMEANLGLV : 101

240      *      : ---ELADISNVSTOGKVAQRDARE-----V--VGNFANQLTESDSSE-----QOPAARYSML--SAVVPPPSSGDTTE-- : 142
      : TIdA : ---E-GVDEIIIVLQTH--NONPPD-----NMMHDDVTETPPAGAIL--AAKELSPSGDTTE-- : 127
      : Taud : ---D-GTYLLQLDQ--AQQR-----ANSMMHDDVTETVEAYPKASIL--SVVAPASSGDTTE-- : 136
      : ACSK : ---D-AEEFARVFD--DSTSS-----GMMHDDVTETVEAYPKASIL--SVVAPASSGDTTE-- : 246
      : YSD : ---GEGYRDTIK--LEGEK-----GKIVTGRGOLPEDSGLLSOVDVFLYAAEIKNVKFGATTE-- : 131
      : PvcB : ---WPGAVLEVEQEGADHIFA-----NNY-----VPIMDCMLETVEFOVHCVDAPGDTDRCTFS : 142
      : GBBB : ---TFGQFWVSNSATNDEPAYE-----DTAYG-SDEIGPDSTED-----FQDTGIQVFCHL--TPAKTSGLV : 225
      : GBBB_CEL : ---SNGVLFDWSKADUSNAY-----TAF-----NPLTDLTRELQGLOFHLCL--VNDATGNSTFV : 239
      : SVYB : ---GLHGTGCDTPKKEGGRNVYR-----TPPEREMILITESHLESWBRKOWFFCE--QPSRVEGATPL : 160
      : CS2 : GRRGLGHTGYRELRSGTVYHDVYPSGAHYLSSETSETTLERHTENAYHLQNYVNYLACS--RADHENAETLV : 175
      : CS1 : GRRGLGHTGYRELRSGTVYHDVYPSGAHYLSSETSETTLERHTENAYHLQNYVNYLACS--RADHERTAATLV : 174

```

Figure 22 (continued)

```

TtGdA      *      320      *      340      *      360      *
Taud      : FCD-MRAAYDALP---RDQSEH-GLRAEH---YALNSRFLLDGTD-YSEAQRNAMP---PVMWPLR---TH : 201
AtsK      : WTS-GIAAYEALS---VPROLES-GLRAEHDFKSPPEYKYRKTREEHORWEAKNPPLLHPVR---TH : 192
YSD       : WAN-TAAAYQELPEPIRELADEKAYHSNEYDYASLKPDIDPAKLEHRKVFSTVYET---EHPVR---V : 202
CAtC      : PAD-TIEADRLS---KPIQDFSTLL-----HVIHSSKEQANSORQGIKRAPV---THIHLR---V : 303
PvCB      : VCD-HALACOEMFA---HLRVDE-EETFE---VRVLERYYYDVS-PDGWKPVPF---TDLGWR-----KM : 188
GBBH      : SI---PAALQIAD---SSELEUNR-----RAGARY-ORSAAH-----YSSRS-----AAPIE-RHPRRE : 189
GBBH_CEL : DSEYCAEKLRNES---PEDEFIC-----NTKISH-HYLEGS-PPSSIHVSYL---EKPVIE-RNSFCN : 281
SYCB      : DGFATAELRIEA---PAAYRIC-----ETVEF-RNKDRH-S-----DYRC---TAPVIA-LDSGE : 289
CS1       : -A-----DIRQVL---AYLPKEV-----ERESK-GLYS-----RT---TAGVE-----PS : 196
CS2       : -G-----SVRKAL---PLIDEKTR-----ARLFDKVPCCVD-----VA---FRGGVDDPGAIAN : 218
          : -A-----SVRKAL---PLIDERTR-----ARLDRMPCCVD-----VA---FRGGVDDPGAIAN : 217

TtGdA      *      380      *      400      *      420      *      440      *
Taud      : AGSG-RKFLFIGA-HAS-HV---EGLPV-----AGRMLLAE---LEHATQREFVYHRNVS---DEVDWDRCVH : 263
AtsK      : PVSG-KQALFVNEGFTT-RH---VDVSE-----KESEALLSEF---FAHITQREFVQWRQCPNDIAFWDRVTQH : 255
YSD       : PISG-ERALQLGH-FVK-RH---KGYSL-----QSOHLFAYH---QGHVTRLENTVWRWEASDVAMDRATQH : 264
CAtC      : PVIK-KKQILVNRASF-RH---VELKR-----QSESLINF---YNLVESHDLQRAKPEHSVDMRRVQH : 367
PvCB      : LIYF-PFDEGQFASWEP-RH---VGFTD-----HETQAFQEL---GAFLKPRYRYKHWEDESLLMDRRVH : 251
GBBH      : FILRPFCEPVEGDASF---NPSEFH---YDGIAPGEORGELLAS---RRCLYHQAHYAHRWRSDDLEADLTLLH : 259
GBBH_CEL : ITQIRF---NPYDRAPFSCNNSSEAS--A---AETIKFYAYERF---SKICHNPONSIEISLRPSEVIFDRFRIH : 348
SYCB      : WEIRL---ANLRAFPQVADQMP-----DYFLAYRRF---IQMTREPRCFTRRLEAQWCFNRRVH : 350
CS1       : WESF-----FGTSERSV---EQRC---BEQGT---DFEWLDCD---TLQLTQCPAVITHPFTTFCRCFNQVQH : 256
          : VRPL-----YGDADDFP---GYDRELLAPEDPA---DKEAVAH---SKALDEVTAUYLEP---DLELIVDFRTH : 280
          : VRPL-----YGDADDFP---GYDRELLAPEDPA---DKEAVAH---SKALDEVTAUYLEP---DLELIVDFRTH : 279

```

	460	480	500	520
Ttfa	: RG-RRYDISAR	ELRRATILDAVV---		: 287
Taud	: -YA-NADYLPOR	IMRRATILGDKPFYRAG---		: 283
YalstK	: -YA-VDYGTQPR	IVRVTLAGEVPVGDQLSRTNKG---		: 301
YsD	: -SAVIDEETPIH	FAFRITQAPERVEDLFLNDENYPSLTLDI---		: 412
CarC	: -EREENDDIVR	RLRGQTADI---		: 273
PvCB	: GREAF--AHRA	PLRVSH-VLHAEPALRN--PHI-ORD---		: 291
GBBH	: SRTSE---QYR	PMCGCY-LSRDNFWAKAIPFL-SGKSQTSI---		: 385
GBBH cel	: ARDAF-PASGE	RFQCY-VDRDELLSR--ILVL-QR---		: 383
YsYb	: ----PYCMGE	ELLEDLL--MFGDRL---	PLRVSYGDSIAEDFVWALIGEAECAPFAWKGDVVMLDN	: 320
CS2	: -ARTPFSPWPK	QRLHRRVYVIRTRDN---	-GEL-SGGERAGDTISFPRR	: 325
CS1	: -ARTPFSPWPK	QRLHRRVYVIRTRDN---	-GOL-SGGERAGDVVAFFPR	: 324

	*	540	*
Tfda	:	----	:
TauD	:	----	:
Alsk	:	----	:
YSD	:	----	:
CarC	:	----	:
PvCB	:	----	:
GBBH	:	----	:
GBBH CEL	:	----	:
Syrb	:	----	:
MLAAHARDPYEPRILVVANGEMTARGDVWOPA	:	----	:
353	:	----	:
CS2	:	----	:
CS1	:	----	:

Figure 23. Alignment of Group III α -KG-dependent dioxygenases

The sequences of proline hydroxylase (Pro4H), mitomycin C biosynthesis protein (MmcH), putative hypophosphite dioxygenase (HtxA) and phytanoyl CoA hydroxylase (PPHYH) are compared. Residues discussed in the text of Chapter 1 are identified with black boxes. Protein accession numbers for the above sequences are the same as in Table 2 (Chapter 1).

MmcH	:	-----*	20	*	-----	40	*	-----	60	*	-----	80	*	-----	100	*	-----	120	*	-----	140	*	-----	160	*	-----	180	*	-----	200	*	-----	220	*	-----										
ProH	:	-----			-----			-----			-----			-----			-----			-----			-----			-----			-----			-----			-----										
HtxA	:	-----			-----			-----			-----			-----			-----			-----			-----			-----			-----			-----			-----										
PPHYH	:	MEQLRAARLQIVLGHGRPSAGAVVAHPTSGT	ISSASF	HPQQFQYTL	DNVN	LTLEQ	K	FVEEN	C	ELV	K	N	L	P	E	D	:																												
MmcH	:	AVFEKLRGLLEVAE	-----	QERENGSAFLY	-----	GGNQ	-----	RVFSL	L	N	K	G	E	E	F	E	Q	N	-----	VQD	-----	PTV	M	L	L	M	E	:																	
ProH	:	REVDCILRRAAALVYA	-----	QDSPD	-	RTLEK	-----	GRTV	-----	RAVHG	C	H	R	R	D	P	V	C	R	D	L	-----	VRH	-----	P	R	L	I	G	P	A	M	:												
HtxA	:	EEVAKILEDVKQELGAIGVASDNET-YQFEK	-----	QDSPD	-	RTLEK	-----	GRTV	-----	RAVHG	C	H	R	R	D	P	V	C	R	D	L	-----	VRH	-----	P	R	L	I	G	P	A	M	:												
PPHYH	:	ADIQRFNEFEK	-----	CR	-----	KEVKPLGLTVMR	-----	VTISK	SEY	AP	SE	K	M	I	T	K	V	Q	D	F	Q	E	K	E	L	E	R	Y	C	T	L	E	L	K	Y	E	:								
MmcH	:	EILGFGFLSSSTHANIA	-----	GG	-----	SRMHL	-----	Q	Y	I	S	W	A	R	E	D	G	M	D	R	H	V	N	V	A	V	L	-----	D	E	A	H	N	G	P	L	L	F	G	S	H	L	L	G	:
ProH	:	QILSGDVYVHQFKINAKAMTG	-----	DVPM	-----	Q	Y	I	S	W	A	R	E	D	G	M	D	R	H	V	N	V	A	V	L	-----	D	E	A	H	N	G	P	L	L	F	G	S	H	L	L	G	:		
HtxA	:	HELGENIRLHNSKINFKESS	-----	AFVQ	-----	Q	Y	I	S	W	A	R	E	D	G	M	D	R	H	V	N	V	A	V	L	-----	D	E	A	H	N	G	P	L	L	F	G	S	H	L	L	G	:		
PPHYH	:	CFTGENIMAMHTMTLINKED	-----	DS	-----	KKTSRHP	-----	Q	Y	I	S	W	A	R	E	D	G	M	D	R	H	V	N	V	A	V	L	-----	D	E	A	H	N	G	P	L	L	F	G	S	H	L	L	G	:

Figure 23. (Continued)

```

MmCH : -----RQP-----*-----240-----*-----260-----*-----280-----*-----300
PROH : LI--DVERRAPAGDGAQWLPQLS-ADLDY--AIDADLLARLTAGRGIESATGPAGSVMVFDGRLW--QTGANTIDRP : 200
HTXA : VY--DHRNVETG-----EFCHAISRSNWD-----EALDPTEGELLTGPVCTVTLHHVVRTLHGSGPNHSTIR : 225
PPHYH : LKPHDYPKWEGG-----VNKMFHGIQD-----YEE-NKARVHLVMEKGDVTFVFFHPLLIHGSGQNKIQGF : 216
                                           : 274

MmCH : HGILNYICRGYVR-----*-----320-----*-----340-----*-----360-----*
PROH : FGVVLVTINRTDN-----ALPAQAAPRPEFLAARD-----ATP-----LVPLPAG-----FSLGMTDGLP--- : 254
HTXA : RFLLLIGYAAADAWPLLGCNGYGDYESLMVSGRSTVFPRMV--ELP-LTVPYPLSMYGDRIFESQRALTQKYY- : 272
PPHYH : KKAISCHFFASADC-----HYIDVKGTSQENIEKEVVGIAHKFFGAENSVNLKDIWMEERARLVKGERTNL : 286
                                           : 338

```


Figure 24. Alignment of complete and partial TfdA sequences.

Deduced TfdA sequences from *Ralstonia eutropha* JMP134(pJP4) (M16730); *Burkholderia cepacia*(pIJB) (AAB47567); *Burkholderia cepacia* sp. RASC (Q45423), RASC; pEMT8 (Terry Marsh, unpublished); *Halomonas* sp. I-18 (U22499); Variovorax (U65531), TFD23 (U43276), *Ralstonia* strain CS (AF182758) are compared. Histidines altered in mutagenesis experiments (Chapter 2) are shown with arrows, invariant residues are shown in gray boxes.

	▼	20	*	40	*	60	*		
pJP4	:	MSVYANFHLFLFAAGVEDIDIRFALG	STEVREIERIMDEKSVLVFRGQPLSDQDQIAFARNFGP	LEGGFIKVNQR	:	75			
pIJB	:	MSINSEYHLFLFVAEYEEADLQCAL	SPTFVVRDVEHQMCKAVLVFRGQPLDQDQIAFARNFGQ	LEGGFIKYNQR	:	75			
RASC	:	MSINSEYHLFLFVGVNDLALQCAL	SPAEDVVRDVENEDQKAVLVFRGQPLDQDQIAFARNFGQ	LEGGFIKYNQR	:	75			
pEMT8	:	MSITSEYHLFLFVGVQDKLALQCAL	SPTFVVRDVEHQMCKAVLVFRGQPLDQDQIAFARNFGQ	LEGGFIKYNQR	:	75			
I-18	:	-----	-----	-----	-----	---			
TFD23	:	-----	-----	-----	-----	---			
Variovorax	:	-----	-----	-----	-----	---			
Ralst-CS	:	-----	-----	-----	-----	---			
		80	*	100	*	120	*	140	*
pJP4	:	PSREKYAELADISNVSLDGKVAQRDAREV	VGNFANQLMHS	SDSSFQOPPAARYSMLSAV	VPFSGGDTFEC	DMRAA	:	149	
pIJB	:	PSREKYAELADISNVSDGKVAQRDAREV	VGNFANQLMHS	SDSSFQOPPAARYSMLSAI	VPFSGGDTFEC	DMTHAT	:	150	
RASC	:	PSREKYAELADISNVSDGKVAQRDAREV	VGNFANQLMHS	SDSSFQOPPAARYSMLSAI	VPFSGGDTFEC	DMRAA	:	149	
pEMT8	:	PSREKYAELADISNVSDGKVAQRDAREV	VGNFANQLMHS	SDSSFQOPPAARYSMLSAI	VPFSGGDTFEC	DMRAA	:	149	
I-18	:	-----	-----	-----	-----	-----	-----	---	
TFD23	:	-----	-----	-----	-----	-----	-----	---	
Variovorax	:	-----	-----	-----	-----	-----	-----	---	
Ralst-CS	:	-----	-----	-----	-----	-----	-----	---	
						DMRAA	:	5	

Figure 24. (continued)

pJP4	:	YDALPRDLSQSELEGRFAEHYALNSRFLIGD	160	Y	180	*	200	Y	*	Y	Y	224
PIJB	:	NLGGRDDLPRELQGRFAEHYALNSRFLIGD										225
RASC	:	YDLPEDFKKELOGRFAEHYALNSRFLIGD										224
DEMT8	:	YDLPEDFKKELOGRFAEHYALNSRFLIGD										224
I-18	:	-DDLPEDFKKELOGRFAEHYALNSRFLIGD										74
TfD23	:	--ALPEDFKKELOGRFAEHYALNSRFLIGD										73
Varioovorax	:	YDLPEDFKKELOGRFAEHYALNSRFLIGD										75
Ralst-CS	:	YDLPEDFKKELOGRFAEHYALNSRFLIGD										79
pJP4	:	EGRMLLAELEHATQREFYIRHRWNVKGDLVM	240	Y	260	*	280	Y	*			287
PIJB	:	EGRMLLAELEHATQREFYIRHRWNVKGDLVM										288
RASC	:	EGRMLLAELEHATQREFYIRHRWNVKGDLVM										297
DEMT8	:	EGRMLLAELEHATQREFYIRHRWNVKGDLVM										287
I-18	:	EGRMLLAELEHATQREFYIRHRWNVKGDLVM										105
TfD23	:	EGRMLLAELEHATQREFYIRHRWNVKGDLVM										104
Varioovorax	:	EGRMLLAELEHATQREFYIRHRWNVKGDLVM										106
Ralst-CS	:	RRRSHAAG-----										87

Literature cited

1. **Nicholas, K. B., N. H. B. Jr., and I. Deerfield, D.W.** 1997. GeneDoc: analysis and visualization of genetic variation. *EMB News* **4**:14.
2. **Nicholas, K. B., and J. Nicholas, H.B.** GeneDoc: Analysis and Visualization of Genetic Variation. <http://www.cris.com/~Ketchup/genedoc.shtml> September, 10 1999
3. **Smith, R. F., and T. F. Smith.** 1992. Pattern-Induced Multi-sequence Alignment (PIMA) algorithm employing secondary structure-dependent gap penalties for comparative protein modelling. *Prot. Engineering* **5**:35-41.
4. **Smith, R. F., B. A. Wiese, M. K. Wojzynski, D. B. Davison, and K. C. Worley.** 1996. BCM Search Launcher--an integrated interface to molecular biology data base search and analysis services available on the World Wide Web. *Genome Res.* **6**:454-462.
5. **Thompson, J. D., D. G. Higgins, and T. J. Gibson.** 1994. CLUSTAL W: improving the sensitivity of progressive multiple sequence alignment through sequence weighting, position-specific gap penalties and weight matrix choice. *Nucl. Acids Res.* **22**:4673-4680.

APPENDIX B

STEREOSPECIFIC DEGRADATION OF THE PHENOXYPROPIONATE HERBICIDE MECOPROP

The following article, Saari, R. E., D. A. Hogan, and R. P. Hausinger (1999)
“Stereospecific degradation of the phenoxypropionate herbicide dichlorprop.” J.
Mol.Catal. B: Enzymatic (6): 421-428 reprinted with permission from Elsevier Science,
is the result of a collaboration between a former graduate student in the Hausinger lab,
Ruth E. Saari, and myself (D.A.H.). In this report, the stereospecific degradation of
dichlorprop, a chiral derivative of 2,4-D, is examined in cell extracts of *Ralstonia*
eutropha JMP134, *Burkholderia cepacia* strain RASC and a mecoprop-degrading strain
Alcaligenes denitrificans. These studies indicate that α -KG-dependent dioxygenases with
altered substrate specificities exist in the environment and suggest that TfdA-like
enzymes can act on substituted phenoxyacetic acids that may more closely resemble the
structure of aromatics liberated during the course of lignin degradation.

Stereospecific degradation of the phenoxypropionate herbicide dichlorprop

Ruth E. Saari ^{a,b}, Deborah A. Hogan ^{a,c}, Robert P. Hausinger ^{a,b,c,*}

^a Center for Microbial Ecology, 160 Giltner Hall, Michigan State University, East Lansing, MI 48824, USA

^b Department of Biochemistry, 160 Gilmer Hall, Michigan State University, East Lansing, MI 48824, USA

^c Department of Microbiology, 160 Giltner Hall, Michigan State University, East Lansing, MI 48824, USA

Received 31 August 1998; accepted 7 December 1998

Abstract

2,4-Dichlorophenoxyacetic acid (2,4-D)/ α -ketoglutarate (α -KG) dioxygenase, TfdA, from *Ralstonia eutropha* JMP134, was purified from recombinant cells and shown by gas chromatographic and colorimetric methods to degrade only the *S* enantiomer of dichlorprop, a phenoxypropionate herbicide. Similarly, cell extracts of *Burkholderia cepacia* RASC, containing a biochemically and genetically related α -KG-dependent dioxygenase, also were shown to oxidize (*S*)-dichlorprop using chiral HPLC and colorimetric methods. In contrast, cell extracts of a mecoprop-degrading strain of *Alcaligenes denitrificans* were shown to catabolize (*R*)-dichlorprop. Although the *A. denitrificans* activity exhibited stereospecificity opposite to that of the JMP134 and RASC strains, its cofactor requirements were found to be characteristic of an α -KG-dependent dioxygenase. A PCR amplification product from the DNA of this strain was shown to encode an amino acid sequence that was 95% and 86% identical to the corresponding region of TfdA in RASC and JMP134, respectively. Thus, closely related herbicide-degrading gene products appear to be capable of exhibiting opposite stereochemical degradative capabilities. © 1999 Elsevier Science B.V. All rights reserved.

Keywords: Stereospecificity; Herbicide; Dichlorprop; α -Ketoglutarate; TfdA

1. Introduction

Ring-substituted phenoxyacetates and phenoxypropionates are widely used as herbicides to control the growth of broadleaf weeds and woody plants [1]. While phenoxyacetates such as 2,4-dichlorophenoxyacetic acid (2,4-D) lack

a chiral carbon atom, phenoxypropionates can exhibit either of two enantiomeric forms because of the methyl group attached to the C-2 carbon atom. Notably, only the *R* enantiomers are active towards plants [2]. A current trend in agriculture is increasing use of only the active enantiomer of chiral herbicides in order to reduce environmental loads of organopesticides [2]. For example, about 75% of dichlorprop (2-(2,4-dichlorophenoxy)propionate) and mecoprop (2-(2-methyl-4-chlorophenoxy)propionate) are sold in their active enantiomeric forms in the European Union, with the expectation that

* Corresponding author. Michigan State University, Center for Microbial Ecology, Department of Microbiology, 160 Giltner Hall, East Lansing, MI, USA. Tel.: +1-517-353-9675; Fax: +1-517-353-8957; E-mail: hausinger@pilot.msu.edu

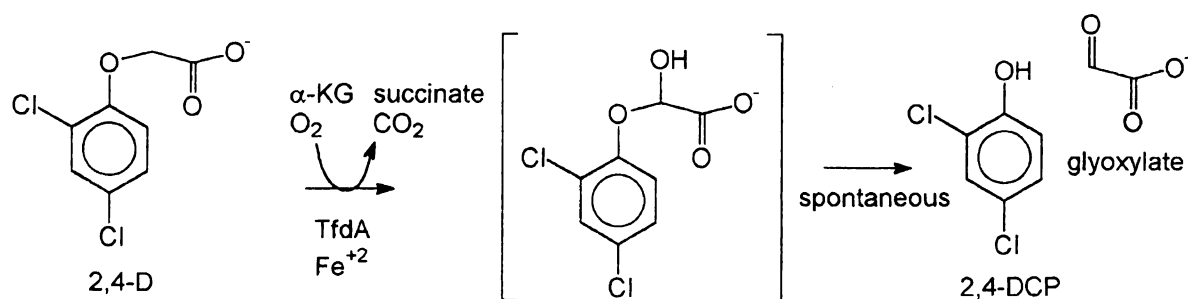
within 5 years only the *R* isomer will be commercially available (R. Akers, personal communication).

Phenoxyacid herbicides are rapidly degraded in soil by bacteria and fungi [1]. One of the best characterized herbicide-degrading organisms is *Ralstonia eutropha* (formerly *Alcaligenes eutrophus* [3]) strain JMP134, capable of using 2,4-D as its sole carbon and energy source. The first step in 2,4-D catabolism is its conversion to 2,4-dichlorophenol (2,4-DCP), catalyzed by the enzyme 2,4-D/ α -ketoglutarate (α -KG) dioxygenase [4] or TfdA [5]. This ferrous ion-dependent enzyme couples the oxidative decarboxylation of α -KG to hydroxylation of the substrate at the C-2 carbon to yield a postulated hemiacetal intermediate which spontaneously decomposes to form 2,4-DCP and glyoxylate [4] (Scheme 1). The chlorinated phenol is subsequently metabolized by a series of well-studied enzymes that eventually generate an intermediate of the tricarboxylic acid cycle [6]. It is important to emphasize, however, that not all 2,4-D-degrading microorganisms use this pathway. The biochemistry of phenoxypropionate degradation is much less well understood than that of 2,4-D. Here too, however, side chain removal to release the corresponding phenol has been shown to be an essential step in catabolism of these compounds (e.g., Refs. [7–14]).

Studies to characterize the stereospecificity of enzymes that degrade phenoxypropionate herbicides can have important biotechnological ramifications. For example, a synthetic process

could be devised in which a particular herbicide is initially synthesized as the racemic mixture, the *S* enantiomer is degraded by a stereoselective enzyme, and the remaining *R* isomer is purified away from the other reaction products which are recycled. As an alternate illustration, the genes encoding an enzyme specific for the *R* isomer could be used to develop genetically engineered crops that are resistant to the herbicide of interest. Genetic engineering has already been used for crop protection from (achiral) phenoxyacetate herbicides: cotton has shown enhanced tolerance towards 2,4-D when *tfdA* was transformed directly into the plant [15] or into root-associated microbes [16].

Here, we demonstrate that purified *R. eutropha* TfdA specifically degrades the *S* enantiomer of dichloroprop and characterize the kinetics of this process. In addition, we establish that *Burkholderia cepacia* strain RASC, a 2,4-D-degrader containing a TfdA with 80% sequence identity to that from JMP134, has the same stereopreference for the *S* enantiomer. By contrast, we show that cell extracts of a strain of *Alcaligenes denitrificans*, intact cells of which are known to utilize the *R* enantiomer of mecoprop [14], specifically degrade the *R* enantiomer of dichloroprop in an α -KG-dependent process. Although the latter activity exhibits opposite stereospecificity from that found in the 2,4-D-degrading strains, we provide evidence that a *tfdA*-like gene is present in *A. denitrificans*, suggesting that all of these enzymes are closely related to each other.



Scheme 1. Reaction catalyzed by TfdA with 2,4-D.

2. Experimental

2.1. Chemicals

(+)-(R)-Dichlorprop was a kind gift from BASF. Racemic and (+)-(R)-mecoprop were generously donated by A.H. Marks. Racemic dichlorprop and 2,4-D were purchased from Aldrich.

2.2. Bacterial strains

R. eutropha JMP134 [17] and *B. cepacia* RASC [18] were obtained from the Research on Microbial Evolution laboratory at Michigan State University. A strain of *A. denitrificans* isolated for its ability to degrade mecoprop [14] was obtained from Hilary Lappin-Scott (University of Exeter).

2.3. Activity assay with colorimetric detection of derivatized phenols

The standard assay mix contained 1 mM α -KG, 50 μ M each of Fe(II) and ascorbate, 1 mM phenoxyacid substrate in 10 mM imidazole buffer (pH 6.75), and enzyme. In studies of cell extracts, the concentrations of selected reagents were varied in some experiments as noted in the text. The iron and ascorbate were either supplied together as iron(II) ascorbate salt or separately as $(\text{NH}_4)_2\text{Fe}(\text{SO}_4)_2$ and ascorbic acid. Reactions were carried out at 30°C and terminated by addition of EDTA to a final concentration of 5 mM. The phenolic product was detected at 510 nm following addition of 4-aminoantipyrene, pH 10 borate buffer, and potassium ferricyanide, as described [19]. Measured extinction coefficients for the 4-aminoantipyrene adducts were 15,700 $\text{M}^{-1} \text{cm}^{-1}$ for 2,4-DCP and 11,300 $\text{M}^{-1} \text{cm}^{-1}$ for 4-chloro-2-methylphenol.

2.4. Preparation of cell extracts and purified enzyme

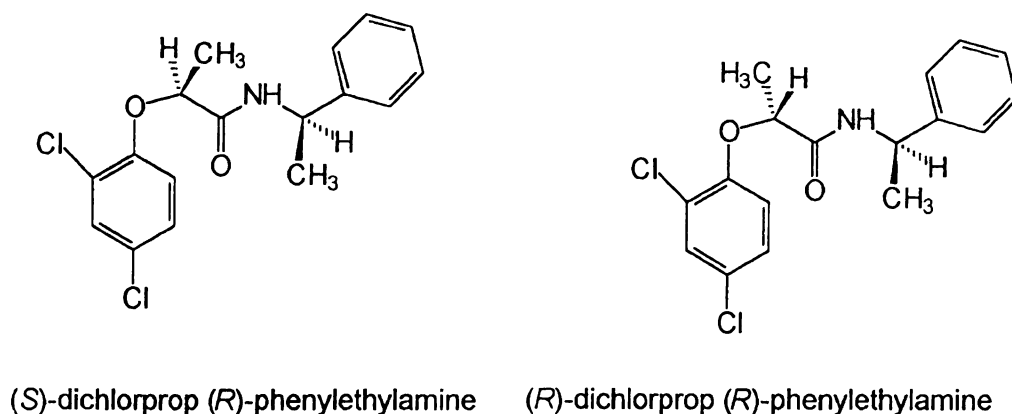
TfdA was purified from *Escherichia coli* DH5 α cells carrying the cloned *R. eutropha*

JMP134 *tfdA* gene on plasmid pUS311 by sequential chromatography on DEAE Sepharose and MonoQ (Pharmacia) columns [4,20].

2,4-D and mecoprop degraders were grown aerobically at 30°C in MMO mineral salts medium [21] with 50 ppm yeast extract and the relevant herbicide at initial concentrations between 1 and 5 mM. Cells were harvested when 60–90% of the herbicide was consumed as measured by disappearance of the chromophore at 230 nm. Cell extracts were prepared by resuspending the bacteria in Tris buffer (pH 7.7) with 1 mM EDTA followed by disruption in a French pressure cell and ultracentrifugation (100,000 $\times g$, 30 min) or centrifugation in a microcentrifuge (16,000 $\times g$, 5 min). Protein concentrations were determined by using the BioRad protein assay with bovine serum albumin as the standard.

2.5. Formation of diastereomers and gas chromatography (GC)

The levels of (*R*)- and (*S*)-dichlorprop in samples were assessed by using a modification of a published GC method [22]. Aqueous reaction mixtures (1 ml) were acidified with 25 μ l of HCl (conc.) and extracted with 1 ml methylene chloride. The organic phase (0.5 ml) was dried under a gentle stream of air, 1 drop of thionyl chloride was added, and the sample was incubated 10 min over a steam bath. Following removal of the thionyl chloride under vacuum, the sample was dissolved in 0.1 ml chloroform with 1 drop of (*R*)-phenylethylamine added, allowed to react 25 min at room temperature to form diastereomers (Scheme 2), dried, and transferred to 0.5 ml of ethyl acetate. An aliquot (1 μ l) of the sample was injected onto a DB-5 column (polymethylsiloxane with 5% phenyl groups; J&W Scientific), with a temperature program set to increase linearly from 200 to 270°C in 7 min, and the analytes were monitored by electron capture detection (rather than the less sensitive flame ionization detection originally used [22]). Peaks were identified by



Scheme 2. Formation of diastereomers of dichlorprop and (R)-phenylethylamine.

comparison with the retention times of the diastereomeric amides of authentic (R)-dichlorprop and (RS)-dichlorprop.

2.6. High pressure liquid chromatography (HPLC)

Dichlorprop was reacted with cell extracts or purified enzyme as described for the activity assay, and the reactions were stopped with 5 mM EDTA. Aliquots were injected onto a Nucleodex α -PM column (4.0 mm i.d. \times 200 mm length; Machery-Nagel, Germany). The eluent was 30% phosphate buffer (50 mM, pH 3) and 70% methanol at a flow rate of 0.7 ml min⁻¹. Species eluting from the column were monitored with UV detection at 230 nm.

2.7. DNA hybridization, amplification and sequencing

Total genomic DNA was isolated from *A. denitrificans* [23] and digested with *Bam*HI. Following separation on a 0.8% agarose gel, the DNA was transferred [23] to a Hybond N membrane (Amersham). Probes for *tfdA*_{RASC} (a 1-kb *Pst*I fragment [18]) and for *tfdA*_{JMP134} (an 801-bp *Sty*I fragment [24]) were labeled with digoxigenin according to the Genius™ System instructions (Boehringer-Mannheim Biochemicals). The membrane was blotted with the probes

at high stringency (68°C, 50% formamide) or low stringency (68°C, no formamide) using the protocol from the same manual.

A. denitrificans DNA was used as template DNA for PCR amplification with TVU and TVL primers which amplify a 360-bp internal fragment of both RASC and JMP134 *tfdA* [25]. The product was purified by using the GFX PCR DNA and gel band purification kit (Pharmacia Biotech) and was sequenced in both directions by using dye terminator chemistry at the MSU-DOE-PRL Plant Biochemistry DNA Sequencing Facility with TVU and TVL as primers. The nucleotide and amino acid sequences of the amplified product (not including the primer sequence) were aligned to those of JMP134 and RASC using protocols in the GCG suite of programs [26].

2.8. Data analysis

Data were fitted to straight lines, exponential decays, or square hyperbola using the program KaleidaGraph (Synergy software). As well, progress curves of 2,4-DCP production vs. time were fitted to Eq. (1) by non-linear regression using the same program.

$$A_t = A_f(1 - e^{-k_{\text{inact}}t}) \quad (1)$$

In this equation, A_t is the absorbance at time t , A_f is the final absorbance, and k_{inact} is the rate of inactivation.

3. Results

3.1. TfdA stereospecificity

The stereospecificity of purified TfdA from *R. eutropha* JMP134 was investigated using two methods. The first approach used derivatization with (*R*)-phenylethylamine followed by GC analysis to separate and quantitate the two diastereomers. During the reaction of racemic dichlorprop with TfdA, the percentage of *S* relative to *R* enantiomer decreased over time, suggesting that this enzyme uses the *S* isomer (Fig. 1). The second procedure used to assess stereospecificity involved a colorimetric assay for 2,4-DCP release. 2,4-DCP was produced by TfdA acting on racemic dichlorprop but not on (*R*)-dichlorprop (Fig. 2), a result in agreement with the GC results for this enzyme. The enzyme lost activity over time due to oxidative inactivation events that are minimized by the presence of ascorbic acid [27]. Based on initial rates, (*S*)-dichlorprop utilization ($0.81 \mu\text{mol min}^{-1} \text{mg}^{-1} \text{protein}$) was 6% of that observed for 2,4-D decomposition ($13 \mu\text{mol min}^{-1} \text{mg}^{-1} \text{protein}$) under saturating substrate concentrations.

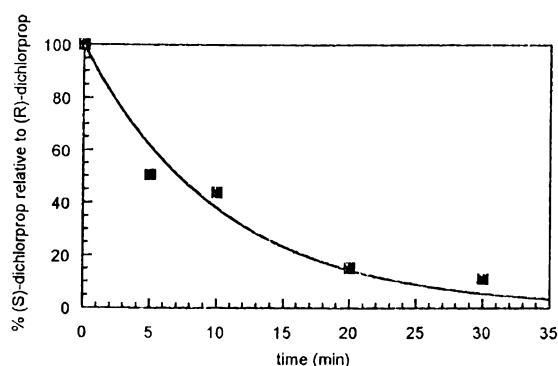


Fig. 1. Stereoselectivity of dichlorprop decomposition catalyzed by TfdA. TfdA from JMP134 ($50 \mu\text{g}$) was incubated with racemic dichlorprop ($100 \mu\text{M}$) and ascorbic acid, ferrous ion, and α -KG using standard concentrations for the indicated time periods. Following extraction, the remaining dichlorprop was converted to the (*R*)-phenylethylamine diastereomers and analyzed by GC/electron capture detection. Data were fitted to an exponential decay with a decay rate of $0.096 \pm 0.011 \text{ min}^{-1}$.

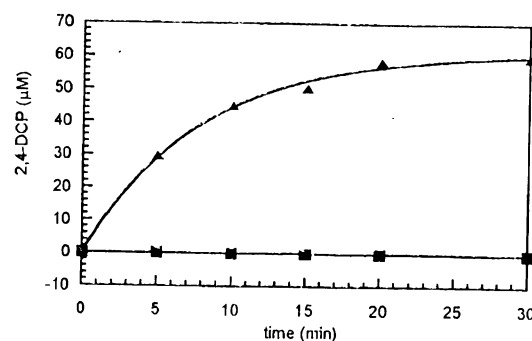


Fig. 2. 2,4-DCP production by TfdA acting on dichlorprop. TfdA from JMP134 ($10 \mu\text{g ml}^{-1}$) was incubated with a racemic mixture of dichlorprop (\blacktriangle) at 2 mM or with (*R*)-dichlorprop at the same concentration (\blacksquare). 2,4-DCP was measured colorimetrically. Data for the racemic dichlorprop were fitted to Eq. (1) ($k_{\text{inact}} = 0.131 \pm 0.004 \text{ min}^{-1}$), while data for the (*R*)-dichlorprop were fitted by linear regression (slope of $-0.02 \mu\text{M min}^{-1}$).

3.2. Herbicide-degrading activities in cell extracts

Cell extracts were examined from JMP134 and two additional phenoxyacid herbicide degraders: *B. cepacia* RASC, a 2,4-D degrader with a TfdA that is 80% identical to that of *R. eutropha* JMP134 [18], and a strain of *A. deni-*

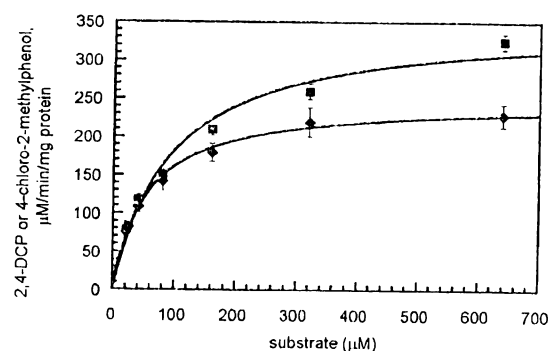


Fig. 3. Kinetic analysis of *A. denitrificans* cell extract activities towards (*R*)-mecoprop and (*R*)-dichlorprop. Cell extracts of *A. denitrificans* were examined for their abilities to decompose (*R*)-dichlorprop (\blacksquare) and (*R*)-mecoprop (\blacklozenge). Initial rates calculated from the phenolic product release (based on 6 min time points, triplicate samples) were fitted to the Michaelis-Menten equation to yield values of $K_m = 91 \pm 16 \mu\text{M}$ and $V_{\text{max}} = 351 \pm 21 \mu\text{M min}^{-1} \text{mg}^{-1} \text{protein}$ for (*R*)-dichlorprop and $K_m = 52 \pm 4 \mu\text{M}$ with $V_{\text{max}} = 247 \pm 6 \mu\text{M min}^{-1} \text{mg}^{-1} \text{protein}$ for (*R*)-mecoprop. Mecoprop velocity data were corrected for $\sim 1\%$ contamination with a phenolic compound presumed to be 4-chloro-2-methylphenol.

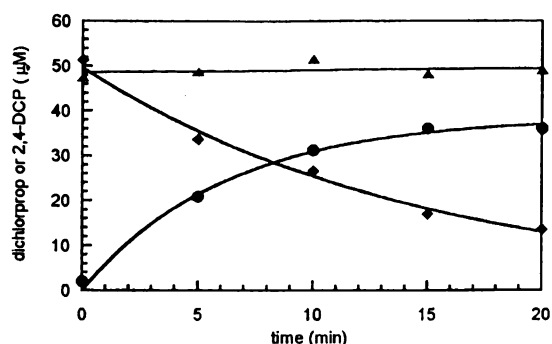


Fig. 4. Stereospecificity of dichlorprop-degrading activity of *A. denitrificans* cell extracts as measured by chiral HPLC. Concentrations of (*S*)-dichlorprop (▲), (*R*)-dichlorprop (◆), and 2,4-DCP (●) were measured at selected time points after incubation of *A. denitrificans* cell extracts (50 μ l) with racemic dichlorprop (0.1 mM) and the standard reaction components. Dichlorprop was quantitated by using chiral HPLC and 2,4-DCP was quantitated colorimetrically. Data for the (*S*)-dichlorprop were fit to a straight line of slope $0.05 \mu\text{M min}^{-1}$, for (*R*)-dichlorprop to exponential decay with an exponent of -0.067 min^{-1} ; and for 2,4-DCP to Eq. (1) with an apparent inactivation rate of 0.16 min^{-1} .

trificans isolated for its ability to degrade (*R*)-mecoprop [14]. Cell extracts of JMP134 and RASC exhibited highest activity towards 2,4-D, but showed $\sim 20\%$ of this activity towards dichlorprop. We attribute the cell extract activity towards phenoxy herbicides in both these strains to TfdA, since Tn5 disruption of the *tfdA* gene in either strain will prevent the conversion of 2,4-D to 2,4-DCP by intact cells [5,18]. By

contrast to the specificity of the abovementioned strains, *A. denitrificans* extracts were most active with phenoxypropionates including mecoprop, dichlorprop, 2-(2,4-dibromophenoxy)propionate, and 2-(4-chlorophenoxy)propionate, with only minor activity towards the phenoxyacetates 2,4-D and 2-chloro-4-methylphenoxyacetic acid (~ 13 fold less than the activity towards dichlorprop). Cell extracts of *A. denitrificans* demonstrated a slightly higher V_{max} towards the dichlorprop than towards mecoprop, the substrate on which it was isolated, but slightly less affinity (higher K_m) (Fig. 3). The *A. denitrificans* activity was dependent on α -KG and ferrous ion, and was rapidly lost (in 2 min) in the absence of ascorbic acid. These cofactor requirements are characteristic of α -KG-dependent dioxygenases.

3.3. Stereospecificity of activity in cell extracts

The stereospecificity of herbicide decomposition by cell extracts was measured using an HPLC column with a chiral stationary phase, which permitted direct separation without prior derivatization of the enantiomers of dichlorprop. In agreement with the results using purified enzyme, cell extracts of JMP134 degraded the *S* enantiomer. Similar results were obtained with

	150	160	170	180	190	200
JMP134	RAAYDALPRDLQSEGLRAEHYALNSRFLGDTDYSEAQRNAMPPVNWPLVRTHAGSGRK					
		: : :	: : : :	: : : :	: : : :	: : : :
<i>A. denitrificans</i>	RAAYDDLPEDFKKELQGLRAEHYALNSRFLGDTDYSESQRNAMPPVSWPLVRTHAGSGRK					
		: : : :	: : : :	: : : :	: : : :	: : : :
RASC	RAAYDDLPEDFKKELQGLRAEHYALHSRFLGDTDYSESQRNAMPPVSWPLIRTHAGSGRK					
		: : : :	: : : :	: : : :	: : : :	: : : :
	170	180	190	200	210	220
	210	220	230	240	250	
JMP134	FLFIGAHASHVEGLPVAEGRMLLAELLEHATQREFVYRHRWNVGDLM					
		: :	: : : :	: : : :	: : : :	: : : :
<i>A. denitrificans</i>	FLFIGAHAGHIEGRPVAEGRMLLAELLEHATQKRFVYRHSWKVGDLM					
		: : : :	: : : :	: : : :	: : : :	: : : :
RASC	FLFIGAHASHIEGRPVAEGRMLLAELLEHATQPKFVYRHSWKVGDLM					
		: : : :	: : : :	: : : :	: : : :	: : : :
	230	240	250	260	270	

Fig. 5. Comparison of an *A. denitrificans* TfdA-like sequence with the enzymes from RASC and JMP134. The deduced sequence encoded by the PCR amplification product arising from *A. denitrificans* DNA was compared to the indicated portions of the RASC and JMP134 TfdA sequences. Identical amino acids are indicated by a solid vertical bar and similar amino acids by a dashed bar.

RASC extracts (data not shown). By contrast, *A. denitrificans* extracts degraded (*R*)-dichlorprop (Fig. 4) with concurrent 2,4-DCP production.

3.4. Molecular biological comparison of strains

The similarity in cofactor requirements among the three strains raised the question of whether the *A. denitrificans* activity was due to a gene related in sequence to those which encode the two TfdA enzymes in the other species. *A. denitrificans* genomic DNA hybridized at low stringency to a probe for *tfdA*_{JMP134} and at high stringency to a segment of *tfdA*_{RASC} (data not shown). Amplification of *A. denitrificans* DNA with primers specific for *tfdA* yielded a 360-bp DNA fragment with a sequence that was 94% identical to that from RASC and 78% to that from JMP134, in a 327-bp overlap. The translated sequence (109 amino acids long) had 95% identity with TfdA from RASC and 86% identity to that from JMP134 (Fig. 5).

4. Discussion

4.1. *R. eutrophus* JMP134 TfdA oxidizes the *S* isomer of phenoxypropionates

α -KG dependent dioxygenases typically exhibit stereoselectivity in the hydroxylations they catalyze (e.g., Refs. [28–31]); thus, it was not surprising to find that *R. eutrophus* JMP134 TfdA oxidizes a single enantiomer (the *S* isomer) of dichlorprop. Based on this result with phenoxypropionate, the enzyme likely catalyzes stereochemically selective oxidation at the *pro-R* position when acting on the prochiral 2,4-D.

4.2. Related gene products can degrade opposite stereoisomers

The above studies demonstrate that the herbicide-degrading activity of *A. denitrificans* exhibits opposite stereochemistry than that found

in strains JMP134 or RASC; yet, each of these activities are α -KG-dependent and the enzymes are likely to be genetically related. The present work extends the conclusions derived from studies with a strain of *Sphingomonas herbicidovorans* that is capable of degrading both enantiomers of mecoprop [32]. In that strain, two α -KG-dependent dioxygenases appear to be present, each specific for a separate enantiomer of the substrate [33]. Based on our findings, it is probable that the two *S. herbicidovorans* enzymes are closely related in sequence. The ability for closely related enzymes to recognize opposite stereoisomers has precedent. For example, recent crystallographic characterization of two tropinone reductases demonstrate the presence of almost identical overall protein folding, but the closely related enzymes exhibit opposite substrate stereoselectivities due to differences in a few charged residues at the active site [34].

4.3. Biotechnological implications

The work described here may have biotechnological applications. An *S* isomer selective dichlorprop-degrading enzyme, such as TfdA, may be used to facilitate the preparation of the desired *R* isomer, while a gene encoding an *R* isomer selective enzyme, such as that in *A. denitrificans*, may be useful for development of herbicide-resistant transgenic plants. Also, in understanding the role of microorganisms in the environmental fate of phenoxypropionates, it is useful to have analytical techniques such as those used in this research capable of distinguishing the enantiomers.

Acknowledgements

We thank Peter Chapman for suggesting that dichlorprop could be used to probe the stereospecificity of TfdA, Paul Loconto of the Engineering Research Labs of MSU for assistance in setting up the GC method and suggesting the

use of electron capture detection, and Hilary Lappin-Scott for providing us with the mecoprop-degrading strain of *A. denitrificans*. This work was supported by the National Science Foundation (MCB9603520), the National Science Foundation–Science and Technology Center Grant DEB9120006, and the Michigan State University Agricultural Experiment Station.

References

- [1] M.A. Loos, in: P.C. Kearney, D.D. Kaufman, (Eds.) *Herbicides: Chemistry, Degradation and Mode of Action*, Vol. 1, Marcel Dekker, New York, 1969, p. 1.
- [2] IUPAC, *Pure Appl. Chem.* 69 (1997) 1335.
- [3] E. Yabuuchi, Y. Kosako, I. Yano, H. Hotta, Y. Nishiuchi, *Microbiol. Immunol.* 39 (1995) 897.
- [4] F. Fukumori, R.P. Hausinger, *J. Bacteriol.* 175 (1993) 2083.
- [5] W.R. Streber, K.N. Timmis, M.H. Zenk, *J. Bacteriol.* 169 (1987) 2950.
- [6] R.P. Hausinger, F. Fukumori, D.A. Hogan, T.M. Sassanella, Y. Kamagata, H. Takami, R.E. Wallace, in: K. Horikoshi, M. Fukuda, T. Kudo (Eds.), *Microbial Diversity and Genetics of Biodegradation*, Japan Scientific Press, Tokyo, 1996, p. 35.
- [7] P. Ludwig, W. Gunkel, H. Hünerfuss, *Chemosphere* 24 (1992) 1423.
- [8] R. Martens, *Pestic. Sci.* 9 (1978) 127.
- [9] M. Nègre, M. Gennari, V. Andreoni, R. Ambrosoli, L. Celi, *J. Environ. Sci. Health B* 25 (1993) 545.
- [10] A.E. Smith, A.J. Aubin, *Can. J. Soil Sci.* 70 (1990) 343.
- [11] A.E. Smith, *Bull. Environ. Contam. Toxicol.* 34 (1985) 656.
- [12] A.E. Smith, *J. Agric. Food Chem.* 33 (1985) 483.
- [13] A.E. Smith, *J. Agric. Food Chem.* 25 (1977) 893.
- [14] V.A. Tett, A.J. Willetts, H.M. Lappin-Scott, *FEMS Microbiol. Lett.* 14 (1994) 191.
- [15] B.R. Lyon, Y.L. Cousins, D.J. Llewellyn, E.S. Dennis, *Transgen. Res.* 2 (1993) 162.
- [16] L. Feng, I.R. Kennedy, *Biotech. Bioeng.* 54 (1997) 513.
- [17] R.H. Don, J.M. Pemberton, *J. Bacteriol.* 145 (1981) 681.
- [18] Y. Suwa, A.D. Wright, F. Fukumori, K.A. Nummy, R.P. Hausinger, W.E. Holben, L.J. Forney, *Appl. Environ. Microbiol.* 62 (1996) 2464.
- [19] R.J. King, K.A. Short, R.J. Seidler, *Appl. Environ. Microbiol.* 57 (1991) 1790.
- [20] F. Fukumori, R.P. Hausinger, *J. Biol. Chem.* 268 (1993) 24311.
- [21] R. Stanier, N. Pelleroni, M. Douderoff, *J. Gen. Microbiol.* 43 (1966) 159.
- [22] B. Blessington, N. Crabb, S. Karkee, A. Northage, *J. Chromatogr.* 469 (1989) 183.
- [23] J. Sambrook, E.F. Fritsch, T. Maniatis, *Molecular Cloning: A Laboratory Manual*, 2nd edn., Cold Spring Harbor Laboratory Press, Cold Spring Harbor, NY, 1989.
- [24] W.E. Holben, B.M. Schroeter, V.G.M. Calabrese, R.H. Olsen, J.R. Kukor, V.O. Biederbeck, A.E. Smith, J.M. Tiedje, *Appl. Environ. Microbiol.* 58 (1992) 3941.
- [25] D.A. Hogan, D.H. Buckley, C.H. Nakatsu, T.M. Schmidt, R.P. Hausinger, *Microb. Ecol.* 34 (1997) 90.
- [26] Wisconsin Package Version 9.0, Genetics Computer Group (GCG), Madison, WI.
- [27] R.E. Saari, R.P. Hausinger, *Biochemistry* 37 (1998) 3035.
- [28] J.E. Baldwin, R.A. Field, C.C. Lawrence, K.D. Merritt, C.J. Schofield, *Tetrahedron Lett.* 34 (1993) 7489.
- [29] J.E. Baldwin, K.D. Merritt, C.J. Schofield, S.W. Elson, K.H. Baggaley, *J. Chem. Soc., Chem. Commun.* (1993), 1301.
- [30] S. Englard, J.S. Blanchard, C.F. Midelfort, *Biochemistry* 24 (1985) 1110.
- [31] E. Leete, D.H. Lucast, *Tetrahedron Lett.* 38 (1976) 3401.
- [32] C. Zipper, K. Nickel, W. Angst, H.-P. Kohler, *Appl. Environ. Microbiol.* 62 (1996) 4318.
- [33] K. Nickel, M.J.-F. Suter, H.-P.E. Kohler, *J. Bacteriol.* 179 (1997) 6674.
- [34] K. Nakajima, A. Yamashita, H. Akama, T. Nakatsu, H. Kato, T. Hashimoto, J. Oda, Y. Yamada, *Proc. Natl. Acad. Sci.* 95 (1998) 4876.

MICHIGAN STATE UNIV. LIBRARIES



31293020799395